1981

Electrocatalysis of the oxidations of some organic compounds on noble-metal electrodes by foreign metal ad-atoms

Ronald W. Tsang
Iowa State University

INFORMATION TO USERS

This was produced from a copy of a document sent to us for microfilming. While the most advanced technological means to photograph and reproduce this document have been used, the quality is heavily dependent upon the quality of the material submitted.

The following explanation of techniques is provided to help you understand markings or notations which may appear on this reproduction.

1. The sign or "target" for pages apparently lacking from the document photographed is "Missing Page(s)". If it was possible to obtain the missing page(s) or section, they are spliced into the film along with adjacent pages. This may have necessitated cutting through an image and duplicating adjacent pages to assure you of complete continuity.

2. When an image on the film is obliterated with a round black mark it is an indication that the film inspector noticed either blurred copy because of movement during exposure, or duplicate copy. Unless we meant to delete copyrighted materials that should not have been filmed, you will find a good image of the page in the adjacent frame. If copyrighted materials were deleted you will find a target note listing the pages in the adjacent frame.

3. When a map, drawing or chart, etc., is part of the material being photographed the photographer has followed a definite method in "sectioning" the material. It is customary to begin filming at the upper left hand corner of a large sheet and to continue from left to right in equal sections with small overlaps. If necessary, sectioning is continued again—beginning below the first row and continuing on until complete.

4. For any illustrations that cannot be reproduced satisfactorily by xerography, photographic prints can be purchased at additional cost and tipped into your xerographic copy. Requests can be made to our Dissertations Customer Services Department.

5. Some pages in any document may have indistinct print. In all cases we have filmed the best available copy.

University
Microfilms
International

300 N. ZEEB RD., ANN ARBOR, MI 48106

Tsang, Ronald W.

ELECTROCATALYSIS OF THE OXIDATIONS OF SOME ORGANIC COMPOUNDS ON NOBLE-METAL ELECTRODES BY FOREIGN METAL AD-ATOMS

Iowa State University PH.D. 1981

Electrocatalysis of the oxidations of some organic compounds on noble-metal electrodes by foreign metal ad-atoms

by

Ronald W. Tsang

A Dissertation Submitted to the
Graduate Faculty in Partial Fulfillment of the
Requirements for the Degree of
DOCTOR OF PHILOSOPHY

Department: Chemistry
Major: Analytical Chemistry

Approved:

Signature was redacted for privacy.

In-Charge of Major Work

Signature was redacted for privacy.

For the Major Department

Signature was redacted for privacy.

For the Graduate College

Iowa State University
Ames, Iowa

1981

TABLE OF CONTENTS

LIST OF TABLES

LIST OF FIGURES

LIST OF ACRONYMS

EF	Enhancement factor
I-E	Current-potential
NHE	Normal hydrogen electrode
QEF	Coulombic enhancement factor
RDE	Rotating disc-electrode
SCE	Saturated calomel electrode

LIST OF SYMBOLS

A	Electrode area
b	Constant
C^b	Concentration in solution bulk
D	Diffusion coefficient
d	Diameter of electrode
E	Electrode potential
E_+	Positive scan limit
E_-	Negative scan limit
E_{dep}	Deposition potential
E^o	Standard reduction potential
E_p	Peak potential
$E_{p,strip}$	Stripping peak potential
EF	Enhancement factor
F	Faraday's constant
ΔG^*	Activation energy
I_ℓ	Limiting current
I_o	Initial current
I_p	Peak current
I_{ss}	Steady-state current
I_t	Current at time t
$I_{t,max}$	Maximum time-dependent current
k	Constant
n	Number of electrons

N_{act}	Effective number of sites
N_{tot}	Total number of sites
Q	Quantity of charge under a peak
R	Gas constant
S	Slope
T	Temperature
t	Time
T_{dep}	Deposition time
δ_{eff}	Effective diffusion layer thickness
δ_{theory}	Theoretical diffusion layer thickness
θ_M	Fractional coverage by metal ad-atoms
θ_{org}	Fractional coverage by organic molecules
v	Kinematic viscosity
ϕ	Potential scan rate
τ_{max}	Time required for anodic current to reach the maximum value
W	Electrode rotation speed

I. INTRODUCTION

The interest in the electrochemical oxidation of organic compounds comes at least in part from the efforts surrounding the development of simple, reliable, efficient and economical fuel cells. The majority of studies involves the electrochemical oxidation of organic compounds at the noble-metal electrodes, particularly the Pt electrode. Pt is a well-known catalyst in the hydrogenation reaction of unsaturated hydrocarbons and is expected, therefore, to be a catalyst for dehydrogenation reactions of organic molecules. The oxidation of many organic compounds involves dehydrogenation as the first step of the reaction sequence. In such cases, Pt provides active sites for the chemisorption of the organic molecules prior to the dehydrogenation step and the chemisorption of the H-atoms produced by dehydrogenation.

Whereas the noble-metal electrodes are preferred for the electrochemical oxidation of certain organic compounds because of the accessibility of a rather large range of positive potential, they are not entirely without problems in practice. Usually, intermediate products of the anodic reactions are strongly adsorbed on the surface of the electrode and these adsorbed compounds poison the surface of the electrode, leading to severe loss of activity. Poisoning is a major cause of the fact that the expected catalytic potential of the noble-metal electrodes has not been fully realized in fuel cells.

Electrochemical methods of quantitative analysis, although proven to be highly sensitive in a wide variety of applications, have not been extensively applied to the determination of organic compounds. This is

a consequence of the above observations resulting from poisoning of the electrode surface. Use of the dropping mercury electrode (DME) in the determination of organic compounds may seem like the logical choice because the surface of the DME is continuously renewable and, therefore, highly reproducible. Fouling or poisoning of the electrode surface is not usually a problem with the DME because the lifetime of each Hg drop is only a few seconds. Unfortunately, most of the anodic reactions involving organic compounds do not take place at a DME (1) because of the limited accessible range of positive potential. Therefore, it seems extremely attractive to search for conditions in which the poisoning phenomenon can be avoided.

Most of the work in electrocatalysis up to the mid-1970s has been concerned primarily with the choice of the electrode material. However, several workers have demonstrated that for a given electrode material, the reactivity of the electrode surface can be dramatically altered by changes of the chemical composition of the double-layer region at the electrode-solution interface. For example, adsorption of iodine on the surface of a Pt electrode has been shown to substantially increase the heterogeneous rate constant for the Sb(V)/Sb(III) couple in a HCl medium (2).

The underpotential deposition of metal atoms, M, on a noble-metal substrate, is a process whereby the metal atoms are deposited in amounts up to a monolayer at potentials more positive than the reversible potential for the M^{+n}/M couple. This phenomenon is due to the strong interactions between the substrate metal and the underpotential-deposited

metal atoms, which are commonly referred to as 'foreign metal ad-atoms'. Recently, the catalytic effects of submonolayer deposits of foreign metal ad-atoms have been observed for several electrochemical reactions on various electrode material. It has been shown that the underpotential deposition of several heavy-metal species substantially increased the heterogeneous rate constants of the Fe(III)/Fe(II) couple on a Au electrode, the reduction of O_2 on a Au electrode, the oxidation of HCOOH on a Pt electrode (3) and the reduction of NO_3^- on a Cu electrode (4). The mechanisms of the electrocatalysis can be drastically different for different electrochemical reactions. Adzic et al. (5) applied in situ reflectance spectroscopy to study the underpotential deposition of Pb on Au electrodes and demonstrated that the surface electronic properties of Au is modified by the underpotential deposition of a submonolayer of Pb ad-atoms. The modification of the electronic properties of the electrode surface is believed to be a consequence of strong interactions between the valence orbitals of the metal ad-atoms and the band structure of the substrate electrode material.

Several workers have extensively studied the electrocatalytic effects of metal ad-atoms on the electrochemical oxidation of simple organic compounds, particularly HCOOH and CH_3OH. The mechanism of the electrocatalysis is still a subject of much controversy. Several workers have proposed that the metal ad-atoms adsorb oxygen-containing species which then react with the organic species adsorbed on adjacent sites of the electrode substrate. Others have proposed that the metal ad-atoms prevent fouling of the electrode surface by blocking the

adjacent surface sites of the electrode which are necessary for the formation of the "poisons". This mechanism is based on the premise that the metal ad-atoms are very evenly distributed on the surface of the electrode. The maximum catalytic effects of the metal ad-atoms would then be expected to be at a maximum when exactly 50% of the electrode surface sites are covered, i.e., $\theta_M = 0.5$. Several workers have claimed that they indeed have evidence that maximum catalytic enhancement is achieved when $\theta_M = 0.5$.

In this research project, the electrocatalytic effects of metal ad-atoms deposited at underpotential was studied extensively for the oxidation of formic acid and dextrose. The electrochemical oxidation of dextrose was examined at Pt and Au electrodes. The catalytic effects of various metal ad-atoms, including Bi, Pb, Tl, Hg, Cd and Ag, on the electrochemical oxidation of dextrose were studied. These studies were performed in the expectation that the metal ad-atoms will substantially increase the steady-state currents for the oxidation of dextrose. The activation energy associated with the electrochemical oxidation of HCOOH was determined for a Pt electrode and a Bi-coated Pt electrode. From the results, it is concluded that the enhancement of the anodic current does not result from the electrocatalysis of the electron-transfer step, but rather from an increase of the rate of desorption of adsorbed poisons.

II. LITERATURE REVIEW

The electrochemical oxidation of several organic compounds at noble-metal electrodes is reviewed. The focus is on simple organic molecules, particularly formic acid (HCOOH). A large proportion of the research done to date has dealt with this compound. The processes that lead to the formation of the catalytic poisons are discussed. Finally, the catalytic effects of various metal ad-atoms are reviewed. Included in this review is a discussion of the mechanisms of these catalytic effects as presented by different workers.

A. Electrochemical Oxidation of Organic Compounds at Noble-Metal Electrodes

Initial analytical applications of noble-metal electrodes occurred ca. 1890. Technical interest in the electrochemical oxidation and reduction of organic compounds was already widespread in Germany in the early 1900s. Haber (6) and Russ (7) examined the electrochemical properties of Au, Pt and other less noble metal electrodes with respect to organic oxidation and reduction reactions. Growing industrial interest in the electrochemical synthesis of organic compounds prompted Weinberg (8) and Rifi (9) to compile extensive lists of electrochemical data for organic compounds at noble-metal and nonnoble-metal electrodes. The organic compounds included in these lists range from simple aliphatic hydrocarbons to complex, naturally occurring N-heterocyclic compounds.

The extensive fuel-cell programs developed in the 1960s have shifted the attention of electrochemists to the electrochemical oxidation of simple organic compounds. Simple organic compounds, such as methanol, formic acid and formaldehyde, have been used in place of hydrogen as the fuel in some low-temperature fuel cells (10). Organic fuels, in liquid form, are easier to handle than hydrogen. Certain organic fuels, such as ethanol, can be obtained relatively inexpensively from the recycling of refuse or waste material.

In an attempt to better understand the mechanisms for the electrochemical oxidation of alcohols to carbon dioxide, many workers turned to fundamental studies of the electrochemical oxidation of formic acid (HCOOH). HCOOH was believed to be an intermediate product in the electrochemical oxidation of alcohols, e.g., CH_3OH, to CO_2. Many workers assumed that the electrochemical oxidation of HCOOH ought to be relatively simple and straightforward. Although the oxidation of HCOOH turned out to be more complicated than initially speculated, detailed studies of this compound nevertheless served as a pathway to the better understanding of the mechanisms involved in the electrochemical oxidation of many simple organic compounds.

In the following sections, mechanisms are discussed for the electrochemical oxidation of simple organic acids, aldehydes and alcohols, followed by description of studies involving the electrochemical oxidation of compounds with higher molecular weights, especially glucose.

1. Simple organic compounds

a. HCOOH on Pt electrodes One of the first extensive investigations of the electrochemical oxidation of HCOOH was made by Müller (11) and Müller and Tanaka (12) who found virtually 100% efficiency for the reaction

$$HCOOH \longrightarrow CO_2 + 2H^+ + 2e \qquad (II\text{-}1)$$

They noted that the limiting current for this reaction is not controlled by the diffusion of HCOOH to the surface of the electrode, i.e., the rate of stirring the electrolyte solution does not affect the limiting current observed. To account for this, they proposed that the rate-limiting step (r.l.s.) involves surface-adsorbed HCOOH, represented as $(HCOOH)_{ad}$.

$$(HCOOH)_{soln} \xrightarrow{Pt} (HCOOH)_{ad} \quad \text{(fast)} \qquad (II\text{-}2)$$

$$(HCOOH)_{ad} \longrightarrow H_2 + CO_2 \quad \text{(r.l.s.)} \qquad (II\text{-}3)$$

$$H_2 \rightleftharpoons 2H^+ + 2e^- \quad \text{(fast)} \qquad (II\text{-}4)$$

Although Brummer and Makrides (13) questioned the mechanistic details proposed by Müller and Tanaka, subsequent work supported the conclusion that surface-adsorbed species are involved. Further proof of the importance of adsorption in the electrochemical oxidation of HCOOH comes from the fact that different electrode materials behave differently towards HCOOH. Capon and Parsons (14) studied the electrochemical oxidation of HCOOH in acidic media for Pt, Pd, Rh, Ir and Au

electrodes. They found that the activities of the electrodes towards HCOOH were in the order Pt > Pd > Rh > Ir > Au.

It is now generally recognized that the electrochemical oxidation of HCOOH on Pt proceeds to CO_2 via a surface-adsorbed intermediate state, but the chemical nature and role of this intermediate state remain the subject of much controversy. In an early paper, Breiter (15) postulated the adsorption of HCOOH molecules, the same view as that held by Müller and Tanaka (11,12). Other workers favored a dissociative adsorption process (13, 16, 17, 18, 19, 20) which could be written

$$(HCOOH)_{soln} \xrightarrow{Pt} (HCOOH)_{ad} \qquad \text{(II-5)}$$

$$(HCOOH)_{ad} \longrightarrow \begin{matrix}(HCOO\cdot)_{ad} \\ \text{or} \\ (\cdot COOH)_{ad}\end{matrix} + (\cdot H)_{ad} \qquad \text{(II-6)}$$

Brummer and Makrides (13) favored the existence of the $(\cdot COOH)_{ad}$ radical while Munson (17) and Piersma et al. (20) postulated that $(HCOO\cdot)_{ad}$ is the surface-adsorbed species. Bagotzky and Vassiliev (21) observed that CH_3OH is able to undergo dissociative adsorption at pH > 14 and that three hydrogen atoms are formed from one molecule of CH_3OH. They inferred from these observations that the C-H bonds in CH_3OH are more likely to break than the O-H bond. Comparisons of HCOOH with CH_3OH suggest that the C-H bond in HCOOH is the one most likely to be broken, resulting in $(\cdot COOH)_{ad}$ as the surface-adsorbed intermediate species. Rhodes and Steigelmann (19) and Brummer (22) suggested $(CO)_{ad}$ as the adsorbed species after comparing intermediate products from CO and HCOOH by a potentiodynamic sweep technique.

However, $(CO)_{ad}$ has not been generally accepted by other workers as the intermediate species.

Of great importance for the understanding of the oxidation reactions of organic compounds is a correct evaluation of the adsorption processes as well as the effect of various factors on the adsorption processes, e.g., concentration, potential, electrode material, etc. In the case of the Pt-group metals, as well as other metals such as Ni, complications can arise because at certain electrode potentials O_2 and H_2 can adsorb on the electrode surfaces in considerable amounts. Nevertheless, several workers have attempted to measure the extent of coverage by organic molecules on Pt and other solid-metal electrodes. Bockris and Swinkels (23) and Bockris et al. (24) used a C^{14}-labelling technique to measure the adsorption of n-decylamine and naphthalene on solid-metal electrodes. This method is the only direct one to have been used for adsorption measurements and has an accuracy within 10-15%. Electrochemical methods have also been used widely for adsorption measurements. In their simplest form, these methods are based on the determination of the quantity of electricity necessary for the oxidation of a monolayer or submonolayer of adsorbed organic molecules on the surface of the electrode. Capon and Parsons (25) used this method to show that in the potential region of 0.4 - 0.8 V vs. the normal hydrogen reference electrode (NHE), the surface of a Pt electrode is approximately 70% covered by adsorbed organic species for 0.5 M HCOOH in 0.5 M H_2SO_4.

More reliable results can be obtained by another type of electrochemical method which is called the "adsorption substitution method" (21). This method involves the measurement of the quantities of electricity necessary to adsorb or desorb a submonolayer of the H-atoms from the surface of the electrode in the absence ($_{S}Q_{H}$) and presence (Q_{H}) of organic compounds. The surface coverage of the electrode by the organic compound is then calculated as

$$\theta_{org} = \frac{{}_{S}Q_{H} - Q_{H}}{{}_{S}Q_{H}} \qquad \text{(II-7)}$$

The accuracy of this method is believed to be within 3-4% of the true value (21). The results of the experiments performed by several workers (13, 21, 26, 27) to measure θ_{org} at Pt electrodes by the method of adsorption substitution are summarized in Table II-1.

Table II-1. Surface coverage (θ_{COOH}) of a Pt electrode by $(\cdot COOH)_{ad}$

[HCOOH] (mM)	θ_{COOH} in the potential region between 0.4 V and 0.8 V vs. NHE
0.1	0.2
1.0	0.5
10.0	0.8
100.0	1.0
1000.0	1.0

The adsorption of $(\cdot COOH)_{ad}$ on Pt is dependent on the potential of the electrode. Brummer and Makrides (13) reported that adsorption ceases at potentials more positive than 0.6 V vs. NHE in $HClO_4$. Other workers reported that adsorption persists until a potential of 0.8 V vs. NHE has been reached (28).

Among workers who agree that $(\cdot COOH)_{ad}$ is the surface adsorbed intermediate species, there is consensus regarding the mechanistic details of the electrochemical steps that follow the chemisorption step. The mechanism is as follows:

$$(HCOOH)_{soln} \xrightarrow{Pt} (\cdot COOH)_{ad} + (\cdot H)_{ad} \qquad \text{(II-8)}$$

$$(\cdot COOH)_{ad} \longrightarrow CO_2 + H^+ + e^- \qquad \text{(II-9)}$$

$$(\cdot H)_{ad} \longrightarrow H^+ + e^- \qquad \text{(II-10)}$$

These steps are commonly referred to as the "main oxidation pathway" for HCOOH on Pt electrodes. As will be discussed in a later section, not all of the $(\cdot COOH)_{ad}$ radicals are oxidized directly to CO_2. Some of them can be transformed to strongly adsorbed species known as 'poisons' which frequently occupy more than one active site on the electrode surface. The multiple-site interactions of the poisons with the Pt substrate lead to very slow rates of oxidation of these poisons in the potential region where HCOOH is oxidized via the main oxidation pathway. Hence, the poisons accumulate on the surface of the electrode and cause deactivation of the electrode surface. The competing reactions can be described as

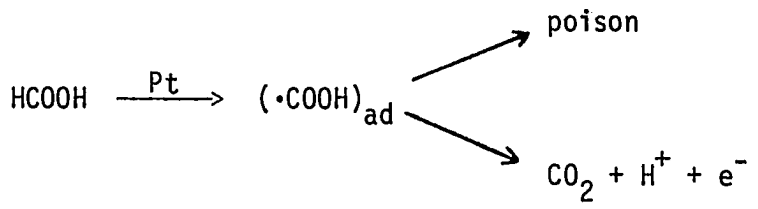

(II-11)

Brummer and Makrides (13) and Jayaram and Lal (29) assumed that Equation II-8 is the rate-limiting step in the main oxidation pathway. They cited the observation that the rate of oxidation of HCOOH is first order with respect to the free Pt surface, the concentration of HCOOH in solution, and the pH. They concluded that the slow step is the non-electrochemical dissociative reaction of $(HCOOH)_{ad}$ (Equation II-8). Breiter (28) assumed that Equation II-9 represents the rate-limiting step although he did not present any concrete evidence for this. However, in view of the fact that the surface-adsorbed •COOH radical can accumulate and lead to the formation of a poison, it is likely that Equation II-9 is the rate-limiting step as Breiter has assumed.

Anodic currents for the oxidation of HCOOH are also observed at 1.4 V vs. NHE in an acidic medium. However, at this positive potential, the surface of the Pt electrode is completely covered by oxide (30) and is free of $(\cdot COOH)_{ad}$ (13, 26, 27, 28). Breiter has proposed that HCOOH molecules are directly oxidized to CO_2 (see Equation II-1) without the preadsorption steps at the oxide-covered electrode at a potential of 1.4 V vs. NHE (28).

b. HCHO and CH_3CHO on Pt electrodes Studies of the electrochemical oxidation of aldehydes have been limited primarily to HCHO and CH_3CHO at Pt electrodes (31-38). As in the case of HCOOH,

electrochemical oxidation of the aldehydes are believed by most workers to proceed via surface-adsorbed intermediate species. None of the workers who have studied the electrochemical oxidation of CH_3CHO has proposed any composition for the intermediate species nor any mechanisms for the electrochemical oxidation of those intermediate species. However, Podlovchenko et al. (31) did mention that:

> "According to electrochemical measurements and the analysis of gases evolved when a Pt electrode is immersed in solutions of saturated alcohols and aldehydes containing more than one carbon atom, dehydrogenation, hydrogenation and self-hydrogenation of the original substances and their decomposition products (mainly along the C_1-C_2 bond) occur on the electrode surface. A steady concentration of $(\cdot H)_{ad}$ on the electrode surface is maintained due to the above process."

More information than that concerning the higher molecular weight aldehydes is available on the electrochemical oxidation of HCHO. Breiter (32) studied the electrochemical oxidation of HCHO on a Pt electrode in a H_2SO_4 medium and concluded that the adsorbed intermediate species are similar to the cases involving the electrochemical oxidation of CH_3OH and HCOOH. He suggested that the net composition of the intermediate species may be $H_2C_2O_3$, which is a composite of $(\cdot CHO)_{ad}$ and $(\cdot COOH)_{ad}$. Loučka and Weber (38) performed a detailed study on the adsorption and electrochemical oxidation of HCHO on Pt electrodes in acid solutions. They pointed out a difficulty in working with HCHO: analytical reagent-grade HCHO is preserved with a substantial amount of CH_3OH. Therefore, solutions of HCHO have to be prepared by distillation from analytical-grade paraformaldehyde into redistilled water and the concentration of HCHO determined iodometrically before each measurement.

Adsorption measurements were performed, and Loučka and Weber discovered that the ability of HCHO to adsorb is higher than that of HCOOH and, furthermore, the total coverage of the electrode can be reached with a concentration of HCHO of about one order of magnitude lower than in the case of HCOOH.

Loučka and Weber (38) suggested that the HCHO molecule is adsorbed into two different states of reactivity:

> "On the one hand, it is adsorbed as a less active substance, A, which is most probably formed by the dehydration of a molecule of formaldehyde with the production of the species $>C=O$ or $>C(OH)_2$. These species are anodically oxidized at potentials $E < +0.6V$, relatively slowly, so that at higher concentrations of formaldehyde, θ_0 reaches the value 1. On the other hand, at the free fraction of the surface, $1 - \theta_0$, formaldehyde is adsorbed as a more active species, B, which gets relatively rapidly anodically oxidized [sic] to CO_2, between $E = +0.3$ and $+0.6V$. The molecules of CO_2 desorb from the surface and the whole process of adsorption of formaldehyde as B and its oxidation can be repeated many times."

The species A of Loučka and Weber can be recognized as the poison that inhibits the electrode surface towards HCHO oxidation. The authors did not propose a structure for the more active species B.

c. CH_3OH and C_2H_5OH on Pt electrodes Several workers have studied the electrochemical oxidation of the simple alcohols on noble-metal electrodes (31, 32, 35, 36, 37, 39, 40, 41, 42, 43, 44). A majority of the work was concerned with the electrochemical oxidation of CH_3OH and C_2H_5OH on Pt electrodes, although Breiter (39) has compared the electrochemical oxidation of CH_3OH on Pt, Pd, Rh, Ir and Au. He found that the order of activities of the electrode materials studied

is Pt > Pd > Rh > Ir > Au. This ordering of the activities is identical to that involving the electrochemical oxidation of HCOOH, as reported by Capon and Parsons (14). Raicheva et al. (35) and Kalcheva et al. (37) reported that C_2H_5OH gives much higher anodic currents than CH_3CHO and concluded that this results because destructive chemisorption plays less of a role in the anodic reaction of the aldehyde than of the alcohol.

Bagotzky and Vassiliev (21) have described the adsorption of CH_3OH on Pt in terms of the Temkin logarithmic isotherm and have considered that the adsorbed species are in equilibrium with the species dissolved in the solution bulk. The Temkin isotherm is described by

$$\theta_{org} = a + 1/f \ln C \qquad \text{(II-12)}$$

where θ_{org} = fractional coverage of the electrode by organic molecules

a = constant

f = inhomogenuity factor

C = concentration of the organic compound.

The adsorption of CH_3OH follows this isotherm over 4 orders of magnitude of the concentration of CH_3OH. Sobkowski and Cinak (43) studied the vapor-phase adsorption of CH_3OH on Pt black and also came to the conclusion that this adsorption is a reversible process. They found that the surface coverage of the Pt by adsorbed CH_3OH increases with increasing pressure and decreases with decreasing pressure.

Kamath and Lal (44) concluded that the adsorbed species from CH_3OH is $(HCO)_{ad}$, arising from the reaction

$$CH_3OH \xrightarrow{Pt} 3(\cdot H)_{ad} + (HCO)_{ad} \qquad \text{(II-13)}$$

They did not elaborate further on the structure of the $(HCO)_{ad}$, but it is probably $(\vdots COH)_{ad}$, attached to 3 surface sites on the surface of the Pt substrate. Sidheswaran (41) proposed the mechanism below for the destructive chemisorption of C_2H_5OH based on the fact that he had discovered HCHO as a product of the electrochemical oxidation of C_2H_5OH.

$$CH_3CH_2OH \longrightarrow (\cdot CH_3)_{ad} + (\cdot CH_2OH)_{ad} \qquad \text{(II-14)}$$

$$(\cdot CH_2OH)_{ad} \longrightarrow (:CHOH)_{ad} + (\cdot H)_{ad} \qquad \text{(II-15)}$$

$$(:CHOH)_{ad} \longrightarrow (\vdots COH)_{ad} + (\cdot H)_{ad} \qquad \text{(II-16)}$$

He proposed that HCHO is formed by breakage of the O-H bond in the species $(\cdot CH_2OH)_{ad}$. The detection of HCHO was made after the addition of aqueous chromotropic acid, 4,5-dihydroxy-2,7-naphthalene disulfonic acid, which forms a violet-pink complex with HCHO.

2. Glucose on Pt electrodes

Several workers have investigated the electrochemical oxidation of organics of higher molecular weights. These included enthylene-glycol (21), glycol-aldehyde (45), glycerol, butanol and oxalic acid (46). This review deals primarily with the electrochemical oxidation of glucose because of the widespread interest in using glucose as a fuel in biological fuel cells and the possibility of in-vivo electrochemical monitoring of the glucose level in diabetic patients.

The idea appeared in the 1960s to use glucose as a fuel in implantable glucose-oxygen fuel cells for cardiac pacemakers because of dissatisfaction over the more conventional power sources (47, 48, 49, 50, 51). Cardiac pacemakers that rely on mercury cells last for only about 2 years (50). Among the various attempts to prolong the life of the power supply, the possibility of generating electricity from the body has been investigated. Massie et al. (52) employed implanted cells with body fluids as the electrolyte. In these cells, Pt was used as the cathode and Al or Zn as the anode. These are galvanic cells in which the anode is oxidized and consumed while oxygen from the blood is reduced at the cathode. Although Tseung et al. (53) showed that an electrochemical cell of this nature can give a satisfactory performance when properly encapsulated, the life of this kind of cell is obviously limited owing to the continuous consumption of the anode.

A biological fuel cell offers the potential of permanency. It can be established in the body by implanting two permanent electrodes inside the body fluids. An analysis of the available oxidants and fuels in the body fluids indicates that an oxygen-glucose cell could serve as an ideal biological fuel cell. In such cells, similar platinized electrodes could be used both as anode and cathode. This necessitates the use of two different membranes to increase the selective permeability of oxygen and glucose towards the cathode and anode, respectively. Wan and Tseung (50) have used different inert materials, e.g., Pt and C, as the cathode and anode, respectively, with good results for in-vivo and in-vitro tests.

Although the majority of the workers are interested in the electrochemical oxidation of glucose because of its potential value as a fuel in biological fuel cells, a few workers are also interested in the *in-vivo* electroanalytical determination of glucose. Chang *et al.* (54) and Gough *et al.* (55) have attempted to use the reactivity of glucose as the basis for the development of an implantable analytical glucose-sensor for long term *in-vivo* monitoring. Since interferences from other biochemicals may pose a severe problem, Gough *et al.* (55) suggested a possible design in which the glucose sensor could be encapsulated in a bio-compatible, semipermeable membrane to prevent the interfering biochemicals from reaching the surface of the working electrode. Glucose molecules which diffuse through the semipermeable membrane would be electrochemically oxidized on the anode at some appropriate value of applied potential to produce a current which could be related to the concentration of glucose in blood.

Fundamental studies involving the electrochemical oxidation of glucose on Pt electrodes have been performed in acidic (56) and alkaline (47) solutions, and buffered media which closely approximate the physiological pH (7.4) of blood (48, 55, 57, 58, 59, 60). Bockris *et al.* (47) and Skon (56) observed that glucose shows a higher reactivity in an alkaline medium than in neutral or acidic media. Bockris *et al.* (47) also compared the behavior of several carbohydrates in alkaline solutions at 80°C and found that the reactivities of the carbohydrates decrease with increasing molecular weight.

The electrochemical oxidation of glucose on a Pt electrode is activation controlled and the rate of stirring the solution has very little effect on the currents observed (56, 58, 60). Several workers have proposed reaction mechanisms for the electrochemical oxidation of glucose on Pt electrodes. Ernst and Heitbaum (58) studied the electrochemical oxidation of glucose in a buffered neutral medium and reported that the glucose molecule is present in the ring form

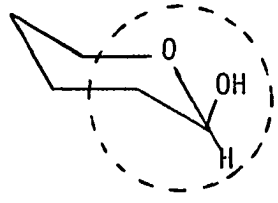

[I]

and that the reaction center is the hemiacetal group (enclosed in dotted circle in [I]) of the glucose molecule. They identified the product of the electrochemical reaction as glucono lactone [II]

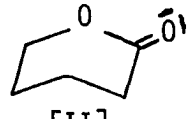

[II]

by mass spectroscopy as well as by pH measurements. Rao and Drake (57) have also analyzed the product of glucose oxidation by thin layer chromatography and concluded that under the experimental conditions they employed, gluconic acid [III] is the only product formed.

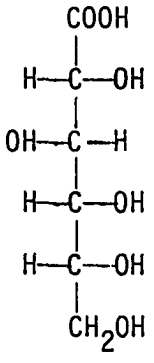

[III]

Other workers reported that gluconic acid is oxidizable further to CO_2 in alkaline media (47, 48, 60).

Another mechanism was proposed by Bockris et al. (47) for the electrochemical oxidation of glucose in acidic media. They observed that the amount of CO_2 evolved from glucose with no current flowing is about 15% of the amount obtained during electrochemical oxidation. From this, these authors postulated that a chemical reaction occurs in the solution cleaving off one carbon atom from each glucose molecule to form CO_2 with simultaneous oxidation of the molecule to $C_5H_8O_7$.

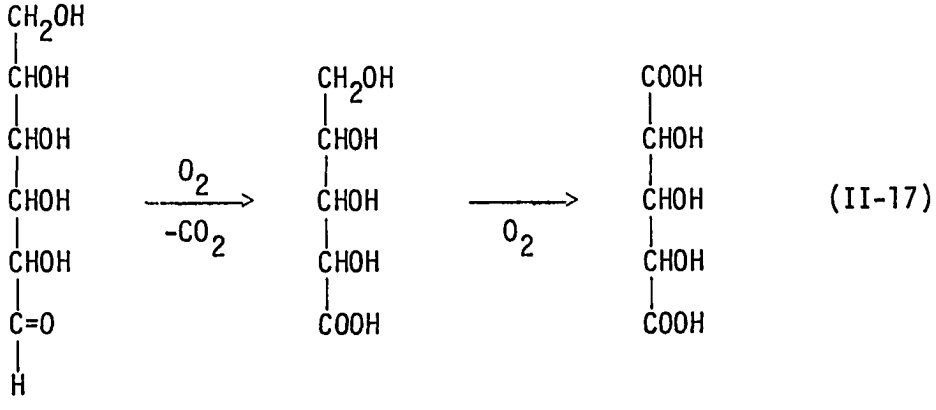

(II-17)

The product of this chemical reaction, $C_5H_8O_7$, is then electrochemically oxidized to CO_2.

$$C_5H_8O_7 + 3H_2O \longrightarrow 5CO_2 + 14H^+ + 14e \qquad \text{(II-18)}$$

According to this scheme, 2.3 electrons would be required per CO_2 molecule evolved, which was in good agreement with their experimental observations.

According to several other workers, glucose also undergoes rearrangement in an alkaline medium to form the corresponding enediol (61, 62). The formation of enediol is acid-base catalyzed with $k_{OH^-} >> k_{H^+}$ (63).

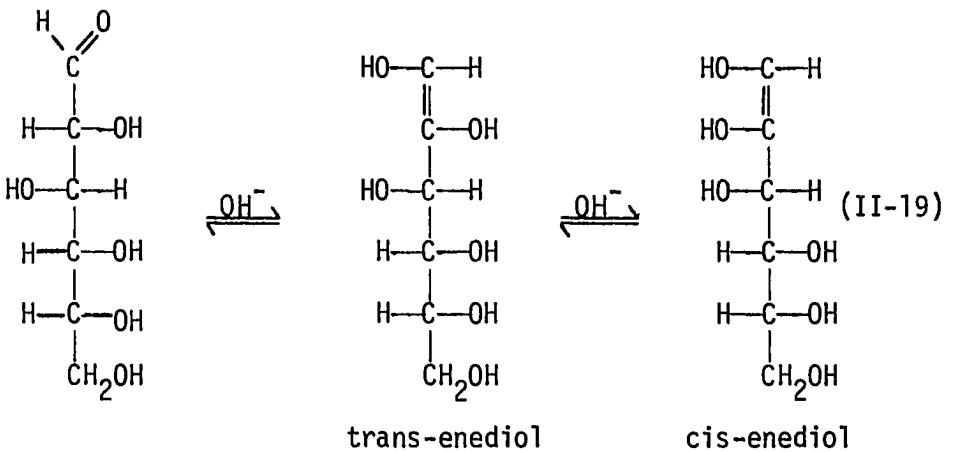

(II-19)

B. Passivation of the Electrode During Oxidation of Organic Compounds

A general problem in the electrochemical oxidation of organic molecules is the progressive decrease of the rate, i.e., current density, of the reaction with time at a given potential and temperature.

This phenomenon of progressive passivation of the electrode is observed in both the electrochemical oxidation of small organic molecules, such as HCOOH (13, 27) and formaldehyde (38), as well as larger molecules such as glucose (60). This phenomenon has been reported at Pt electrodes (13, 27, 38, 60) as well as Pd and Au electrodes (14). Although the passivation of the electrode during the oxidation of organic compounds has been explained by the inhibiting effects of adsorbed impurities from the solution, most workers agree that a large part of the effect is due to the accumulation of strongly bound intermediate species, "poisons", produced during the oxidations. The strongly bound intermediate species block the active sites on the surface of the electrode, resulting in a decrease of the effective area of the electrode and hence a decrease in current density.

Even when the potential of the electrode is continuously scanned, as in cyclic voltammetry, the presence of the poisons is still evident. This is manifested in the form of peak-shaped I-E curves instead of well-defined limiting-current plateaus.

Various workers have proposed mechanisms for the formation of the poisoning species. For the electrochemical oxidation of HCOOH on a Pt electrode, Angerstein-Koglowska et al. (64) have proposed that the poison is formed as a consequence of a dimerization reaction between adjacent $(\cdot COOH)_{ad}$ adsorbed on the surface of the electrode

$$(\cdot COOH)_{ad} + (\cdot COOH)_{ad} \xrightarrow{Pt} ((:COOH)_2)_{ad} \qquad \text{(II-20)}$$

$((:COOH)_2)_{ad}$ is presumably the poison that causes passivation of the electrode surface. Angerstein-Koglowska et al. (64) also proposed that the poison may be $(\vdots COH)_{ad}$, which is formed by a dimerization-disproportionation reaction between bulk HCOOH and $(\cdot COOH)_{ad}$.

$$HCOOH + (\cdot COOH)_{ad} \longrightarrow (\vdots COH)_{ad} + CO_2 + H_2O \qquad (II\text{-}21)$$

This is based on the observation that if HCOOH is injected into a cell with initial potentials in the double-layer region, the potential immediately drops but CO_2 is evolved for a short time. Capon and Parsons (25) suggested that a reaction between HCOOH and $(\cdot COOH)_{ad}$ may also lead to the formation of $(:C(OH)_2)_{ad}$.

$$HCOOH + (\cdot COOH)_{ad} \longrightarrow (:C(OH)_2)_{ad} + H^+ + CO_2 + e^- \qquad (II\text{-}22)$$

If the electrode potential is in the region where H-atoms may be present on the surface of the electrode, e.g., at the negative potential limits, the poisons may be produced by a reaction between $(\cdot COOH)_{ad}$ and H-atoms (25).

$$(\cdot COOH)_{ad} + (\cdot H)_{ad} \longrightarrow (:C(OH)OH)_{ad} \qquad (II\text{-}23)$$

$$(:C(OH)OH)_{ad} + (\cdot H)_{ad} \longrightarrow (\vdots COH)_{ad} + H_2O \qquad (II\text{-}24)$$

It was reported that the reaction between dissolved HCOOH and $(\cdot H)_{ad}$ is very slow (25) and, therefore, Equations II-23 and II-24 are the dominant reaction paths.

The species $(\vdots COH)_{ad}$ has also been suggested as the poison formed in the electrochemical oxidation of CH_3OH and HCHO on a Pt electrode (14, 38, 65, 66)

$$CH_3OH \longrightarrow (\vdots COH)_{ad} + 3H^+ + 3e^- \qquad \text{(II-25)}$$

$$HCHO \longrightarrow (:CO)_{ad} + 2H^+ + 2e^- \qquad \text{(II-26)}$$

$$(:CO)_{ad} \downarrow (\cdot H)_{ad} \longrightarrow (\vdots COH)_{ad}$$

Most workers agree that $(\vdots COH)_{ad}$ is the major poison formed in the electrochemical oxidation of simple organic compounds on a Pt electrode. Regardless of the true structure of the poisons, they are not desorbed and are slow to undergo further oxidations.

Poisons are also formed in the electrochemical oxidation of simple organics on a Pd electrode. However, the interaction between $(\cdot H)_{ad}$ and $(\cdot COOH)_{ad}$ (see Equations II-23 and II-24) apparently does not take place on a Pd electrode (14, 67). This conclusion is based on the experimental observation that no difference in anodic currents is observed whether or not the electrode potential has been in the region where the adsorption of $(\cdot H)_{ad}$ can take place. Adzic et al. (67) suggested that $(\cdot C(OH)_2)_{ad}$ is the main poison formed in the electrochemical oxidation of HCOOH on a Pd electrode. This poison is formed by a dimerization-disproportionation reaction between bulk HCOOH and surface-adsorbed •COOH radicals (see Equation II-22).

Although it is generally agreed that poisons are also formed in the electrochemical oxidation of the more complicated organic molecules,

there is almost no speculation on the compositions of such poison species. Rao and Drake (57) proposed that gluconic acid, the product of the electrochemical oxidation of glucose on a Pt electrode, may be the poison in that reaction. However, there is controversy whether gluconic acid can be oxidized directly to CO_2 (57, 60). Ernst and Heitbaum (58) have also proposed a structure ([IV]) for the poison formed in the electrochemical oxidation of glucose on a Pt electrode

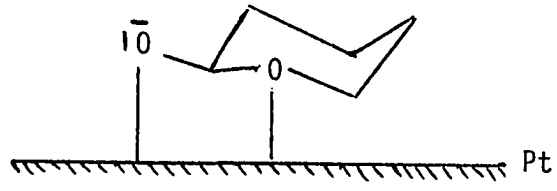

[IV]

C. Electrocatalysis of the Oxidation of Organic Compounds on Chemically Modified Electrodes

In this section, the electrocatalysis of organic oxidation on three basic types of chemically modified electrodes is reviewed. Also presented are the different models of electrocatalysis as presented by various workers in this field.

1. The phenomena of electrocatalytic effects

a. Electrodes modified by metal ad-atoms The deposition of submonolayer quantities of many metal species on noble-metal substrates has been studied extensively (68, 69, 70, 71, 72, 73, 74, 75). Depositions on Au electrodes have been followed by electrochemical

as well as optical methods (76, 77). When a strong interaction exists between the deposited atoms and the substrate, deposition can occur at potentials substantially positive of the reversible potential (E°). This phenomenon is referred to as "underpotential deposition". An interpretation of the underpotential deposition of metals based on the work function of the metals has been developed (78, 79). The spatial arrangement of the metal ad-atoms deposited at underpotential on Pt and Pd substrates has been discussed (80, 81). The inhibitory effects of metal ad-atoms deposited at underpotential on the evolution of hydrogen have also been reported (82, 83, 84).

The electrochemical oxidation of HCOOH on Pt electrode is catalyzed by submonolayer quantities of deposited Pb (85, 86, 87, 88), Bi (85, 87, 89), Tl (85, 87) and Cd (85, 87). Copper was reported to give only a slight enhancement (90) and, in general, other transition metals were observed to inhibit the electrochemical oxidation of HCOOH on Pt electrodes. The catalytic benefit for the various metal ad-atoms tested decreased in the order Pb > Bi > Tl > Cd > Cu (85). The peak currents for the electrochemical oxidation of HCOOH on Pt were observed to be increased up to 70X by Pb ad-atoms, but only 3-4X by Cd ad-atoms (85).

Metal ad-atoms deposited at underpotential also catalyze oxidation of HCOOH on noble-metal electrodes other than Pt. Adzic et al. (67) have reported the catalytic effects of Pb, Bi, Cd, Tl and Ag for the electrochemical oxidation of HCOOH on a Pd electrode. However, the catalytic effects of the ad-atoms on Pd were not as large as those

observed for the Pt electrode, and the ordering of the catalytic effects was also found to be different from the case of the Pt electrode (67). For the Pd electrode, the catalytic benefit of the metal ad-atoms decreased in the order Cd > Pb > Ag > Tl = Bi. Despic et al. (91) reported that Pb, Bi and Tl also enhanced the electrochemical oxidation of HCOOH on a Rh electrode.

Various workers have searched for effective catalysts for the electrochemical oxidation of CH_3OH. The majority of these workers have reported that Sn ad-atoms have a catalytic effect on Pt electrodes (92, 93, 94, 95, 96). Janssen and Moolhuysen (93) have prepared Pt-Sn catalysts by electrochemical deposition as well as a novel immersion technique. They reported that a Pt-Sn catalyst prepared by the immersion technique has comparable catalytic activity to one prepared by conventional electrodeposition. Andrew et al. (95) reported that Sn enhanced the electrochemical oxidation of CH_3OH on Pt by 50X. Watanabe and Motoo (97, 98) reported that submonolayer quantities of Ru or Au ad-atoms enhanced the electrochemical oxidation of CH_3OH on Pt and Pd electrodes. Janssen and Moolhuysen (92) prepared 26 different Pt-based binary catalysts and studied their catalytic effects for the electrochemical oxidation of CH_3OH. They found that the highest activities are observed for systems displaying the greatest stabilization of the zero-valent state of the adsorbed metal. They also found that Pb, Bi and Ag, while being catalysts for the electrochemical oxidation of HCOOH on Pt electrodes, inhibit the electrochemical oxidation of CH_3OH on Pt.

Catalytic effects of metal ad-atoms deposited at underpotential for the electrochemical oxidation of HCHO have been reported (66, 99, 100, 101). Among the various metals studied, Sb, As, Re, Te, Sn, Ge, Bi and Pb were found to be effective catalysts for the electrochemical oxidation of HCHO on Pt electrodes.

The effects of metal ad-atoms deposited at underpotential for the electrochemical oxidation of carbon monoxide, ethylene glycol and ascorbic acid have also been reported. The oxidation of carbon monoxide was found to be catalyzed by Sn (102), As (103) and Ru (104) ad-atoms. The oxidation of ethylene glycol was found to be catalyzed by Pb (3), and that of ascorbic acid by Pb, Tl, Hg, Ag and Sb (105).

b. Electrodes prepared by alloying The electrochemical oxidation of CH_3OH on alloy electrodes has been studied by Janssen and Moolhuysen (92, 96). The alloy electrodes were prepared by leaching Al from Raney-type catalysts ($Pt_{1-y}X_yAl_4$) with KOH, or they were prepared by melting mixtures of the appropriate metals. Pt-Sn and Pt-Ti alloys were studied and were found to greatly enhance the electrochemical oxidation of CH_3OH over that for pure Pt electrodes. Unfortunately, the nonnoble metal components of the alloy electrodes tended to leach out preferentially under the test conditions employed, and the badly corroded electrodes lost their catalytic activities. The alloy electrodes that did not corrode had catalytic activities comparable to those prepared by electrodeposition.

c. Electrodes chemically modified by nonmetallic species Not much information is available on the electrocatalysis of organic oxidation by surface-adsorbed nonmetallic ad-atoms or molecules.

However, several workers did report that the adsorption of such species as I^-, S and CH_3CH were found to enhance the electrochemical oxidation of HCOOH on Pt electrodes (64, 106, 107).

2. The origins of the electrocatalytic effects

Various workers have proposed different mechanisms to account for the electrocatalytic effects of metal ad-atoms. Examination of these various mechanisms suggest that each one has a logical basis and could be valid for different groups of metal ad-atoms.

a. The third-body effect This model has its basis in the speculation that the strongly adsorbed poisons are formed by the dimerization of intermediate species, e.g., $(\cdot COOH)_{ad}$, adsorbed at adjacent sites on the surface of the electrode. The metal ad-atoms are proposed to be deposited on the substrate metal in such a way as to occupy alternate sites on the surface of the electrode. With such an arrangement, the active intermediate species cannot get close enough to undergo the dimerization reaction to form the poisons. Adzic et al. (67, 85, 88), Motoo and Watanabe (89), and Angerstein-Koglowska et al. (64) have concluded that this mechanism is operative for the heavy-metal ad-atoms Hg, Bi, Pb, Tl and Cd, which are referred to as the "third bodies". This model cannot fully explain why some metals act as "third bodies" to decrease the formation of poisons and other metals do not. The model does not explain the differences observed in the catalytic effects of different metals.

b. The suppression of hydrogen adsorption This model was proposed by Spasojevic et al. (66) for the oxidation of HCOOH. According to the model, the poisons are formed via the interaction between surface-adsorbed •H and •COOH radicals (see Equations II-23 and II-24). The metal ad-atoms inhibit the adsorption of H-atoms through site exclusion and thereby reduce the extent of interaction between $(\bullet H)_{ad}$ and $(\bullet COOH)_{ad}$. This, in turn, leads to a decrease in the amount of poisons formed.

c. The bi-functional mechanism Motoo and Watanabe (100) proposed this theory to explain the enhancement effects observed for a group of metal ad-atoms in the oxidation of CH_3OH, HCHO and CO on Pt. According to this model, an oxygen atom, or an oxygen-containing species such as a •OH radical, is adsorbed on a metal ad-atom, while the organic radical is adsorbed on a neighboring noble-metal site. Assuming that the ad-atoms are distributed uniformly on the electrode surface, the adsorbed organic radicals can then be oxidized by the oxygen species while the two are in close proximity. This theory has been applied to Sn, Ge, As and Ru ad-atoms (100, 101, 102, 103, 104, 105). Koch et al. (101) derived a mathematical expression that was used to relate the catalytic currents to the free energy of adsorption of oxygen on the metal ad-atoms.

$$i = K Z a_A^{1/2} \exp(-\Delta\bar{G}_o^o/4RT + F\phi/RT) \qquad \text{(II-27)}$$

where i = current

K = constant

Z = parameter to account for the reaction zone being between 2 phases

a_A = activity of the dissolved organic compounds

$\Delta\bar{G}_O^o$ = free energy of adsorption of oxygen

ϕ = electrode potential

R, T and F have the usual meanings.

From this expression, they were able to predict the catalytic activities of various metal ad-atoms for the electrochemical oxidation of HCHO and found good agreement with experimental results. According to this model, a metal ad-atom will act as a catalyst if oxygen is adsorbed by the ad-atoms at potentials more negative than by the substrate, and if the reactant is not adsorbed on the ad-atoms.

III. ELECTROCHEMICAL OXIDATION OF FORMIC ACID ON A PLATINUM ELECTRODE IN ACIDIC MEDIA: THE EFFECTS OF VARIOUS METAL AD-ATOMS

A. Introduction

Cyclic voltammetry was used to study the effects of various metal ad-atoms on the electrochemical oxidation of HCOOH on a Pt rotating disc electrode (Pt-RDE) in 0.10 M or 0.50 M H_2SO_4. Two procedures were used to control and vary the fractional coverage (θ_M) of the electrode surface with respect to the metal ad-atoms. The first procedure, designated as Procedure A, involved the electrodeposition of the metal ad-atoms at a constant potential (E_{dep}) for different values of deposition time (T_{dep}) in a solution of a fixed concentration of the corresponding metal ions. The second procedure, designated as Procedure B, involved the standard addition of a stock solution of the metal ions to the solutions under study while the potential of the electrode was caused to scan in a cyclic fashion until a reproducible θ_M was achieved. Procedure B was found to be preferable because of the ease with which θ_M could be varied without the necessity of manual interruption of the applied potential waveform. Based on the experimental observations, conclusions were made as to whether the metal ad-atoms act as catalysts, i.e., the reactions are made more reversible, or whether the metal ad-atoms act as so-called "third bodies" to prevent the formation of the poisoning species, thereby enhancing the peak current (I_p) for the anodic reactions without affecting the reversibility of the reactions.

B. Experimental

The three-electrode potentiostat was a RDE-3 from Pine Instrument Co., Grove City, PA. The rotator was a Pine Instrument PIR. The Pt-RDE, with an area of 0.43 cm^2, was also from Pine Instrument Co. The reference electrode was a saturated calomel electrode (SCE) from Corning Scientific Instruments. The counter electrode was a 24-gauge Pt wire 5 inches in length, 3 inches of which was usually submerged in the electrolyte solution. Current-potential (I-E) curves were recorded on a Hewlett Packard 7035B x-y recorder. The electrochemical cell was a conventional three-compartment cell which provided separation of the working, reference and counter electrodes. This cell was also equipped with connections to a nitrogen cylinder for deareation of the solution. The equipment used has been described in detail elsewhere (108).

Solutions of the supporting electrolyte were prepared by dilution of reagent-grade concentrated H_2SO_4 to 0.10 M or 0.50 M with triply distilled water. Stock solutions, each containing 1.000×10^{-3} M Hg(I), Ag(I), Tl(I), Pb(II), Bi(III) or Cu(II), were prepared by dissolving the corresponding nitrates in triply distilled water and diluting to the mark in volumetric flasks. A 1.000×10^{-3} M stock solution of Cd(II) was prepared from $3CdSO_4 \cdot 8H_2O$ in the same manner. Solutions (0.25 M) of HCOOH in 0.10 M or 0.50 M H_2SO_4 were prepared by direction addition of concentrated, reagent-grade HCOOH (19.7 M) to the supporting electrolyte.

All electrolyte solutions were deaerated by dispersing N_2 through them prior to the recording of the I-E curves. During the recording

of the I-E curves, a blanket of N_2 was maintained above the electrolyte solution to prevent the back diffusion of O_2 into the electrolyte solution.

The daily start-up procedure involved the conditioning of the surface of the Pt-RDE by continuous cycling of the electrode potential at a rate of 6 V min^{-1} while the rotating electrode was immersed in the supporting electrolyte. The cycling of the electrode potential was continued until consecutive I-E curves were reproducible. The reproducibility of the I-E curves was an indication that the surface of the electrode had been cleaned of adsorbed impurities and had reached a reproducible state of electrochemical activity. Changes in the I-E curves of an electrode preconditioned in this manner were taken to reflect only the electrochemical behavior of the electroactive species introduced into the cell. All I-E curves were recorded at the ambient temperature (22-27°C).

C. Effects of Electrodeposited Cd, Pb, Hg, Bi, Tl, Ag and Cu on the Electrochemical Oxidation of 0.25 M HCOOH on the Pt-RDE in H_2SO_4

1. Solubility of heavy-metal sulfates in 0.10 M and 0.50 M H_2SO_4

There was some concern that several of the heavy-metal ions to be studied would precipitate as their corresponding sulfates in the supporting electrolyte. Solubility data (109) revealed that the sulfates of Pb(II), Hg(I), Ag(I) and Tl(I) are only slightly soluble salts. Therefore, calculations of solubility were performed to

determine the maximum concentrations of the metal ions permissible in 0.10 M and 0.50 M H_2SO_4 without causing precipitation. The concentrations of SO_4^{2-} in 0.10 M and 0.50 M H_2SO_4 were estimated on the basis of the acid dissociation constants for H_2SO_4 to be 9.85×10^{-3} M and 1.13×10^{-2} M, respectively. These values of concentration were used, together with the solubility product constants (k_{sp}) of the individual metal sulfates, to calculate the maximum permissible concentrations of the corresponding metal ions. All activity coefficients were taken to be unity. The results of these calculations were tabulated in Table III-1. Care was taken in the experiments to ensure that the amount of metal ions added to the solutions under study would not lead to formation of the insoluble sulfates.

Table III-1. Maximum permissible concentration ($[M(n)]_{max}$) of selected heavy-metal ions in 0.10 M and 0.50 M H_2SO_4

Metal ion M(n)	$[M(n)]_{max}$ in 0.10 M H_2SO_4 (M)	$[M(n)]_{max}$ in 0.50 M H_2SO_4 (M)
Hg(I)	8.5×10^{-4}	7.9×10^{-4}
Ag(I)	4.9×10^{-4}	4.6×10^{-4}
Tl(I)	6.0×10^{-1}	5.6×10^{-1}
Cd(II)	VNR[a]	VNR
Pb(II)	2.0×10^{-6}	1.8×10^{-6}
Bi(III)	VNR	VNR

[a]VNR - virtually no restriction.

2. Cyclic voltammetry at a Pt-RDE in 0.10 M H_2SO_4

The I-E curves for the Pt-RDE, recorded at various rates of potential scan (ϕ), are shown in Figure III-1. When the potential of the electrode is scanned in a positive direction from the initial value of 0.0V vs. SCE, virtually no current is observed until the potential of the electrode has reached 0.5V vs. SCE. At potentials more positive than 0.5V vs. SCE, the surface of the Pt-RDE is oxidized to Pt oxide (PtO) with concomitant flow of anodic current. The process of forming PtO proceeds at a relatively constant rate during the positive scan of the electrode potential in the region of E > 0.6V, as reflected by the plateau on the anodic curve. The applied potential is sufficiently high at 1.3V vs. SCE so that H_2O is oxidized to produce O_2 and the anodic current increases rapidly. Following reversal of the potential scan at 1.3V, the current is observed to drop almost immediately to zero since the driving force for the formation of additional oxide no longer exists. The potential of the electrode is not high enough for E < 0.8V vs. SCE to maintain the PtO and a cathodic peak is observed for reduction of PtO to Pt. Two overlapping peaks are observed on the negative scan for E < 0.0V vs. SCE. These result from the reduction of H^+ to produce surface-adsorbed H-atoms. The H^+ ions in the acidic solution are rapidly reduced to H_2 at -0.3V vs. SCE and the cathodic current increases dramatically as the potential of the electrode is further decreased. Two overlapping anodic peaks are observed upon reversal of the potential scan to the positive direction.

Figure III-1. I-E curve of the Pt-RDE in 0.10 M H_2SO_4

Electrode rotation speed (W): 400 rev min^{-1}

Potential scan rate (ϕ): ——— 2 V min^{-1}

····· 4 V min^{-1}

------- 6 V min^{-1}

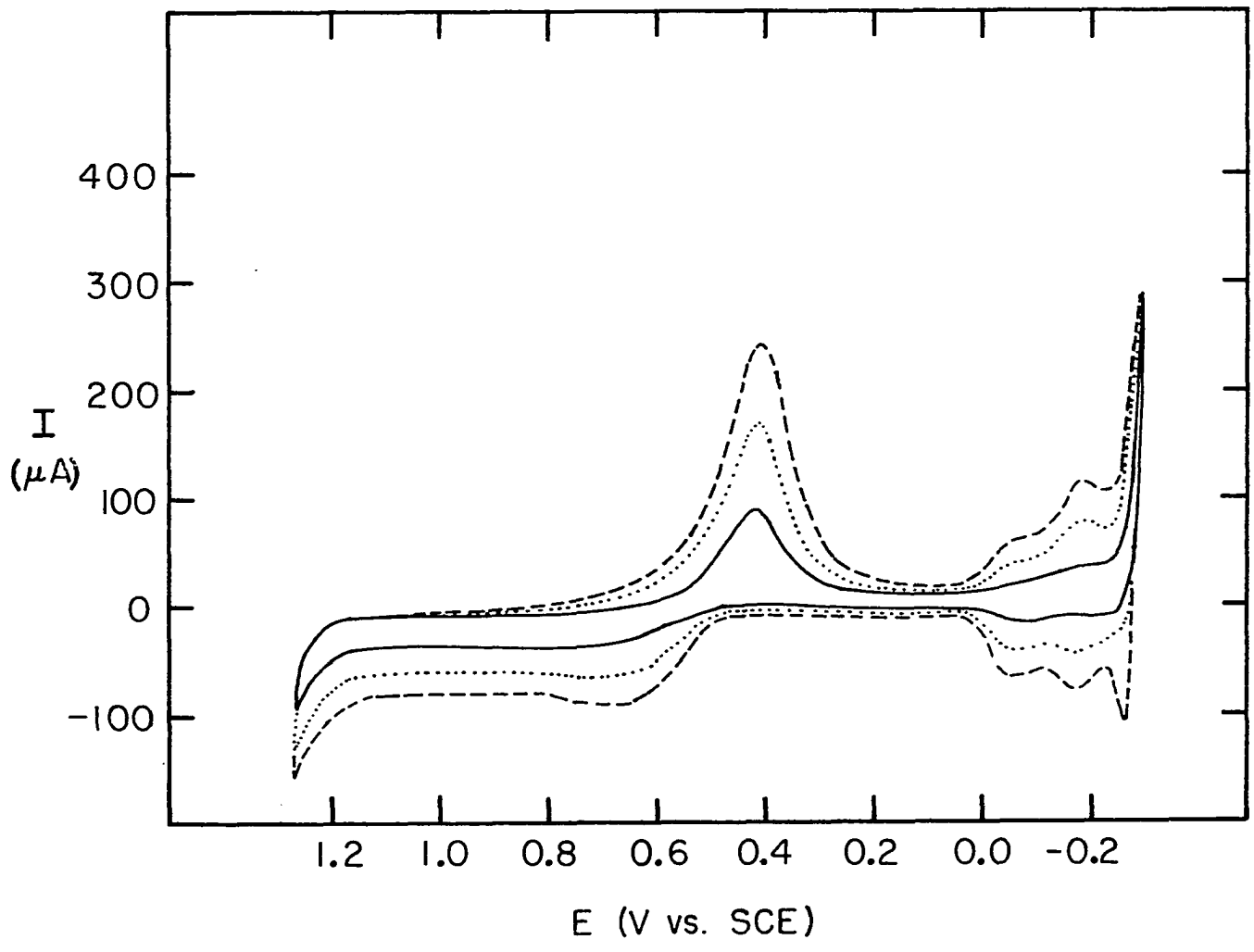
400
300
200
100
0
-100
I
(μA)
1.2
1.0
0.8
0.6
0.4
0.2
0.0
-0.2
E (V vs. SCE)

These peaks are associated with the oxidation and desorption of the adsorbed H-atoms.

The currents associated with all the electrochemical processes described above, except for the production of O_2 and H_2, are directly proportional to ϕ, as shown in Figure III-1. This is expected for surface-controlled electrochemical processes. A mass-transport controlled process, on the other hand, is not sensitive to changes in ϕ but is affected rather by the rate of stirring of the solution containing the electroactive species. The rate of mass transport at the surface of a RDE can be conveniently increased by increasing the rotation speed (W) of the electrode.

The I-E curves obtained for 0.25 M HCOOH in 0.10 M H_2SO_4 are displayed in Figures III-2 and III-3. In Figure III-2, the curves were recorded at a single value of w while ϕ was varied. Peaks A, B and C are observed on the positive scan with values of peak potential (E_p) equal to 0.25V, 0.60V and 1.20V vs. SCE, respectively. Peak D is observed on the negative scan with E_p equal to 0.4V vs. SCE. The values of peak current (I_p) for Peaks C and D are directly proportional to ϕ. E_p of Peak A is not significantly affected while the value for Peak B is shifted positive by about 50 mV when ϕ is increased from 1.0 to 6.0 V min^{-1}. I_p values for Peaks A and B are not affected by changes in ϕ.

Peaks A and D, although drastically different in their I_p values, may actually represent the same electrochemical process. This may be best understood by following the I-E curves through one cycle of the

Figure III-2. I-E curves of the Pt-RDE in a solution of 0.10 M H_2SO_4 and 0.25 M HCOOH

Electrode rotation speed (W): 400 rev min^{-1}

A, B, C and D: anodic peaks

Potential scan rate (ϕ): ——— 2 V min^{-1}

····· 4 V min^{-1}

- - - - - - - 6 V min^{-1}

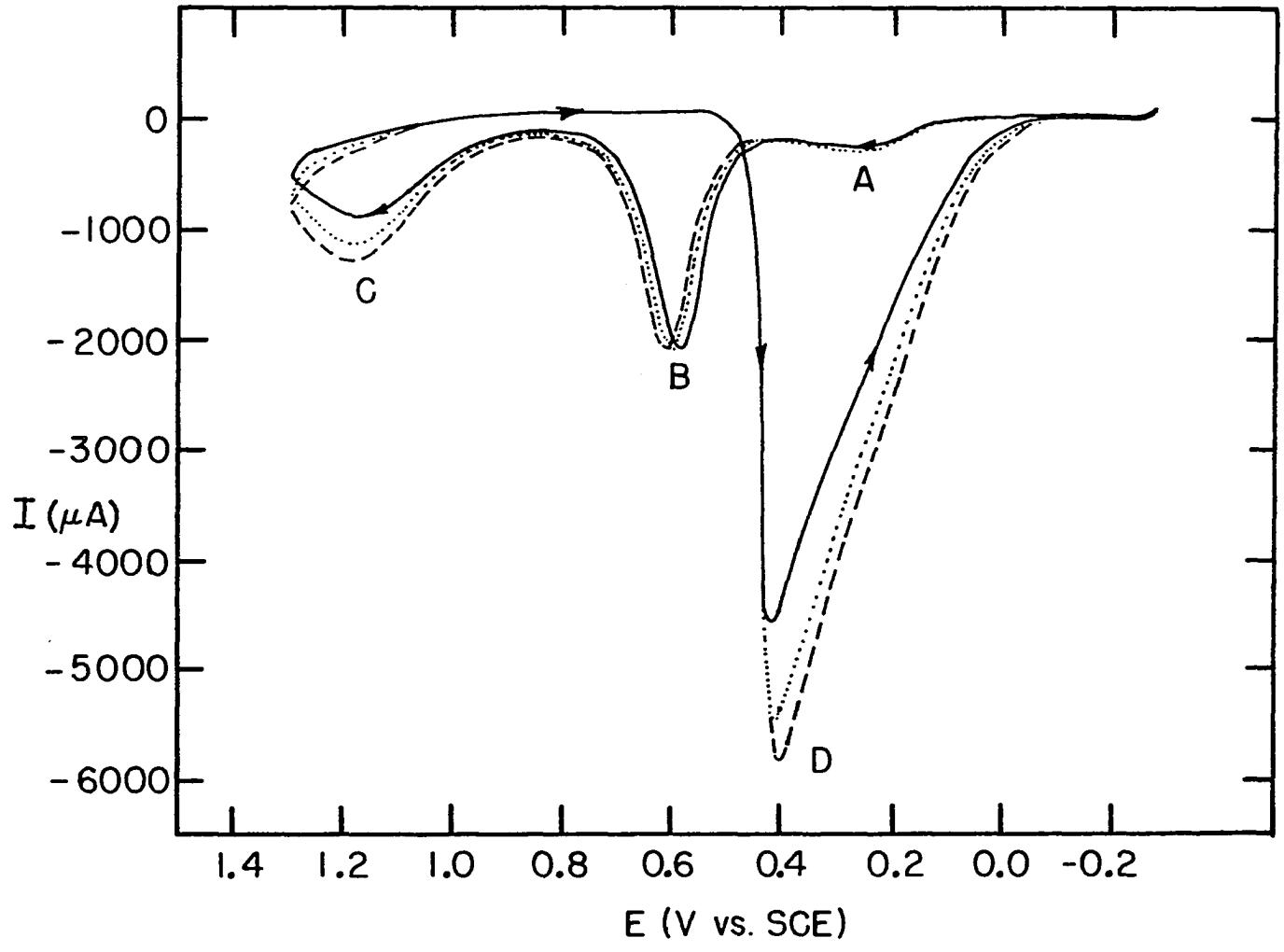
0
-1000
-2000
-3000
I (μA)
-4000
-5000
-6000
A
B
C
D
1.4
1.2
1.0
0.8
0.6
0.4
0.2
0.0
-0.2
E (V vs. SCE)

Figure III-3. I-E curves of the Pt-RDE in a solution of 0.25 M HCOOH and 0.10 M H_2SO_4

Potential scan rate (ϕ): 4 V min^{-1}

A, B, C and D: anodic peaks

Electrode rotation speed (W): ------- 0 rev min^{-1}

····· 2500 rev min^{-1}

——— 4900 rev min^{-1}

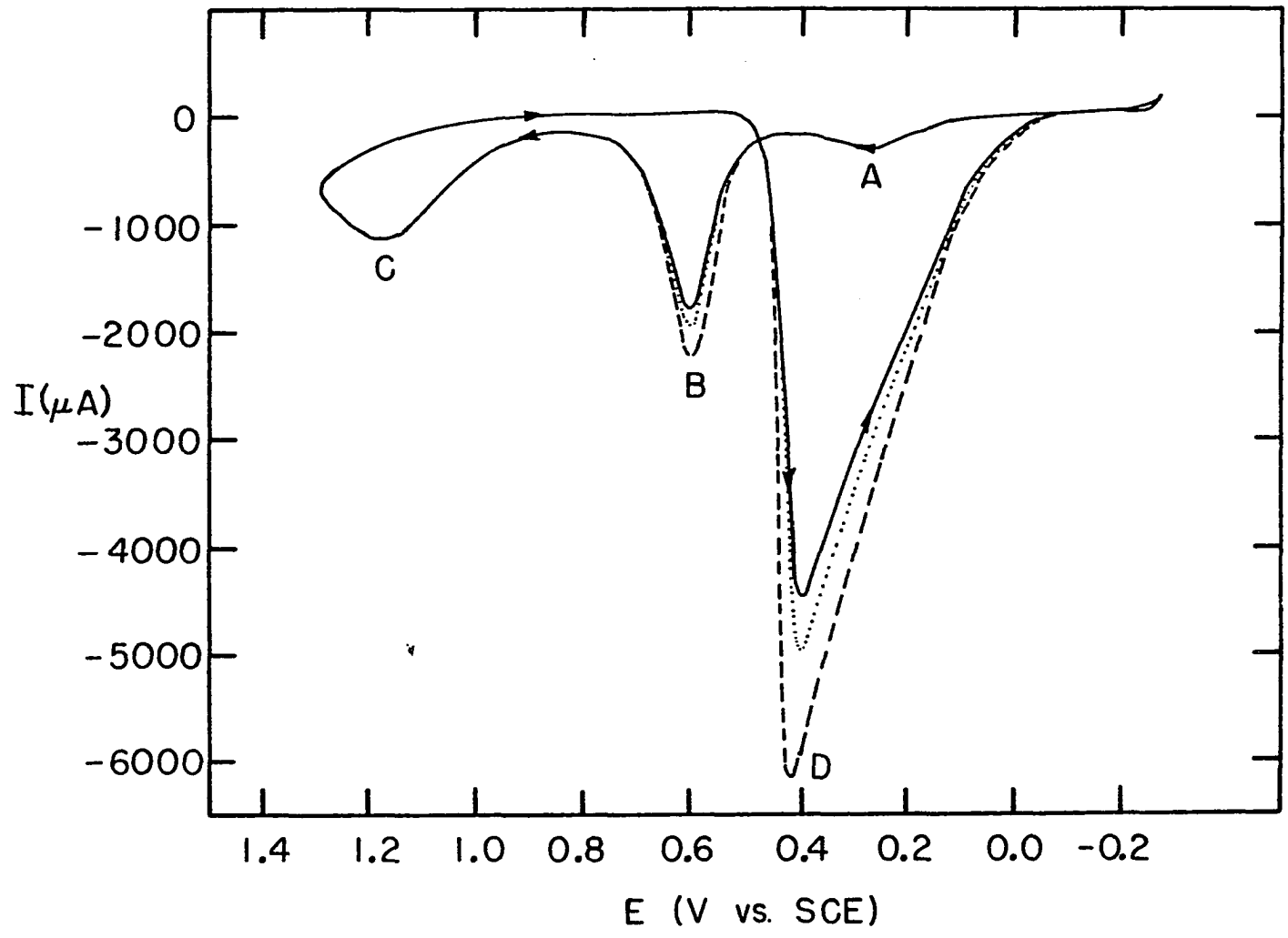
0
-1000
-2000
-3000
-4000
-5000
-6000
I(μA)
A
B
C
D
1.4
1.2
1.0
0.8
0.6
0.4
0.2
0.0
-0.2
E (V vs. SCE)

potential scan starting at 0.0V vs. SCE. The surface of the electrode is severely poisoned at 0.0V and the poisoning species is not removed from the surface of the electrode until the potential of the electrode is scanned to a region where the Pt is oxidized to PtO. The relatively small anodic current for Peak A obtained during positive potential scan indicates that, although the electrode is severely poisoned, a small fraction of the surface is not covered by the poisoning species and the main oxidation pathway of HCOOH is operative on the clean Pt sites. Peaks B and C, also obtained during the positive potential scan, but in the potential region where the surface of the electrode is covered by oxide, is attributed to the oxidation and removal of the poisoning species from the electrode surface. Hence, the surface of the electrode is free from poisons for E = 1.3V vs. SCE. However, the current is observed to drop to zero upon reversal of the direction of potential scan. Examination of the residual I-E curves of the Pt-RDE shown in Figure III-1 reveals that the surface of the Pt-RDE is covered by oxide at electrode potentials more positive than 0.5V vs. SCE and is, therefore, not active for the oxidation of HCOOH. The active Pt surface is regenerated as soon as the oxide is reduced at E < 0.5V vs. SCE on the negative scan. On the newly regenerated, clean Pt sites, the adsorption and oxidation of HCOOH commences, giving rise to a large anodic peak, Peak D. The fall-off of the anodic current for E < 0.4V vs. SCE is attributed to the combination of two factors. First, the potential-dependent heterogeneous rate-constant of the oxidation reaction is decreased as the potential of the electrode is

decreased, i.e., $E < E^{\circ}$. Secondly, the poison species are formed and begin to accumulate on the surface of the electrode concurrently with the main oxidation process. The surface of the electrode may be almost totally covered by the poison during the negative scan when the value of E reaches -0.1V vs. SCE. At this point, the anodic current will have falled to zero because of the poisoning phenomenon, irrespective of the potential dependency of the heterogeneous rate constant. It can be speculated, based on the foregoing discussion, that both Peaks A and D are associated with the main oxidation process of HCOOH and the difference in the peak currents of the two peaks is due only to the difference in the number of clean Pt sites available.

The I-E curves shown in Figure III-3 were recorded as a function of W for a constant value of ϕ. The peak currents for Peaks B and D decrease with increases in W, but the peak currents for Peaks A and C are not affected by changes in W. The simple mass-transport limited reaction of an electroactive species at a RDE is predicted to increase rather than decrease as a linear function of $W^{1/2}$. The following mechanism is proposed to qualitatively explain the inverse dependence of the anodic currents for Peak D on W.

$$(HCOOH)_{soln} \xrightarrow{Pt} (HCOOH)_{ad} \qquad \text{(fast)} \qquad \text{(III-1)}$$

$$(HCOOH)_{ad} \longrightarrow (\cdot H)_{ad} + (\cdot COOH)_{ad} \qquad \text{(fast)} \qquad \text{(III-2)}$$

$$(\cdot COOH)_{ad} + (HCOOH)_{ad} \rightleftharpoons (\vdots COH)_{ad} + CO_2 + H_2O \qquad \text{(slow)} \qquad \text{(III-3)}$$

$$(\cdot COOH)_{ad} \longrightarrow CO_2 + H^+ + e^- \qquad \text{(slow)} \qquad \text{(III-4)}$$

$$(\cdot H)_{ad} + e^- \longrightarrow H^+ \qquad \text{(fast)} \qquad \text{(III-5)}$$

The anodic current observed before significant fouling has occurred is due to the electrochemical processes described by Equations III-4 and III-5, which occur repeatedly on the clean Pt sites. The nonelectrochemical process, described by Equation III-3, leads to the poisoning of the electrode by $(\vdots COH)_{ad}$ which is attached to three adjacent active sites on the Pt substrate (41) and which is not further oxidized in the potential region of Peak D. The presence of $(\vdots COH)_{ad}$ decreases the total number of active sites on the electrode surface at which the electrochemical reactions described by Equations III-4 and III-5 may occur. The rate of formation of $(\vdots COH)_{ad}$ is limited by the rate of mass transport of CO_2 away from the electrode surface, as indicated by Equation III-3. The rate of this process is directly proportional to $W^{1/2}$ and hence the rate of formation of $(\vdots COH)_{ad}$ is also proportional to $W^{1/2}$. The anodic current observed, which depends on the total number of Pt sites not covered by $(\vdots COH)_{ad}$ is decreased at higher values of W because of the consequential increase in the rate of formation of the poison. This gives rise to the experimentally observed inverse dependence of $I_{p,D}$ on $W^{1/2}$. A plot of $I_{p,D}$ vs. $W^{1/2}$ is shown in Figure III-4. A straight line with a slope of -23.2 μA $rev^{-1/2}$ $min^{1/2}$ is obtained.

3. Effects of metal ad-atoms on the electrochemical oxidation of 0.25 M HCOOH on the Pt-RDE in 0.10 M H_2SO_4: ad-atoms deposited by Procedure A

Procedure A (see section III.A) was used to electrochemically deposit the metal ad-atoms onto the Pt-RDE. The metal ions were added

Figure III-4. Dependence of the peak current of Peak D (negative potential scan) on the rotation speed of the Pt-RDE

Supporting electrolyte: 0.10 M H_2SO_4

Electroactive species: 0.25 M HCOOH

Potential scan rate (ϕ): 6 V min^{-1}

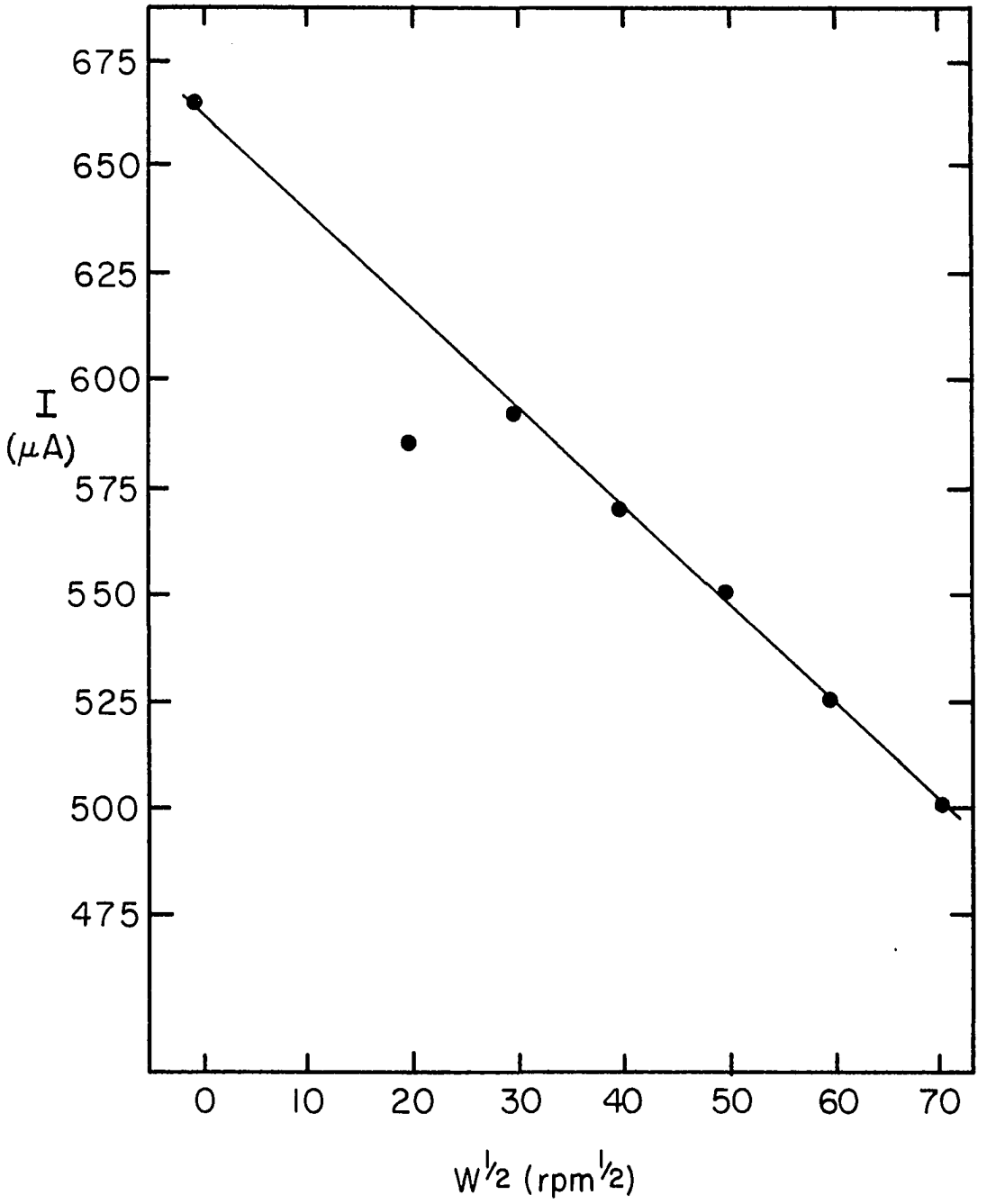
675
650
625
600
575
550
525
500
475
I
(μA)
0
10
20
30
40
50
60
70
W^1/2 (rpm^1/2)

to the solution under study while the potential of the electrode was scanned continuously in a cyclic manner. When E reached 1.3V vs. SCE on the positive sweep, the value was stepped to 0.0V or -0.2V. The potential was then held at 0.0V or -0.2V vs. SCE for varying amounts of time, T_{dep}, during which the electrodeposition of the metal ad-atoms occurred. Upon the expiration of T_{dep}, the scanning of the potential was resumed in a positive direction and the I-E curves recorded. The programming of the electrode potential in this manner was performed in order that the fouling of the electrode by the poisons do not occur extensively prior to or during the electrodeposition of the metal ad-atoms. I-E curves were recorded by this procedure for the supporting electrolyte and for the supporting electrolyte containing HCOOH. These I-E curves were then compared to those recorded in the presence of the metal ad-atoms so that characterizations of the effects of the ad-atoms could be made.

a. Cd ad-atoms The I-E curve of the Pt-RDE obtained in the absence and presence of 1.00×10^{-5} M Cd(II) are shown in Figure III-5. Two anodic peaks of interest, A' and B', are observed during the positive scan in the region from 0.0V to 0.4V vs. SCE when T_{dep} is 2 min or more. Only one peak, B', is observed for T_{dep} equal to 0 min. The reversible potential for the electrochemical reduction of Cd(II) to Cd(0), $E^{\circ}_{Cd(II)/Cd(0)}$, is -0.65V vs. SCE (110). Hence, Peaks A' and B', with E_p more positive than $E^{\circ}_{Cd(II)/Cd(0)}$, are concluded to be associated with the electrochemical oxidation (stripping) of Cd ad-atoms deposited at underpotential. Under experimental conditions that restrict the

Figure III-5. I-E curves for the deposition of Cd ad-atoms on the Pt-RDE in 0.10 M H_2SO_4

Electrode rotation speed (W): 400 rev min^{-1}

Potential scan rate (ϕ): 6 V min^{-1}

Deposition potential (E_{dep}): 0.0V *vs.* SCE

A' and B': stripping peaks

——— Cd(II) absent, T_{dep} = 0 sec

····· 1.00 x 10^{-5} M Cd(II), T_{dep} = 0 sec

------- 1.00 x 10^{-5} M Cd(II), T_{dep} = 120 sec

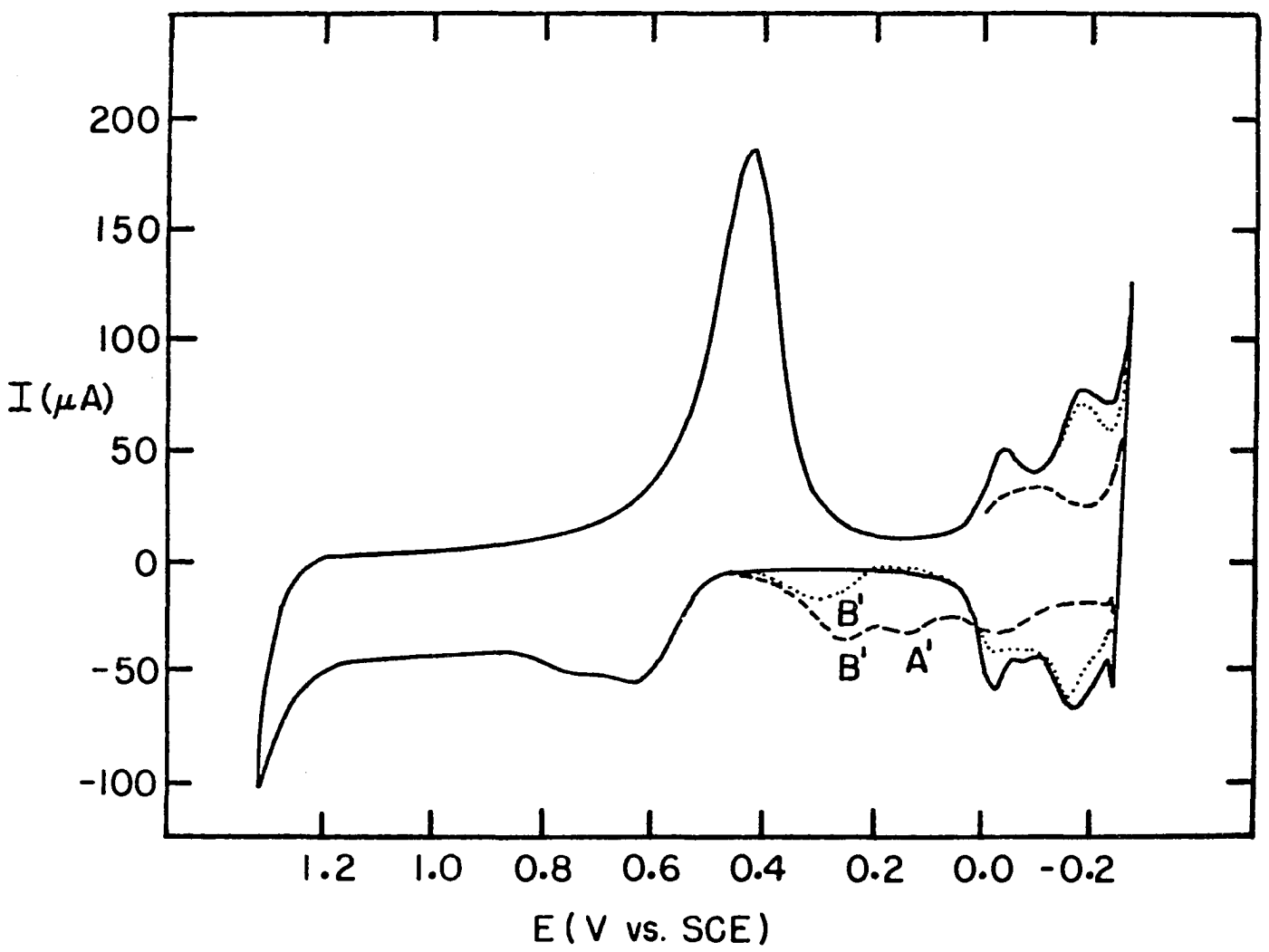
200
150
100
I (μA)
50
0
-50
-100
B'
B'
A'
1.2
1.0
0.8
0.6
0.4
0.2
0.0
-0.2
E (V vs. SCE)

amount of Cd ad-atoms deposited, such as low Cd(II) concentration and/or short T_{dep}, only Peak B' is observed, indicating that the surface of the electrode is partially covered by Cd ad-atoms deposited in a single state, perhaps as isolated ad-atoms. At higher concentrations of Cd(II) and/or longer T_{dep}, dual peaks, A' and B', are obtained indicating the deposition of the Cd ad-atoms in more than one state, perhaps as isolated ad-atoms with no Cd-Cd interactions as well as aggregates of the ad-atoms. It is assumed that underpotential deposition occurs for only the deposition of a monolayer of Cd, for which strong Pt-Cd interaction is possible. Therefore, at a potential of 0.20V vs. SCE, the electrode surface is concluded to be covered by the equivalent of approximately 0.5 monolayer of ad-atoms. According to the models of electrocatalysis proposed by various workers (see Section II, C.2), Cd and Pt sites must co-exist for the Cd-ad-atoms to exert catalytic effects. It is apparent from the foregoing discussion that such a condition exists only for $0.2V < E < 0.4V$. Therefore, it is expected that the catalytic effects of the Cd ad-atoms will be greatest in this potential region.

Another feature of Figure III-5 warrants notice. The hydrogen adsorption and desorption peaks, in the region from 0.0V to -0.2V vs. SCE, are decreased somewhat when Cd(II) is added to the supporting electrolyte. This is due to the fact that the Cd ad-atoms block some of the Pt sites on the surface of the electrode, thereby decreasing the number of Pt sites on which the adsorption of H-atoms can take place. As T_{dep} is increased from 0 to 2 min, a further decrease in the peak

heights of the hydrogen adsorption and desorption peaks is observed, together with an increase in the peak height of Peak B' and the appearance of Peak A'. This indicates that more Cd ad-atoms are deposited as T_{dep} is increased. Deposition times of more than 2 min do not result in an increase in the amount of Cd ad-atoms deposited at underpotential under the experimental conditions employed.

The I-E curves of the Pt-RDE in a solution of 0.10 M H_2SO_4 containing 0.25 M HCOOH in the absence and presence of 2.00×10^{-4} M Cd(II) are shown in Figure III-6. The I-E curve obtained for the electrochemical oxidation of HCOOH is altered quite dramatically by the Cd ad-atoms. The height of the Peak A obtained during the positive scan is increased 5X by the presence of the Cd ad-atoms. Peak D obtained on the negative scan is suppressed about 13% by the Cd ad-atoms, but this is compensated by the appearance of the new peak, E. Perhaps the enhancement effects of the Cd ad-atoms is most dramatically demonstrated by Peak E. The onset of Peak E at 0.3V *vs.* SCE is in the potential region where a submonolayer of Cd ad-atoms is formed on the surface of the Pt-RDE, as demonstrated by the presence of Peaks A' and B' in Figure III-5 (see previous discussion on the electrodeposition of Cd ad-atoms).

$I_{p,D}$ shows a negative dependence on $W^{1/2}$ in the presence of the Cd ad-atoms, just as is observed in the absence of the ad-atoms. However, in the presence of the Cd ad-atoms, this negative dependence of $I_{p,D}$ on $W^{1/2}$ is much less than in the absence of the ad-atoms. The slope of a plot of $I_{p,D}$ *vs.* $W^{1/2}$ is only -2.0 μA $rev^{-1/2}$ $min^{1/2}$ in the presence of

Figure III-6. I-E curves of the Pt-RDE in a solution of 0.25 M HCOOH and 0.10 M H_2SO_4 in the absence and presence of Cd(II)

Electrode rotation speed (W): 400 rev min^{-1}

Potential scan rate (ϕ): 6 V min^{-1}

Deposition potential (E_{dep}): -0.2V vs SCE

Deposition time (T_{dep}): 30 sec

A, B, C, D and E: anodic peaks

——— 0.00 M Cd(II)

------- 2.00×10^{-4} M Cd(II)

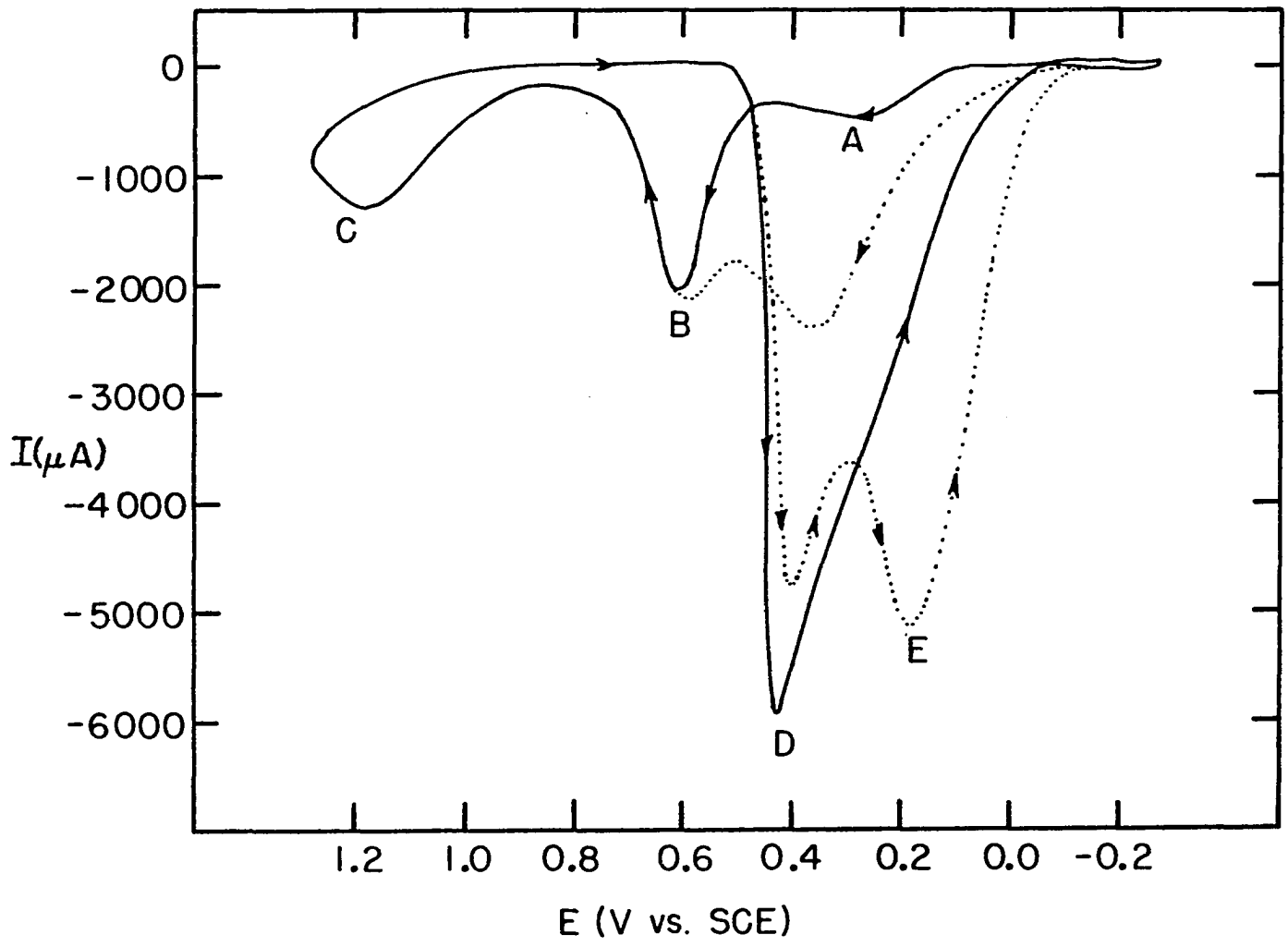
0
-1000
-2000
-3000
I(μA)
-4000
-5000
-6000
A
B
C
D
E
1.2
1.0
0.8
0.6
0.4
0.2
0.0
-0.2
E (V vs. SCE)

the Cd ad-atoms, vs. -23.2 μA $rev^{-1/2}$ $min^{1/2}$ in the absence of the ad-atoms. This illustrates that the Cd ad-atoms effectively decrease the formation of poisons as described by the mechanisms in Equations III-1 to III-3.

It is demonstrated in Figure III-6 that the presence of Cd(II) in the solution has no effect on Peaks B and C because these peaks appear in a region of potential for which no Cd ad-atoms remain on the electrode surface.

b. Pb ad-atoms The I-E curves for the Pt-RDE in the presence of 9 μM Pb(II) in 0.10 M H_2SO_4 are shown in Figure III-7. The reversible potential for the reaction

$$Pb(II) + 2e \rightleftharpoons Pb(0) \qquad \text{(III-6)}$$

is -0.37V vs. SCE (110). The wave attributed to the stripping of the Pb ad-atoms is located in the region more positive than 0.4V vs. SCE. This is considerably greater than the potential for the stripping of the Cd ad-atoms and is interpreted as the result of the stronger interaction of Pt with Pb in comparison to Cd. Adzic et al. (67) have noted that the Cd-Pd interaction is also weak. Holding the electrode potential at 0.0V vs. SCE for extended periods of time increases the surface coverage of the Pt-RDE by the Pb ad-atoms. Wave W appears in addition to the other peaks and waves for $T_{dep} > 1$ min.

The effect of the Pb ad-atoms on the electrochemical oxidation of HCOOH is demonstrated in Figure III-8. The enhancement by the Pb ad-atoms is most noticeable in Peak A, which is obtained during positive

Figure III-7. I-E curves for the deposition of Pb ad-atoms on the Pt-RDE in 0.10 M H_2SO_4

Electrode rotation speed (W): 400 rev min^{-1}

Potential scan rate (ϕ): 6 V min^{-1}

Deposition potential (E_{dep}): 0.0V vs. SEC

[Pb(II)]: 9.000×10^{-6} M

W: stripping wave

——— T_{dep} = 0 sec

····· T_{dep} = 60 sec

------- T_{dep} = 180 sec

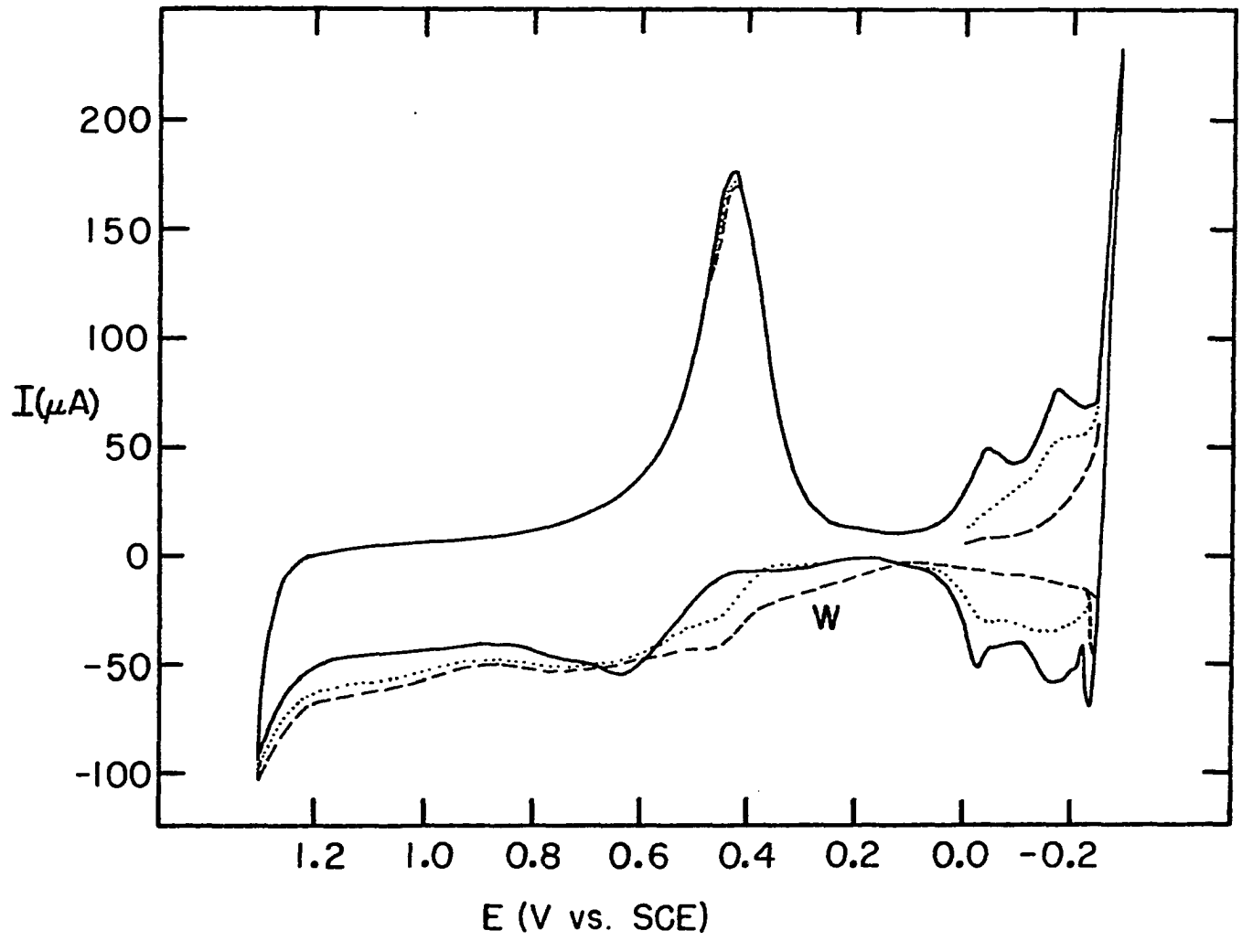
200
150
100
I(μA)
50
0
-50
-100
W
1.2
1.0
0.8
0.6
0.4
0.2
0.0
-0.2
E (V vs. SCE)

potential sweep. In the presence of the Pb ad-atoms, $I_{p,A}$ is increased 7.6X over that obtained for the case in which Pb ad-atoms are absent. When T_{dep} is increased from 0 to 30 sec, the enhancement of $I_{p,A}$ increases to 18.4X. The enhancement factor (EF), defined as the ratio of the catalyzed peak current to the uncatalyzed peak current, is decreased slightly for T_{dep} > 30 seconds. For example, EF is 16.8 with T_{dep} equal to 45 seconds. This is in contrast to the case of the Cd ad-atoms, where T_{dep} has no effect on EF. The catalyzed peak currents and EF increase with increases in W for small values of W, but decrease with increases in W for high values of W. This can be explained on the basis that the rate of deposition of the Pb ad-atoms increases with W, causing saturation of the electrode surface with respect to the ad-atoms at high values of W. Consequently, EF and the catalyzed peak-currents decrease slightly. The effects of W and T_{dep} on EF are shown in Table III-2 and Figures III-9 and III-10.

It is demonstrated in Figure III-8 that $I_{p,B}$ is also enhanced by the Pb ad-atoms, although the degree of enhancement is much less than that obtained for $I_{p,A}$. $I_{p,D}$ obtained during the negative potential scan is not affected by the Pb ad-atoms, but a slight shoulder on Peak D in the potential region between 0.2V and 0.4V *vs.* SCE observed in the presence of the ad-atoms is concluded to result from a slight increase in the rates of the electrochemical processes. This peak is also not affected in any way by increasing T_{dep}. This is understandable because, regardless of T_{dep}, all of the Pb ad-atoms deposited at -0.2V *vs.* SCE have been stripped from the surface of the electrode by the time E is

Figure III-8. I-E curves of the Pt-RDE in a solution of 0.25 M HCOOH and 0.10 M H_2SO_4 in the absence and presence of Pb(II)

Electrode rotation speed (W): 400 rev min^{-1}

Potential scan rate (ϕ): 6 V min^{-1}

Deposition potential (E_{dep}): -0.20V *vs.* SCE

A, B, C and D: anodic peaks

——— 0.00 Pb(II), T_{dep} = 0 sec

------- 1.00 x 10^{-5} M Pb(II), T_{dep} = 0 sec

····· 1.00 x 10^{-5} M Pb(II), T_{dep} = 30 sec

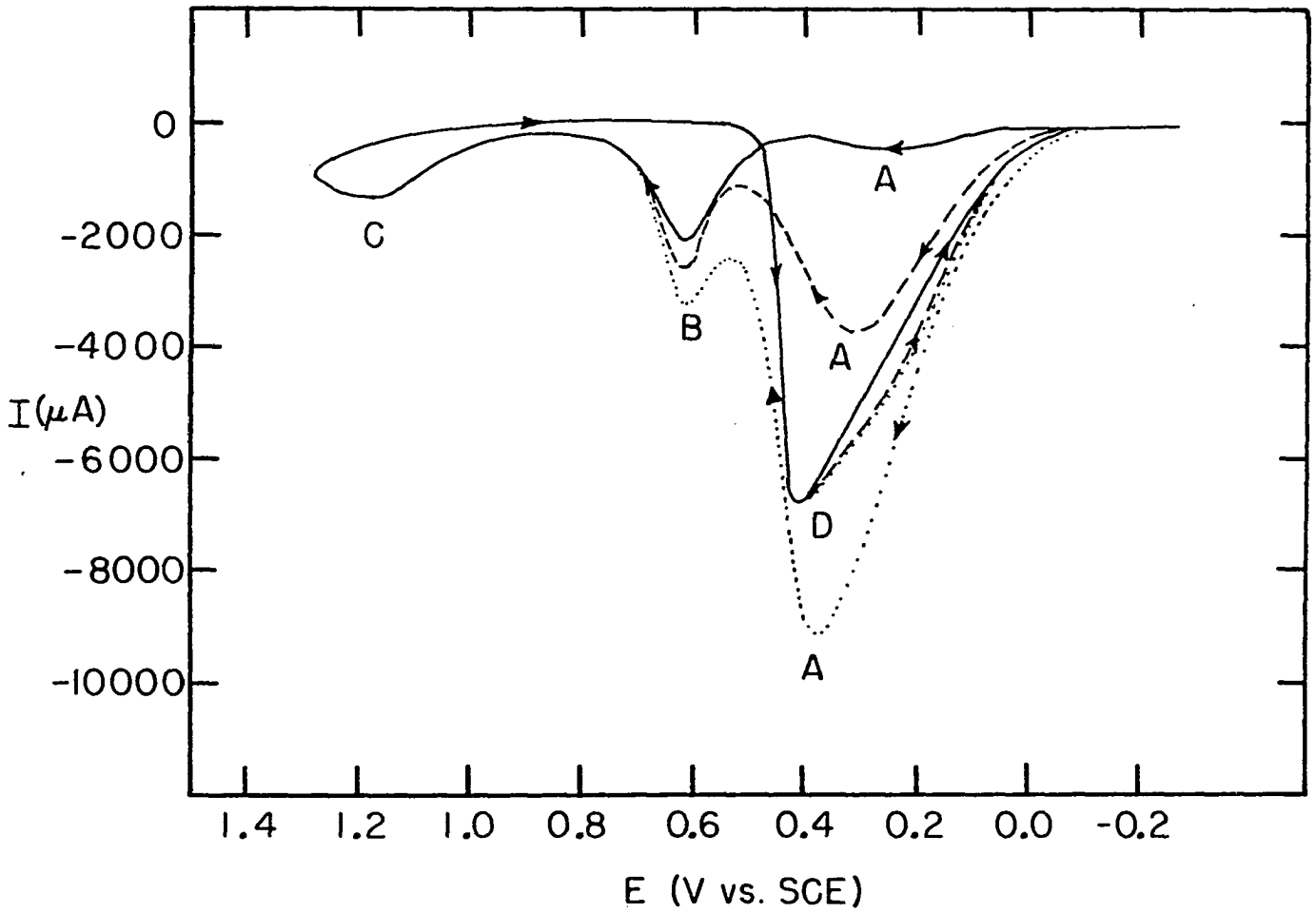
0
-2000
-4000
I(μA)
-6000
-8000
-10000
C
B
A
A
D
A
1.4
1.2
1.0
0.8
0.6
0.4
0.2
0.0
-0.2
E (V vs. SCE)

Table III-2. Dependence of the enhancement factor of Peak A (EF_A) (see Figure III-8) on $W^{1/2}$ and T_{dep}: obtained during the electrochemical oxidation of 0.25 M HCOOH on the Pt-RDE in the presence of 10.0 μM Pb(II) and 0.10 M H_2SO_4

$W^{1/2}$ ($rev^{-1/2}$ $min^{1/2}$)	T_{dep} (sec)	EF_A
20	0	7.6
	15	16.6
	30	18.4
	45	16.8
30	0	11.0
	15	20.4
	30	19.8
	45	19.6
40	0	13.2
	15	22.0
	30	21.8
	45	21.0
50	0	22.0
	15	22.0
	30	21.0
	45	20.5
60	0	14.4
	15	21.5
	30	20.6
	45	20.2

Figure III-9. Dependence of the enhancement factor (EF) of Peak A obtained during the electrochemical oxidation of HCOOH on the deposition time (T_{dep}) of Pb ad-atoms

[HCOOH]: 0.25 M

[Pb(II)]: 1.00×10^{-5} M

[H_2SO_4]: 0.10 M

Deposition potential (E_{dep}): -0.20V *vs.* SCE

Potential scan rate (ϕ): 6 V min^{-1}

Electrode: Pt-RDE

Electrode rotation speed (W): —●—●—●— 400 rev min^{-1}

—▲—▲—▲— 900 rev min^{-1}

—■—■—■— 1600 rev min^{-1}

—o—o—o— 2500 rev min^{-1}

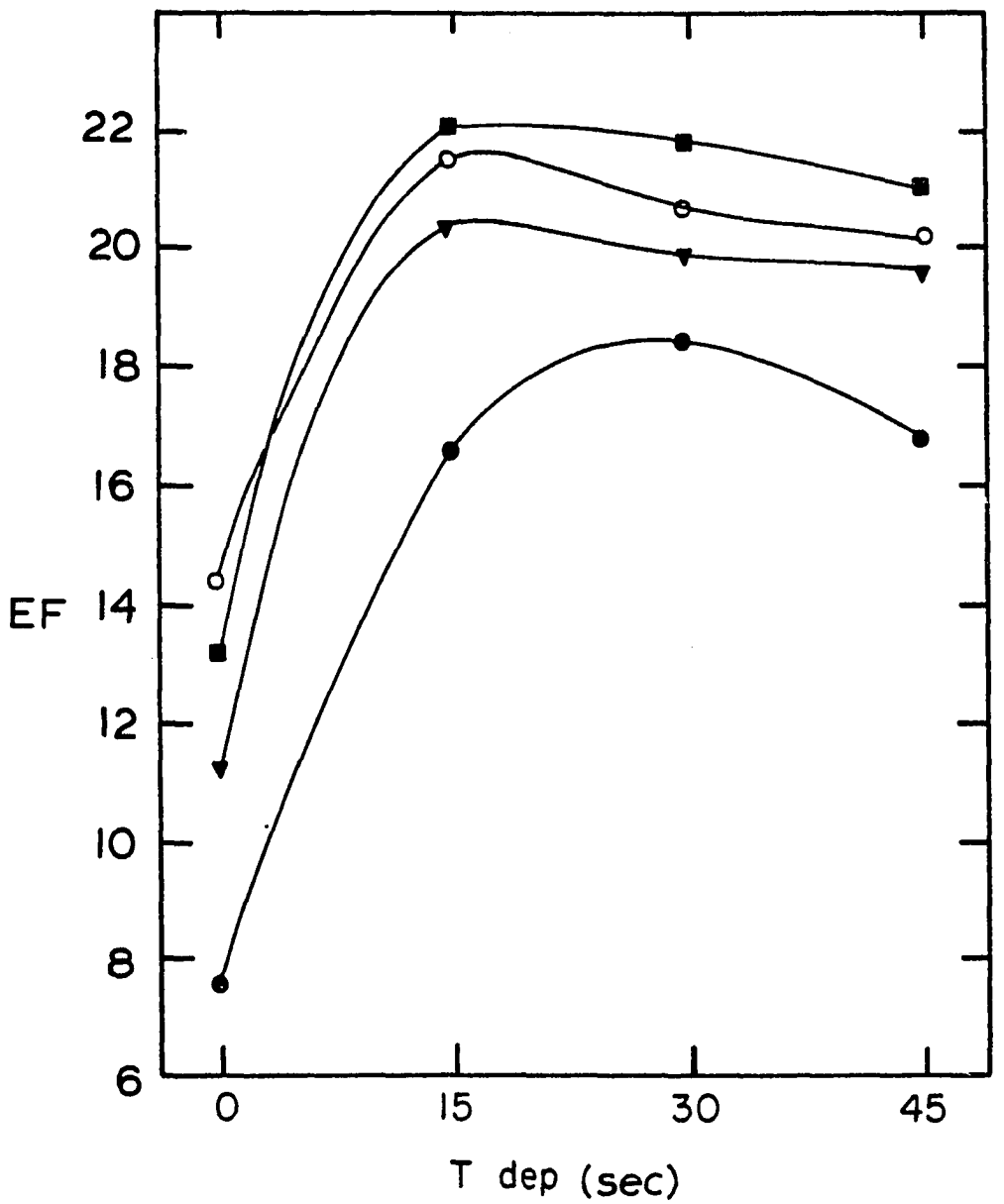
22
20
18
16
EF 14
12
10
8
6
0
15
30
45
T dep (sec)

Figure III-10. Dependence of enhancement factor (EF) of Peak A obtained during the electrochemical oxidation of HCOOH on the rotation speed (W) of the Pt-RDE

[HCOOH]: 0.25 M

[Pb(II)]: 1.000×10^{-5} M

$[H_2SO_4]$: 0.10 M

Potential scan rate (ϕ): 6 V min^{-1}

Deposition potential: -0.2V vs. SCE

—●—●—● T_{dep} = 0 sec

—▲—▲—▲ T_{dep} = 15 sec

—■—■—■ T_{dep} = 45 sec

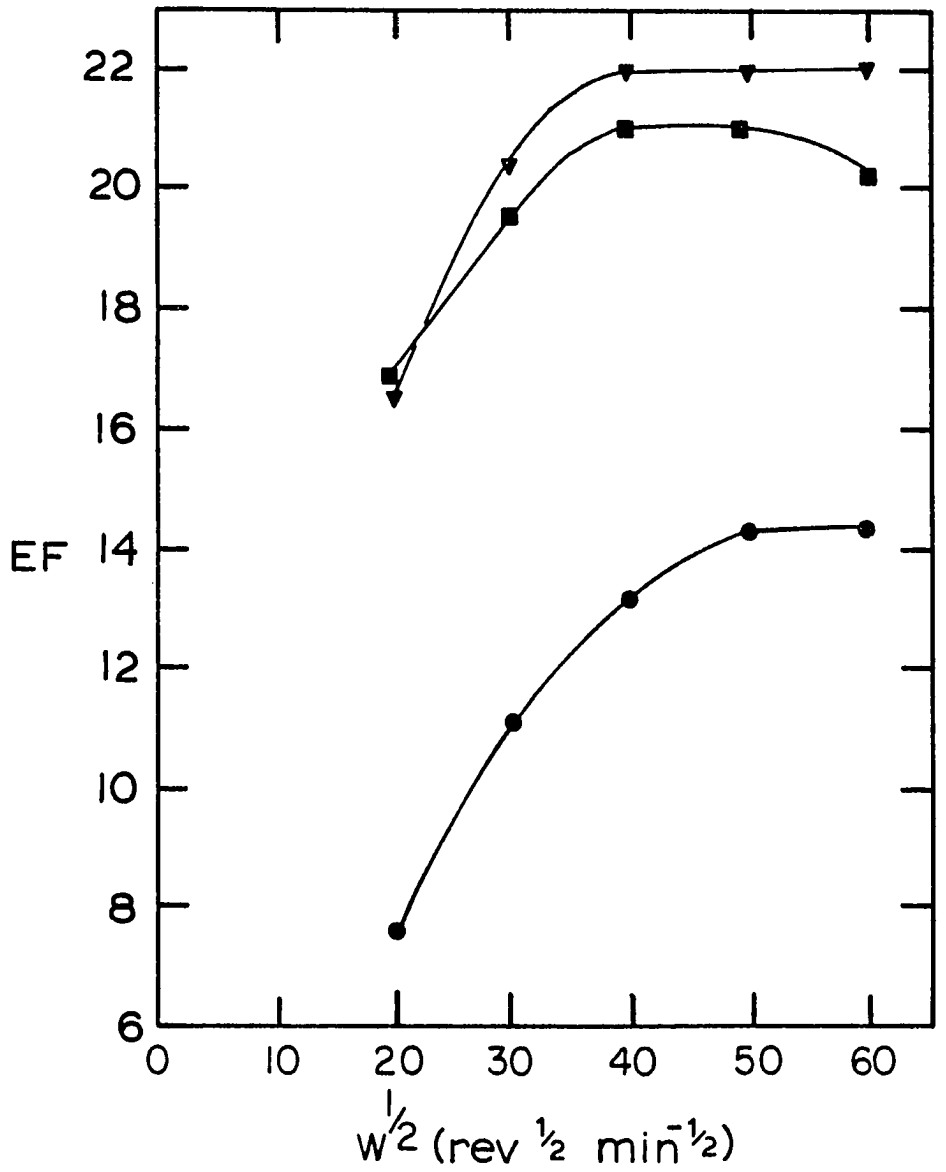
22
20
18
16
EF 14
12
10
8
6
0
10
20
30
40
50
60
W1/2 (rev 1/2 min-1/2)

scanned to the positive potential limit of 1.3V vs. SCE. Therefore, during the negative scan, the coverage of Pb ad-atoms at the potential region of Peak D is reproducible and independent of T_{dep}.

c. Hg ad-atoms The I-E curves for the Pt-RDE in a solution of 5.00 μM Hg(I) in 0.10 M H_2SO_4 are shown in Figure III-11. Comparison of Figure III-11 with Figures III-5 and III-7 reveals that under similar experimental conditions of T_{dep}, but much lower concentration of the metal ions, Hg is deposited to a greater extent on the Pt-RDE than either Pb or Cd. This is reflected in the very large stripping peak for Hg even with T_{dep} equal to 0 sec. The peak potential for the stripping of Hg is 0.9V vs. SCE, indicating that the interaction of Pt with Hg is stronger than that for either Pb or Cd. The Hg ad-atoms are stripped from the surface of the electrode concurrently with the formation of PtO. Once again, the hydrogen adsorption and desorption processes are suppressed by the Hg ad-atoms.

The I-E curves for the electrochemical oxidation of 0.25 M HCOOH in the presence of 5.00 μM Hg(I) are shown in Figure III-12. The effects of the Hg ad-atoms are unusual in two aspects. First, Peak A obtained during the positive potential scan is completely suppressed in the presence of the ad-atoms even with T_{dep} equal to 0 sec. This can be explained by the fact that, due to the strong Hg-Pt interaction, the deposition of the Hg ad-atoms proceeds at a mass-transport limited rate, causing the Pt substrate to be completely saturated with respect to the ad-atoms even with T_{dep} equal to 0 sec. Secondly, the peak currents of Peak D obtained during the negative potential sweep shows dependence on

Figure III-11. I-E curves for the deposition of Hg ad-atoms on the Pt-RDE in 0.10 M H_2SO_4

Electrode rotation speed (W): 400 rev min^{-1}

Potential scan rate (ϕ): 6 V min^{-1}

Deposition potential (E_{dep}): -0.20V *vs.* SCE

[Hg(I)]: 5.000×10^{-6} M

——— T_{dep} = 0 sec

····· T_{dep} = 120 sec

------- T_{dep} = 240 sec

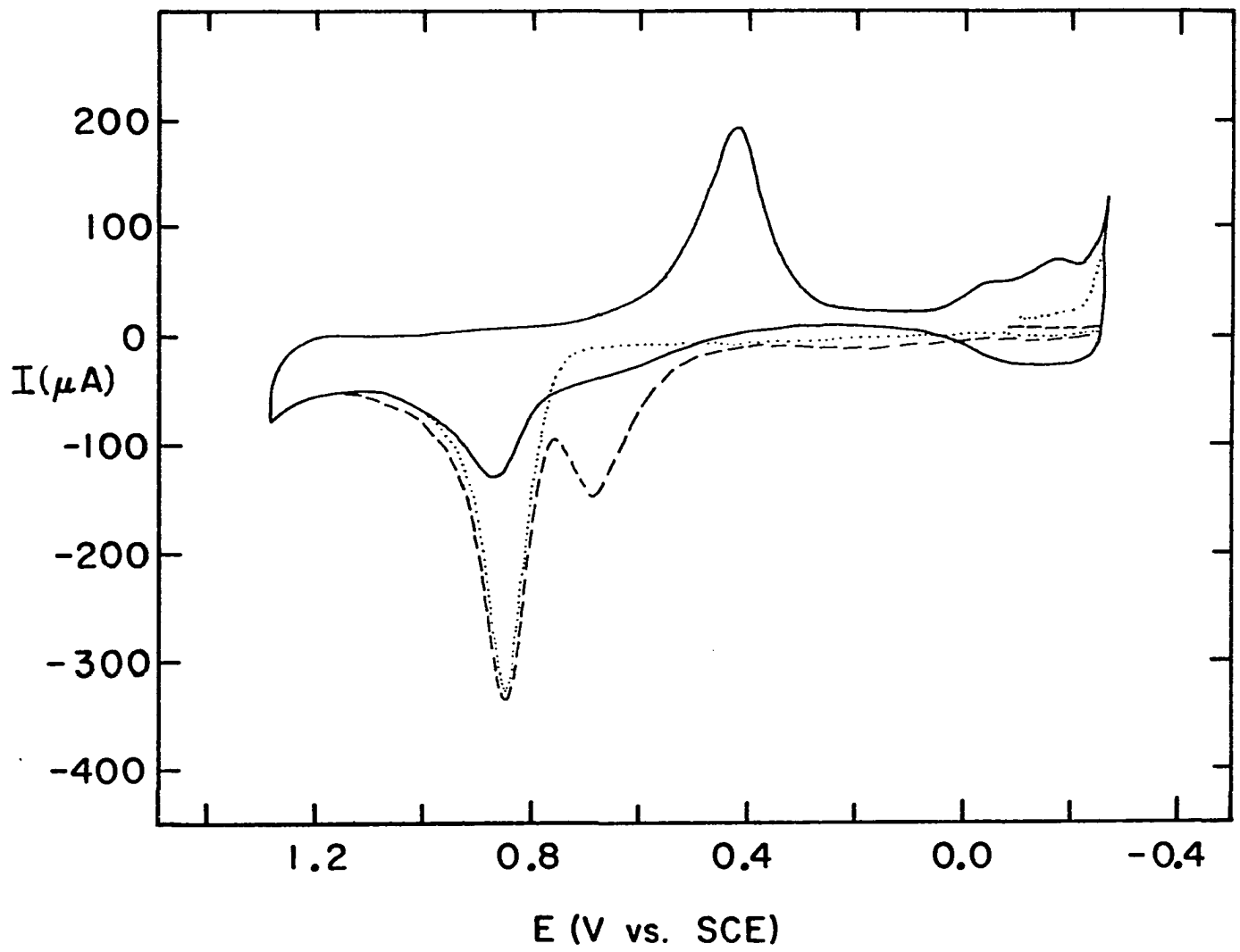
200
100
0
I(μA)
-100
-200
-300
-400
1.2
0.8
0.4
0.0
-0.4
E (V vs. SCE)

Figure III-12. I-E curves of the Pt-RDE in a solution of 0.25 M HCOOH and 0.10 M H_2SO_4 containing 5.00×10^{-6} M Hg(I)

Electrode rotation speed (W): 400 rev min^{-1}

Potential scan rate (ϕ): 6 V min^{-1}

Deposition potential: -0.20V vs. SCE

A, B, C and D: anodic peaks

——— T_{dep} = 0 sec

····· T_{dep} = 120 sec

------- T_{dep} = 240 sec

-·-·-·- T_{dep} = 420 sec

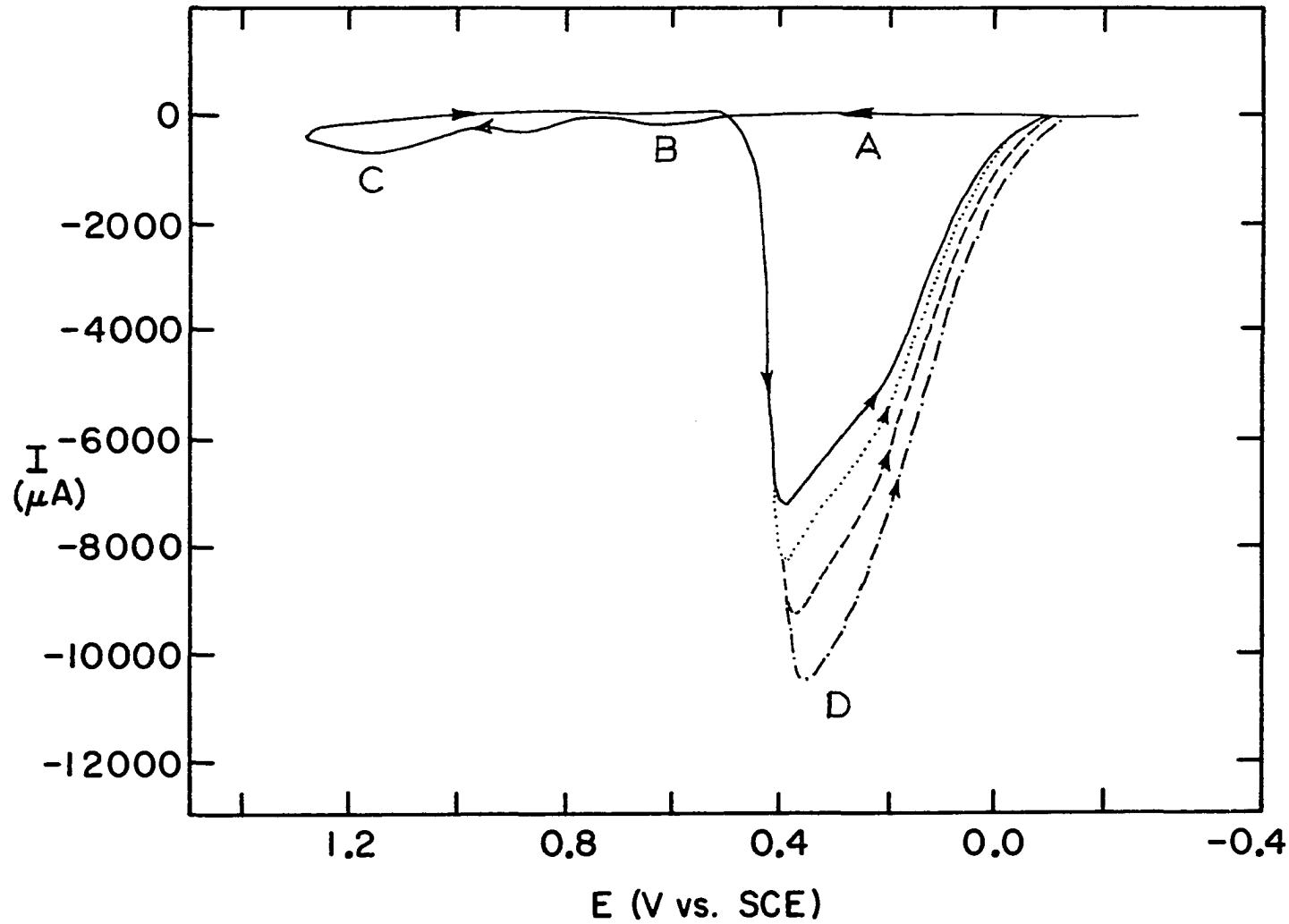
0
-2000
-4000
-6000
-8000
-10000
-12000
I
(μA)
1.2
0.8
0.4
0.0
-0.4
E (V vs. SCE)
A
B
C
D

T_{dep}, increasing with increases in T_{dep}. That this is not expected to occur was discussed in the previous section concerning the Pb ad-atoms. No logical explanation can be proposed to explain the phenomenon.

d. Cu ad-atoms The deposition of Cu ad-atoms at under-potential on a Pt-RDE is also extensive. The Cu ad-atoms are stripped from the Pt substrate in the potential region from 0.6V to 0.9V vs. SCE. The coverage of the Pt-RDE by the Cu ad-atoms increases with increasing T_{dep}. Cu ad-atoms also suppress the adsorption and desorption processes of H-atoms.

The effect of the Cu ad-atoms on the electrochemical oxidation of HCOOH is that of inhibition and all the peaks associated with the oxidation of HCOOH are decreased in size whether obtained during the positive or negative potential scan. Because the effect of Cu ad-atoms is only inhibitory, no I-E curves are shown for this species.

4. Effects of metal ad-atoms on the electrochemical oxidation of 0.25 M HCOOH on the Pt-RDE in 0.5 M H_2SO_4: ad-atoms deposited by Procedure B

Procedure B, used to control the coverage (θ_M) of the Pt-RDE by the metal ad-atoms, involved the variation of the concentration of the metal ions in the supporting electrolyte or HCOOH solutions. Additions of metal ions from a 1.00 mM stock solution to produce final concentrations in the μM range generally involved changes of less than 1% in the volume of the solutions to which the additions were made. The potential of the electrode was continuously scanned between the limits while the standard additions of the metal ions were performed and the I-E curves were recorded after they had become reproducible. The effect of the

standard addition of Bi(III), Pb(II), Tl(I), Ag(I) and Cd(II) was studied for the electrochemical oxidation of HCOOH in 0.50 M H_2SO_4.

a. Bi ad-atoms The I-E curves obtained at the Pt-RDE in the absence of HCOOH for several concentrations of Bi(III) are shown in Figure III-13. The presence of Bi(III) increases the height of the peak associated with the reduction of PtO at 0.42V vs. SCE. Adzic et al. (67) attributed this increase to the reduction of metal ions to the corresponding ad-atoms. However, calculations of the limiting current (I_ℓ) for the reaction

$$Bi(III) + 3e \rightleftharpoons Bi(0) \qquad \text{(III-7)}$$

using the Levich Equation

$$I_\ell = 0.2\ nFAD^{2/3}v^{-1/6}W^{1/2}C^b \qquad \text{(III-8)}$$

with n = number of electrons transferred = 3 eq $mole^{-1}$

F = Faraday constant = 96487 coulombs eq^{-1}

A = area of the electrode = 0.43 cm^2

D = diffusion coefficient of Bi(III) $\approx 1 \times 10^{-5}$ cm^2 sec^{-1}

v = kinematic viscosity of the solution ≈ 0.01 cm^2 sec^{-1}

W = rotation speed of the RDE = 400 rev min^{-1}

C^b = concentration of Bi(III) = 4.00×10^{-7} M

yielded a value of 0.20 μA for a solution containing 4.00×10^{-7} M of Bi(III). This is about 300X less than the experimentally observed increase of 58 μA in the peak current for the oxide reduction. Therefore, although there is little doubt that the reduction of Bi(III)

Figure III-13. I-E curves for the deposition of Bi ad-atoms on the Pt-RDE in 0.50 M H_2SO_4

Electrode rotation speed (W): 400 rev min^{-1}

Potential scan rate (ϕ): 6 V min^{-1}

——— 0.00 M Bi(III)

····· 4.000×10^{-7} M Bi(III)

------- 2.000×10^{-6} M Bi(III)

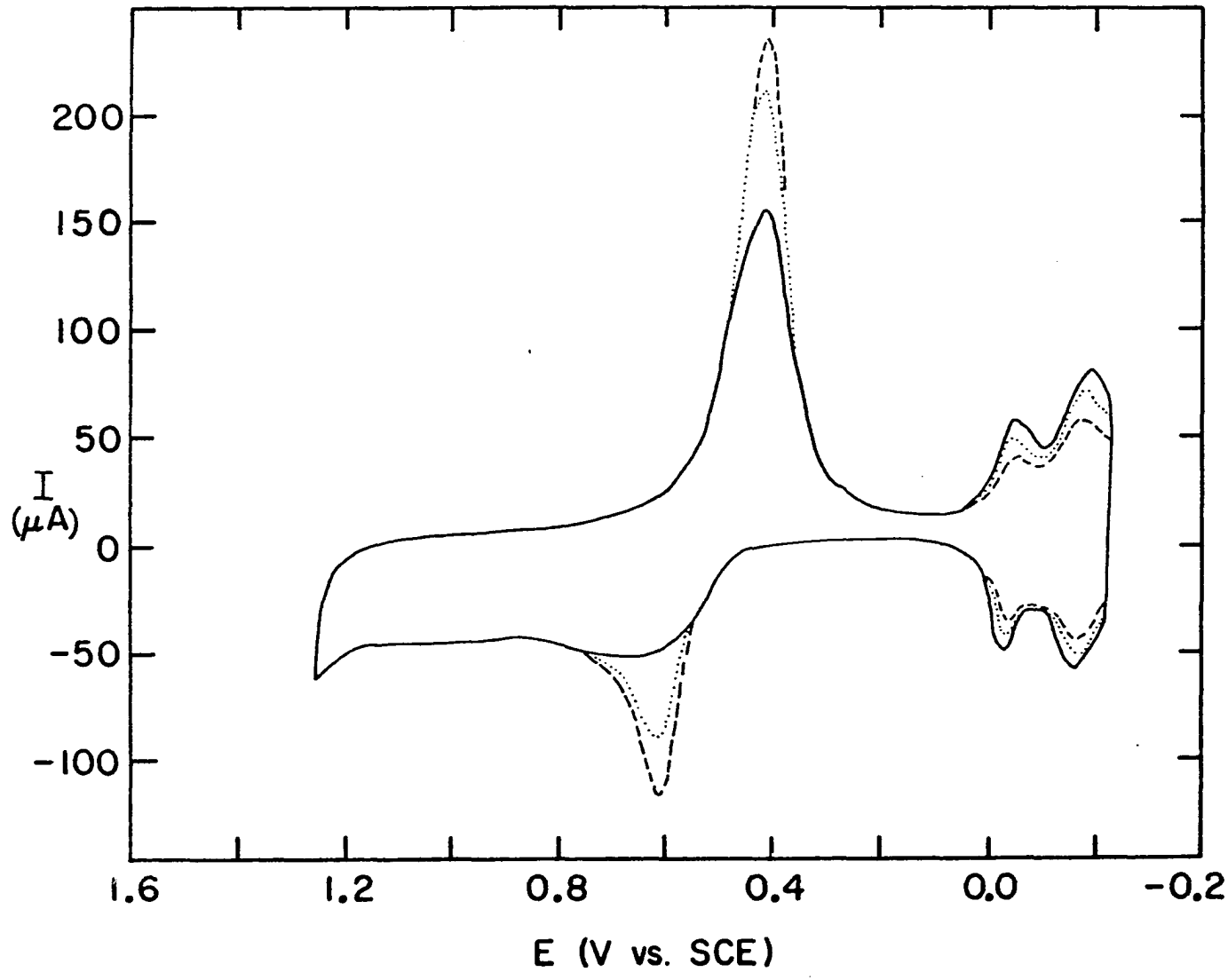
200
150
100
50
I
(μA)
0
-50
-100
1.6
1.2
0.8
0.4
0.0
-0.2
E (V vs. SCE)

is concurrent with the reduction of PtO, the increase in the peak current for oxide reduction must be due to processes other than the reduction of Bi(III) transported to the surface of the electrode from the bulk of the solution. Cadle and Bruckenstein (72) have demonstrated that a large fraction of Bi(III) does not leave the surface of the electrode during the oxidation of Bi to Bi(III). Hence, it is concluded that the increase in the peak current of the PtO reduction peak is due to the reduction of the absorbed Bi(III).

The dependence of θ_{Bi} on the concentration of Bi(III) is demonstrated by the increase in the height of the stripping peak at 0.6V *vs.* SCE with increases in the concentration of Bi(III) in solution. θ_{Bi} can be conveniently estimated by the method of adsorption substitution, which is described by Equation II-7 for the case involving the coverage of the electrode by organic species. θ_{Bi} increases with increasing concentration of Bi(III). The dependence of θ_M on the concentration of Bi(III) is shown in Table III-3 and Figure III-14.

Table III-3. Dependence of θ_{Bi} on the concentration of Bi(III)

[Bi(III)] (μM)	θ_{Bi}
0.00	0.00
2.00	0.08
5.00	0.16
10.00	0.25
15.00	0.29
20.00	0.38
25.00	0.44
30.00	0.52
35.00	0.58
40.00	0.62
45.00	0.67
55.00	0.78

Figure III-14. Dependence of the fractional coverage (θ_M) of the Pt-RDE by the metal ad-atoms on the concentration of the corresponding metal ions ($[M^{+n}]$)

Supporting electrolyte: 0.5 M H_2SO_4

Electrode rotation speed (W): 400 rev min^{-1}

Potential scan rate (ϕ): 6 V min^{-1}

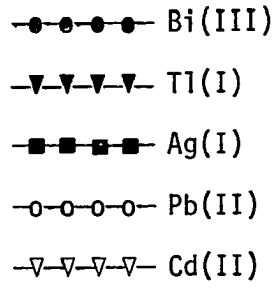

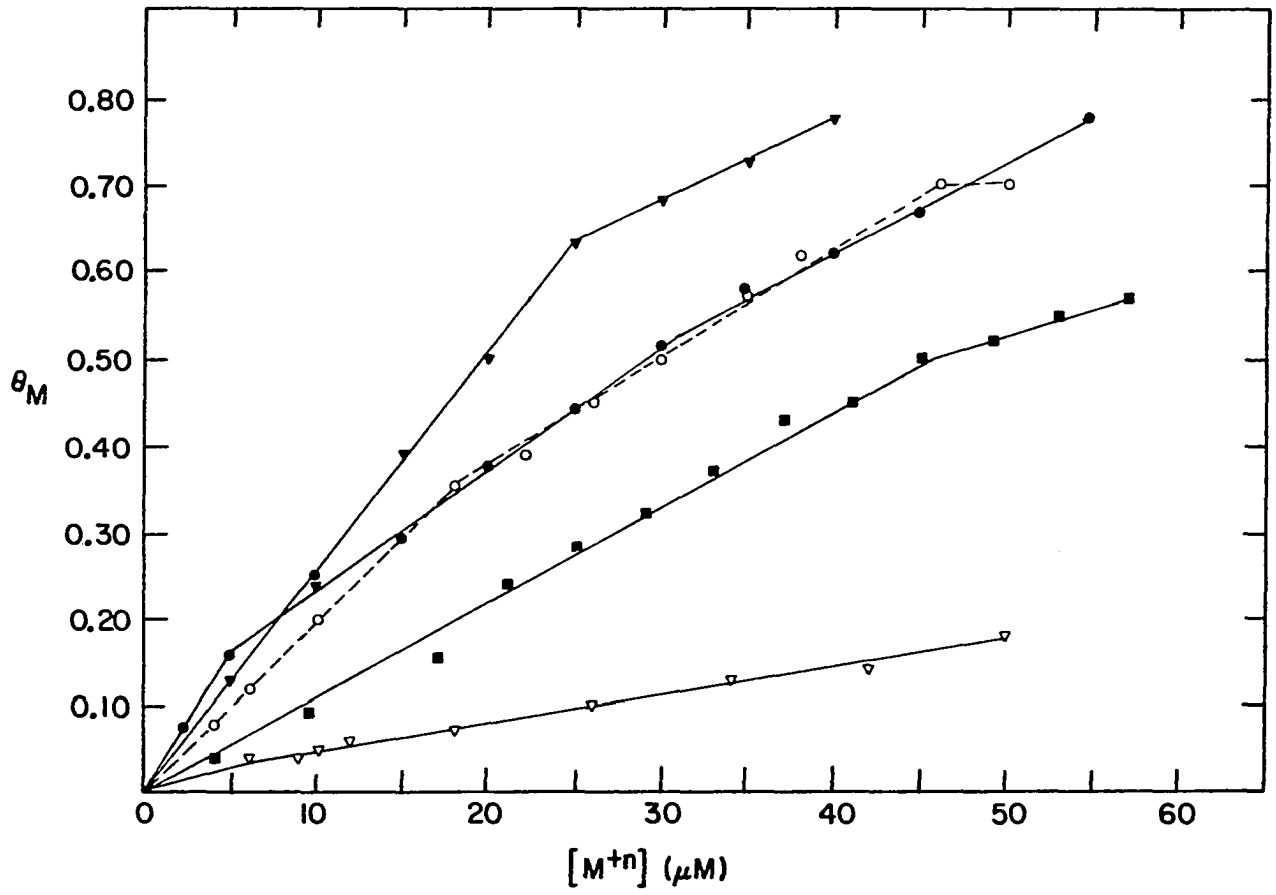
0.80
0.70
0.60
0.50
0.40
0.30
0.20
0.10
θ_M
0
10
20
30
40
50
60
$[M^{+n}]$ (μM)

As shown in Figure III-15, Bi ad-atoms enhance the electrochemical oxidation of HCOOH for both Peak A and Peak D obtained during the positive and negative potential scan, respectively. The Bi ad-atoms shift the potentials of Peaks A and D in the negative direction, and a tentative conclusion is made that the Bi ad-atoms have a catalytic effect on the heterogeneous rate constant for the electrochemical oxidation of HCOOH. The values of $I_{p,A}$, $I_{p,D}$, EF_A and EF_D as a function of the concentration of Bi(III) are presented in Table III-4 and plotted in Figures III-16, III-17, III-18 and III-19, respectively.

Table III-4. Dependence of $I_{p,A}$, $I_{p,D}$, EF_A and EF_D on the concentration of Bi(III) during the electrochemical oxidation of 0.25 M HCOOH on the Pt-RDE in 0.50 M H_2SO_4

[Bi(III)] (μM)	$I_{p,A}$ (μA)	$I_{p,D}$ (μA)	EF_A	EF_D
0.00	300	3800	1.0	1.0
3.00	1800	4000	6.0	1.1
5.00	2700	4150	9.0	1.1
7.00	3425	4300	11.4	1.1
10.00	4000	4500	13.3	1.2
15.00	3775	4950	12.6	1.3
20.00	2650	5500	8.8	1.5
25.00	1650	6050	5.5	1.6
30.00	960	6650	3.2	1.8
40.00	700	7700	2.3	2.0
50.00	700	8600	2.3	2.2
70.00	700	9800	2.3	2.6
90.00	700	10600	2.3	2.8

Figure III-15. I-E curves of the Pt-RDE in a solution of 0.25 M HCOOH and 0.5 M H_2SO_4 in the absence and presence of Bi(III)

Electrode rotation speed (W): 400 rev min^{-1}

Potential scan rate (ϕ): 6 V min^{-1}

A, B, C and D: anodic peaks

——— 0.00 M Bi(III)

------- 3.2×10^{-6} M Bi(III)

····· 8.4×10^{-6} M Bi(III)

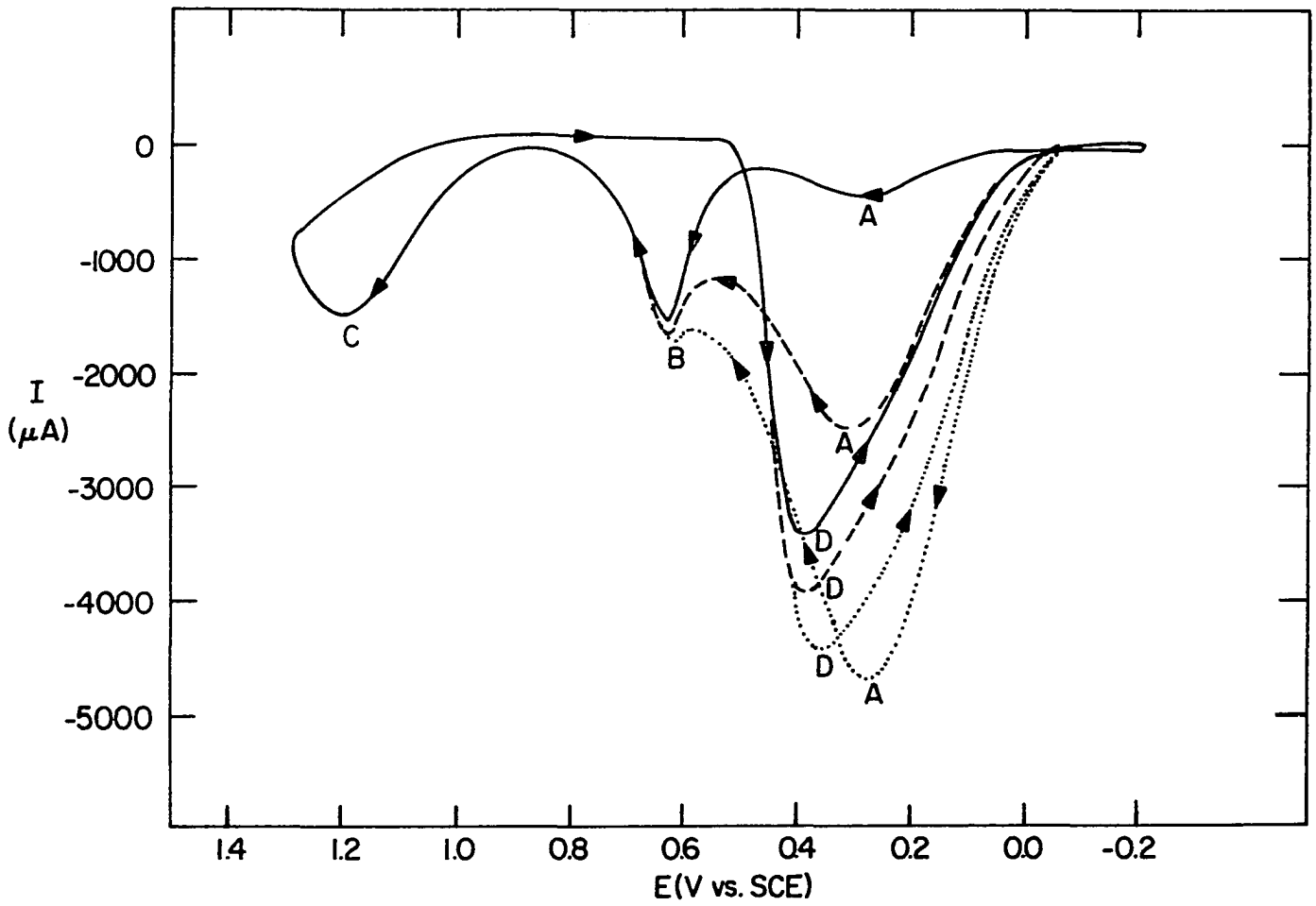
0
-1000
-2000
-3000
-4000
-5000
I
(μA)
C
B
A
A
D
D
D
A
1.4
1.2
1.0
0.8
0.6
0.4
0.2
0.0
-0.2
E(V vs. SCE)

Figure III-16. Dependence of the peak current of Peak A ($I_{p,A}$) on the concentration of the metal ions ($[M^{+n}]$) during the electrochemical oxidation of 0.25 M HCOOH in 0.50 M H_2SO_4

Electrode rotation speed (W): 400 rev min^{-1}

Potential scan rate (ϕ): 6 V min^{-1}

-●-●-●- Bi(III)

-▼-▼-▼- Tl(I)

-o-o-o- Pb(II)

-■-■-■- Ag(I)

-∇-∇-∇- Cd(II)

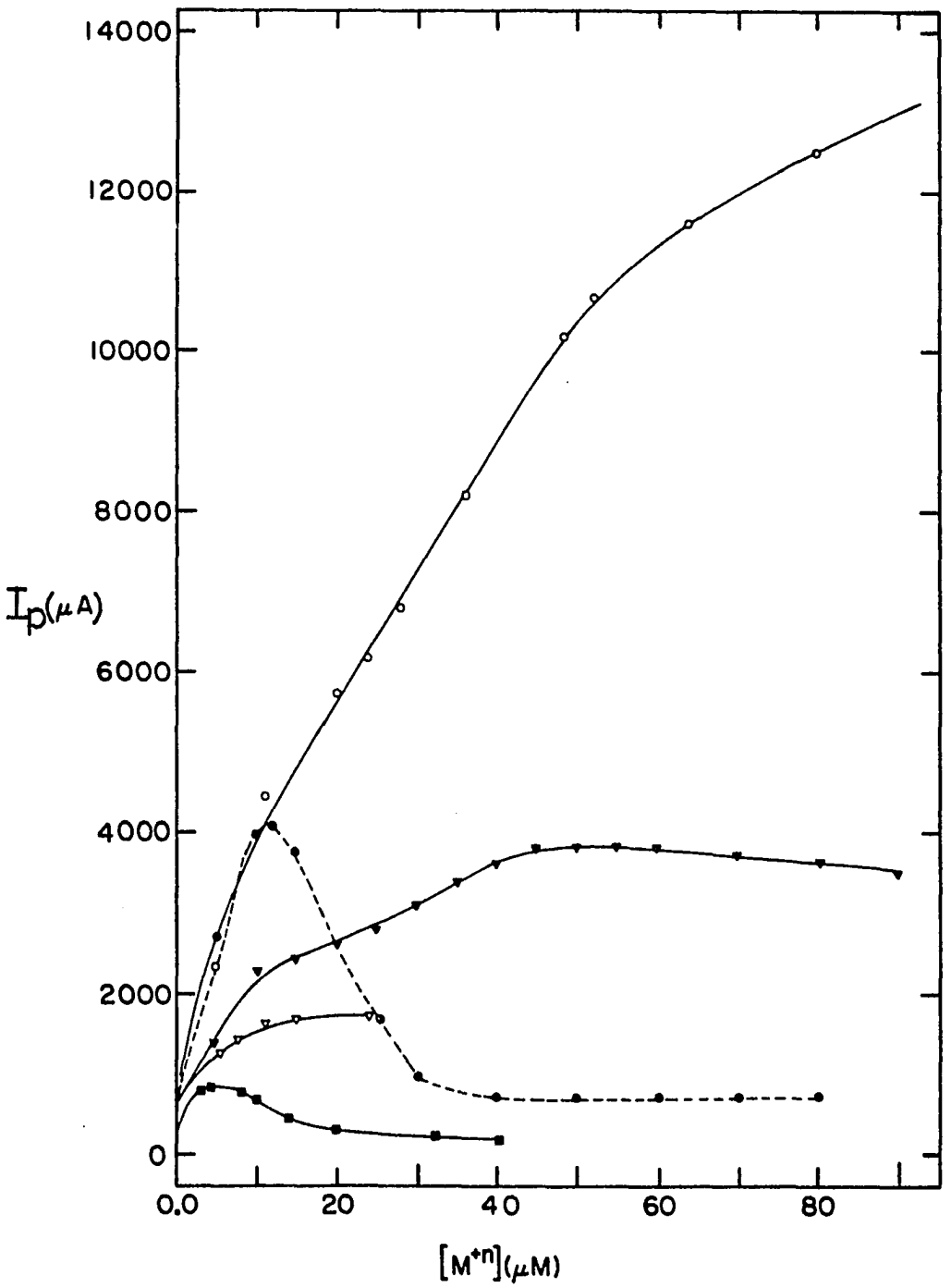
14000
12000
10000
8000
6000
4000
2000
0
$I_p(\mu A)$
0.0
20
40
60
80
$[M^{+n}](\mu M)$

Figure III-17. Dependence of the peak current of Peak D ($I_{p,D}$) on the concentration of the metal ions ($[M^{+n}]$) during the electrochemical oxidation of 0.25 M HCOOH in 0.50 M H_2SO_4

Electrode rotation speed (W): 400 rev min^{-1}

Potential scan rate (Φ): 6 V min^{-1}

-●-●-●- Bi(III)

-▼-▼-▼- Tl(I)

-■-■-■- Ag(I)

-o-o-o- Pb(II)

-∇-∇-∇- Cd(II)

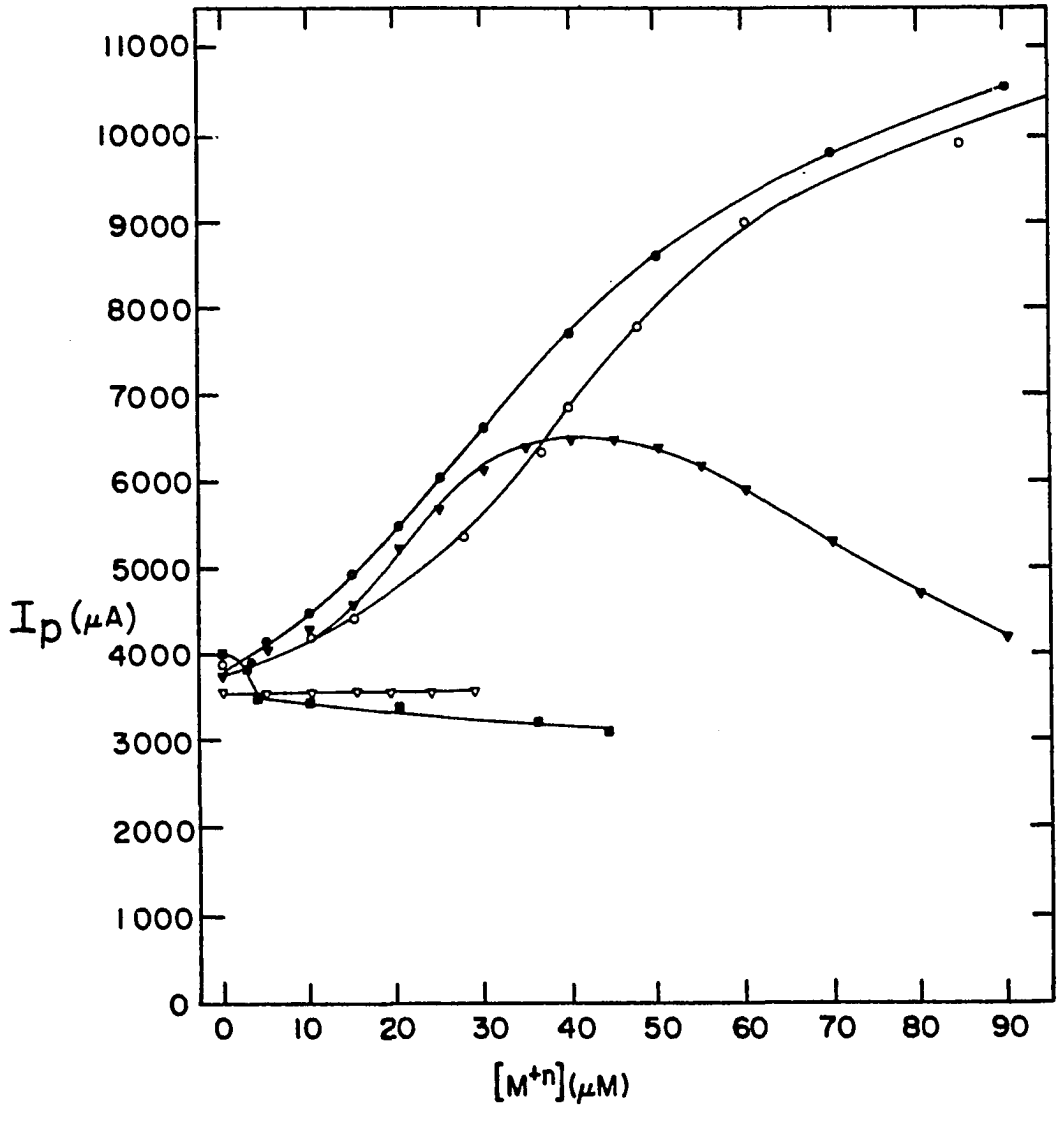
11000
10000
9000
8000
7000
6000
5000
4000
3000
2000
1000
0
I_p (μA)
0
10
20
30
40
50
60
70
80
90
[M+n](μM)

Figure III-18. Dependence of the enhancement factor for Peak A (EF_A) on the concentration of the metal ions ($[M^{+n}]$) during the electrochemical oxidation of 0.25 M HCOOH in 0.50 M H_2SO_4

Electrode rotation speed (W): 400 rev min^{-1}

Potential scan rate (ϕ): 6 V min^{-1}

-●-●-●- Bi(III)

-▼-▼-▼- Tl(I)

-■-■-■- Ag(I)

-o-o-o- Pb(II)

-∇-∇-∇- Cd(II)

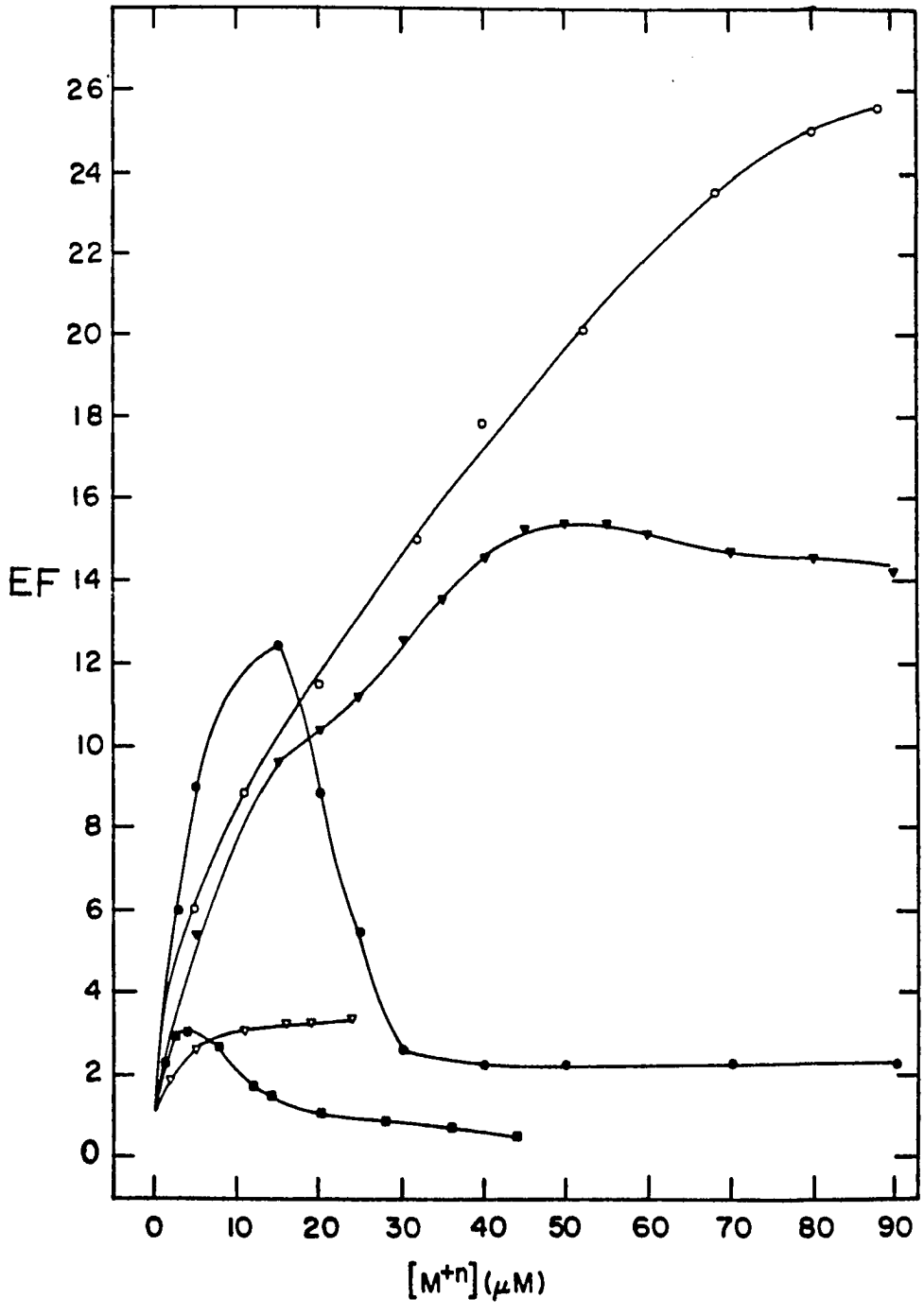
EF
26
24
22
20
18
16
14
12
10
8
6
4
2
0
0
10
20
30
40
50
60
70
80
90
[M+n] (μM)

Figure III-19. Dependence of the enhancement factor for Peak D (EF_D) on the concentration of the metal ions ($[M^{+n}]$) during the electrochemical oxidation of 0.25 M HCOOH in 0.50 M H_2SO_4

Electrode rotation speed (W): 400 rev min^{-1}

Potential scan rate (ϕ): 6 V min^{-1}

-●-●-●- Bi(III)

-▼-▼-▼- Tl(I)

-■-■-■- Ag(I)

-o-o-o- Pb(II)

-∇-∇-∇- Cd(II)

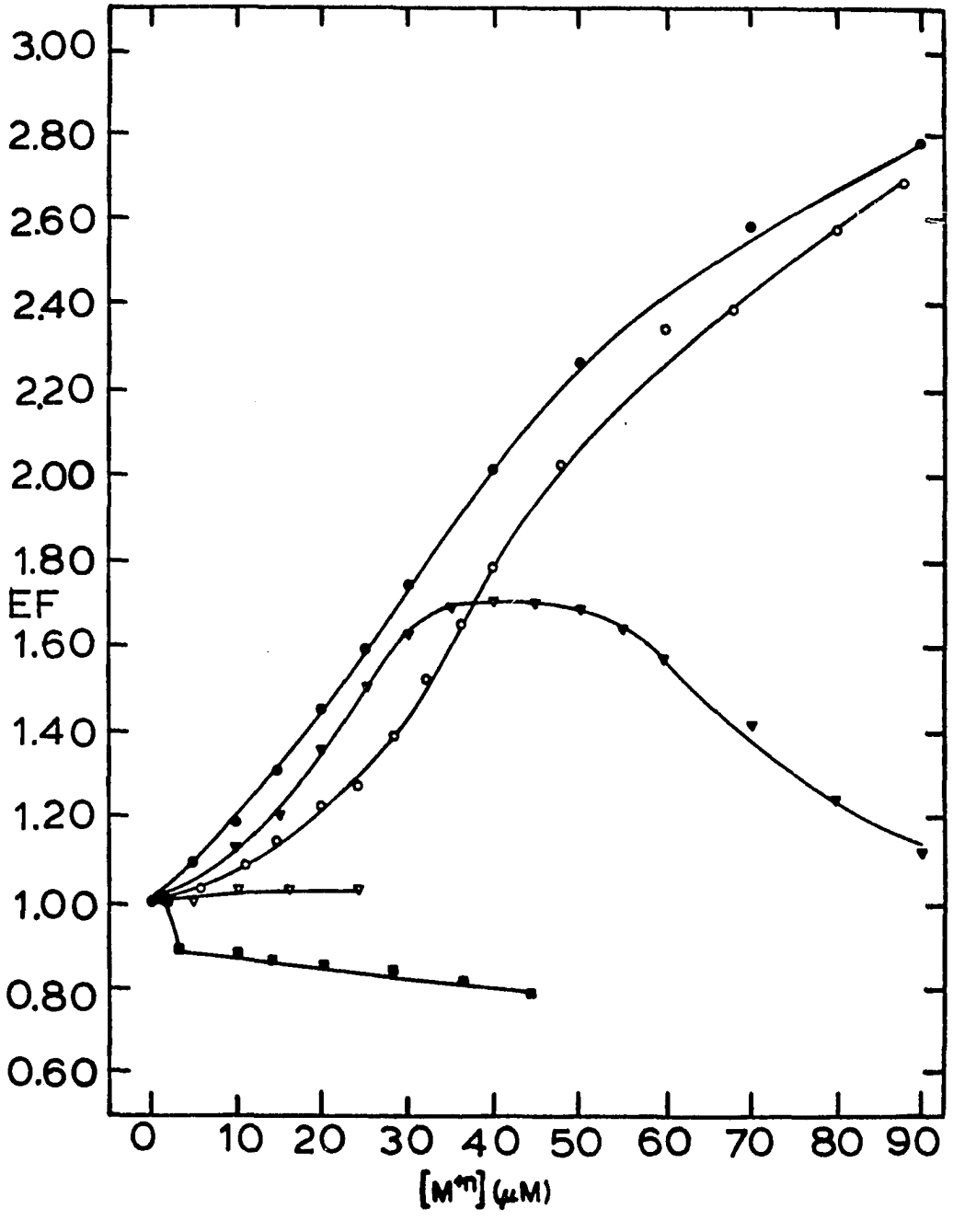
3.00
2.80
2.60
2.40
2.20
2.00
1.80
EF
1.60
1.40
1.20
1.00
0.80
0.60
0
10
20
30
40
50
60
70
80
90
[M^m] (μM)

b. Tl ad-atoms The I-E curves obtained by cyclic voltammetry at the Pt-RDE in the presence of Tl(I) in 0.5 M H_2SO_4 are shown in Figure III-20. The peak potential for the stripping of Tl ad-atoms is 0.7V vs. SCE, which is about 100 mV more positive than observed for the Bi ad-atoms. A highly visible faradaic wave is obtained during the negative potential scan with a half-wave potential of 0.95V vs. SCE. The anodic branch of this wave is dependent on W but independent of ϕ and is attributed to the oxidation of Tl(I) to Tl(III). The cathodic branch of the wave is dependent on ϕ but independent of W and is attributed to the reduction of adsorbed Tl(III) formed during the preceding oxidation of Tl(I). The observation that the cathodic branch of the wave is independent of W points to the possibility that only a specific fraction of the Tl(III) formed is adsorbed on the surface of the electrode. Probably, $\theta_{Tl(III)}$ is at its maximum value for those experimental conditions. The presence of the Tl ad-atoms suppresses the process of hydrogen adsorption and desorption.

The dependence of θ_{Tl} on the concentration of Tl(I) is shown in Table III-5 and plotted in Figure III-14. The plot shown in Figure III-14 is linear for low concentrations of Tl(I), but a decreased slope is obtained at higher concentration of Tl(I). It is shown by extrapolation of the plot for low [Tl(I)] to $\theta_{Tl} = 1.0$ that approximately 40 μM Tl(I) will result in virtual saturation of the surface of the electrode. This value is recognized as only an estimate, at best.

The effect of the Tl ad-atoms on the electrochemical oxidation of HCOOH is shown in Figure III-21. The Tl ad-atoms greatly increase the

Figure III-20. I-E curves for the deposition of Tl ad-atoms on the Pt-RDE in 0.50 M H_2SO_4

Electrode rotation speed (W): 400 rev min^{-1}

Potential scan rate (ϕ): 6 V min^{-1}

——— 0.00 M Tl(I)

····· 2.00×10^{-5} M Tl(I)

------- 4.00×10^{-5} M Tl(I)

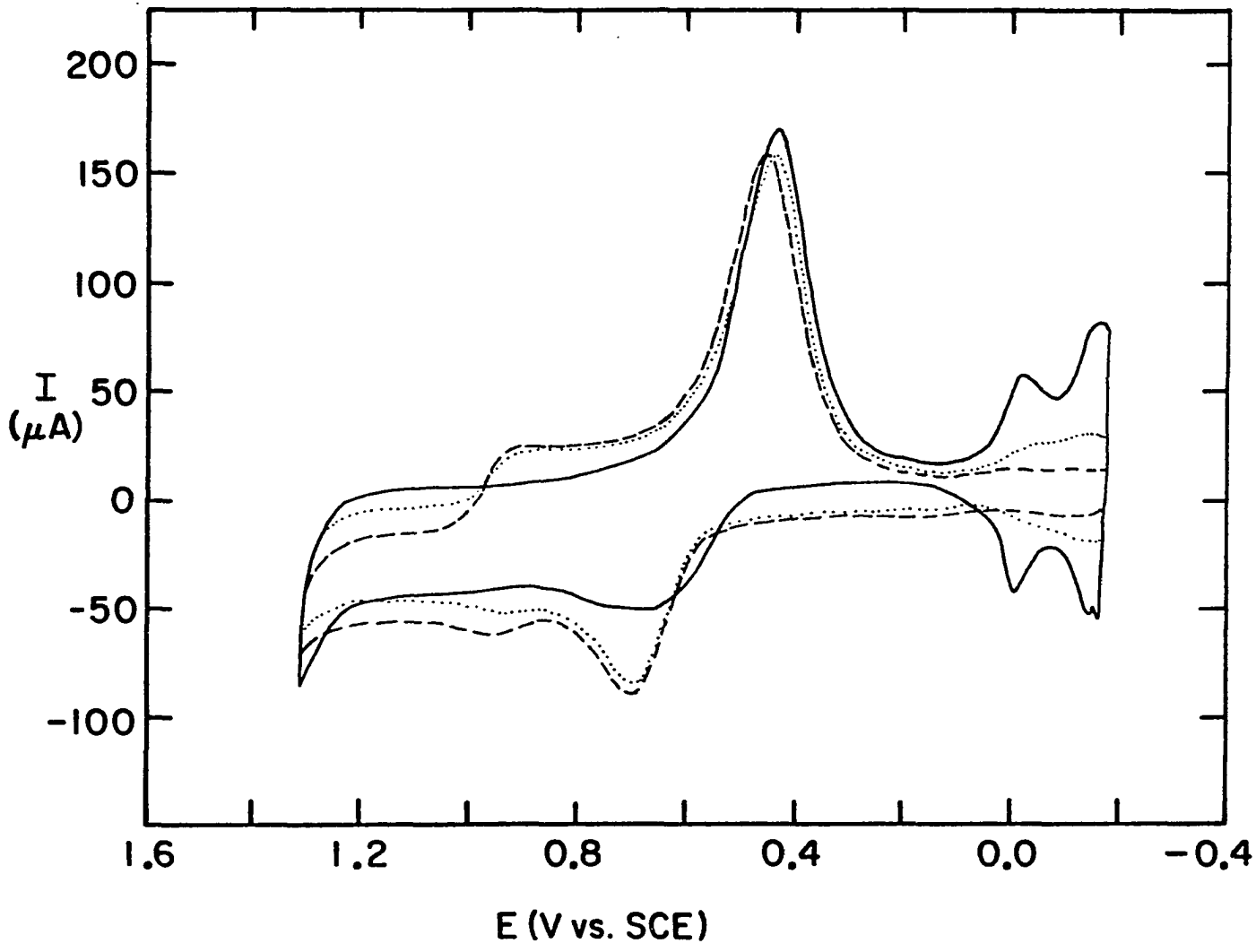
200
150
100
I
(μA)
50
0
-50
-100
1.6
1.2
0.8
0.4
0.0
-0.4
E (V vs. SCE)

Table III-5. Dependence of θ_{Tl} on the concentration of Tl(I)

Tl(I) (μM)	θ_{Tl}
0.0	0.00
5.0	0.13
10.0	0.24
15.0	0.39
20.0	0.50
25.0	0.63
30.0	0.68
35.0	0.73
40.0	0.78

peak currents of Peaks A and D. The effect on Peak A is similar to the case already discussed involving Bi ad-atoms. However, Tl ad-atoms not only enhance the peak currents of Peak D obtained during the negative potential scan, but also broaden the peak width measured at half-peak height and shift E_p to more negative potentials. For θ_{Tl} in excess of the optimal value, the peak current decreases, the peak width at half-peak height decreases and E_p is shifted back slightly towards the more positive potentials. The optimal value for θ_{Tl} occurs for a concentration of approximately 50 μM Tl(I), corresponding to a value of $\theta_{Tl} = 0.88$. The value of 0.88 for θ_{Tl} is estimated by extrapolation of the plot of θ_{Tl} vs. [Tl(I)] shown in Figure III-14. The values of $I_{p,A}$, $I_{p,D}$, EF_A and EF_D as a function of the concentration of Tl(I) are tabulated in Table III-6 and plotted in Figures III-16, III-17, III-18 and III-19, respectively.

Figure III-21. I-E curves of the Pt-RDE in a solution of 0.25 M HCOOH and 0.50 M H_2SO_4 in the absence and presence of Tl(I)

Electrode rotation speed (W): 400 rev min^{-1}

Potential scan rate: 6 V min^{-1}

A, B, C and D: anodic peaks

——— 0.00 M Tl(I)

····· 10.00 x 10^{-6} M Tl(I)

------- 30.00 x 10^{-6} M Tl(I)

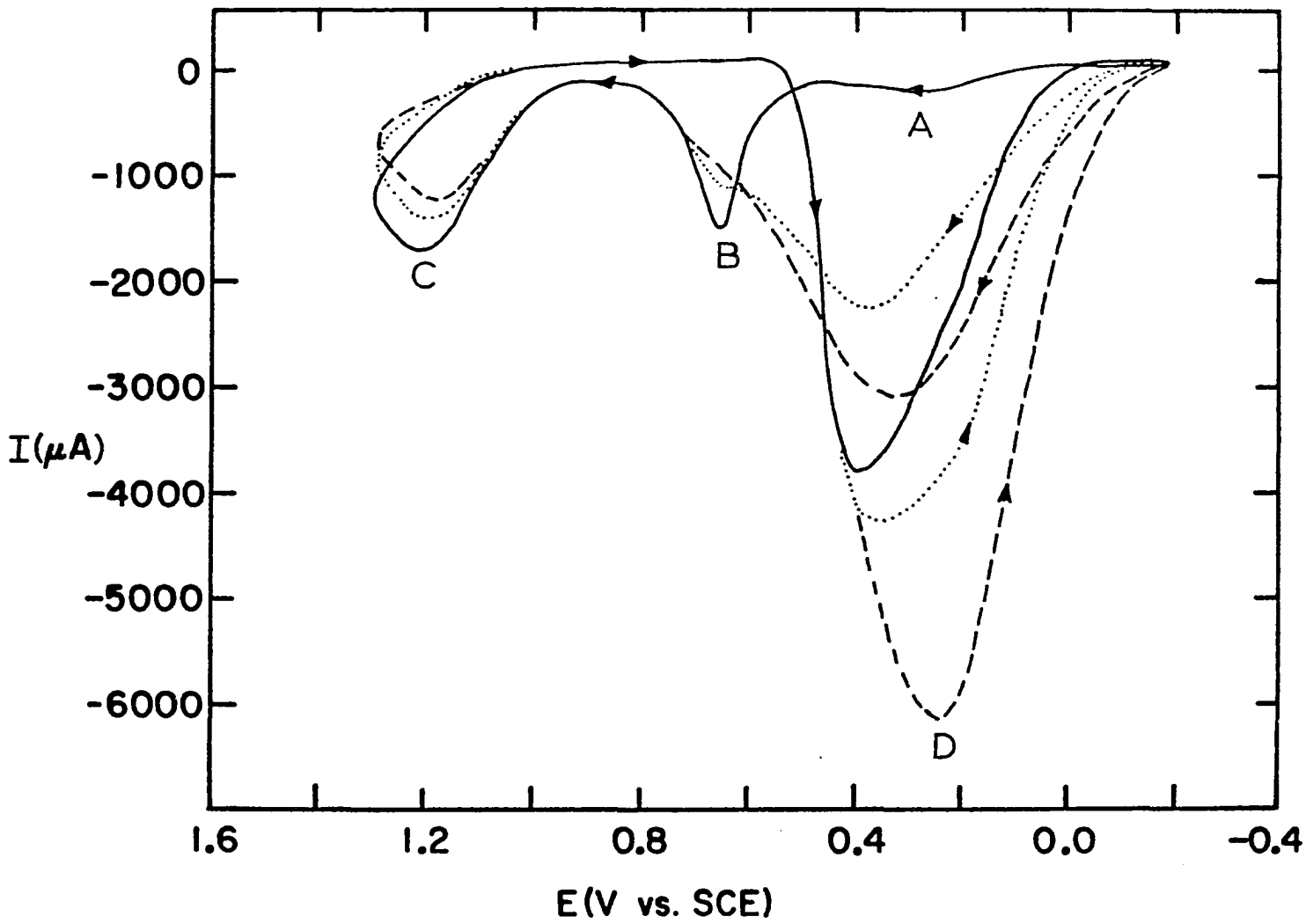
0
-1000
-2000
-3000
-4000
-5000
-6000
I(μA)
A
B
C
D
1.6
1.2
0.8
0.4
0.0
-0.4
E(V vs. SCE)

Table III-6. Dependence of $I_{p,A}$, $I_{p,D}$, EF_A and EF_D on the concentration of Tl(I) during the electrochemical oxidation of 0.25 M HCOOH on the Pt-RDE in 0.50 M H_2SO_4

[Tl(I)] (μM)	$I_{p,A}$ (A)	$I_{p,D}$ (A)	EF_A	EF_D
0.0	250	3800	1.0	1.0
5.0	1350	4050	5.4	1.1
10.0	2300	4300	9.2	1.1
15.0	2400	4575	9.6	1.4
20.0	2600	5250	9.6	1.4
25.0	2800	5700	10.4	1.5
30.0	3150	6175	11.2	1.6
35.0	3400	6400	12.6	1.7
40.0	3650	6500	13.6	1.7
45.0	3825	6500	14.6	1.7
50.0	3850	6400	15.3	1.7
55.0	3850	6225	15.4	1.6
60.0	3800	5975	15.2	1.6
70.0	3725	5350	14.9	1.4
80.0	3650	4700	14.6	1.2
90.0	3575	4250	14.3	1.1

c. Ag ad-atoms The deposition and stripping of Ag ad-atoms is portrayed in Figure III-22. The peak potential for the stripping of Ag ad-atoms is 0.85V vs. SCE, which is more positive than those of Tl, Bi, Pb and Cd. The value of $E^{\circ}_{Ag(I)/Ag(0)}$ is 0.55V vs. SCE. The oxidation of the Pt substrate to PtO commences at 0.6V vs. SCE during the positive scan when the Ag ad-atoms are absent (see solid curve in Figure III-22). However, the presence of Ag ad-atoms delays the formation of PtO to slightly more positive potentials. The dependence

Figure III-22. I-E curves for the deposition of Ag ad-atoms on the Pt-RDE in 0.50 M H_2SO_4

Electrode rotation speed (W): 400 rev min^{-1}

Potential scan rate (ϕ): 6 V min^{-1}

——— 0.00 M Ag(I)

····· 5.00×10^{-6} M Ag(I)

- - - - - - - 2.50×10^{-5} M Ag(I)

-·-·-·- 4.10×10^{-5} M Ag(I)

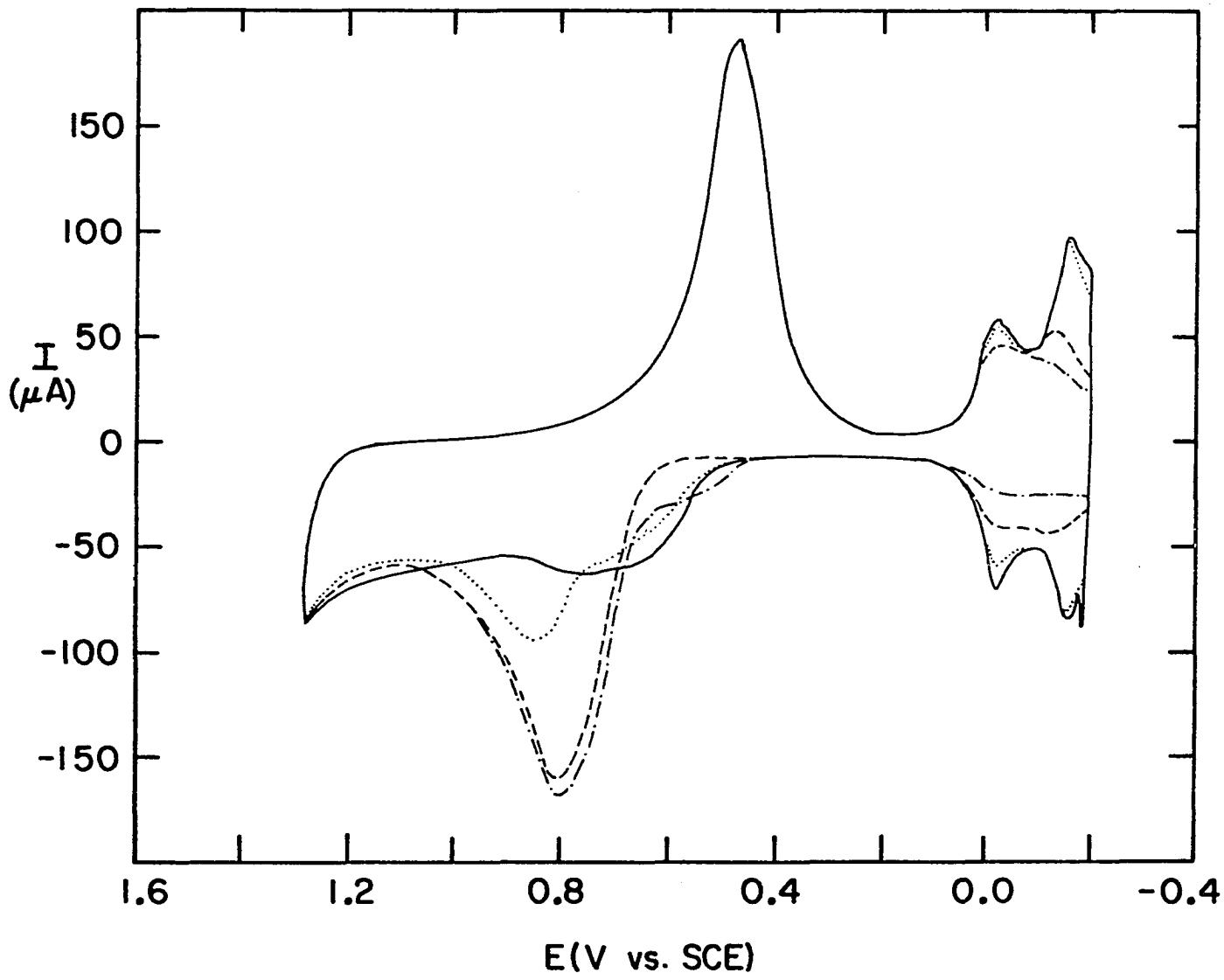
150
100
50
0
-50
-100
-150
I
(μA)
1.6
1.2
0.8
0.4
0.0
-0.4
E(V vs. SCE)

of θ_{Ag} on the concentration of Ag(I) is shown in Table III-7 and Figure III-21.

Table III-7. Dependence of θ_{Ag} on the concentration of Ag(I)

[Ag(I)] (μM)	θ_{Ag}
0.0	0.00
4.0	0.04
9.0	0.09
13.0	0.10
17.0	0.15
21.0	0.24
25.0	0.28
29.0	0.32
33.0	0.37
37.0	0.43
41.0	0.45
45.0	0.50
49.0	0.52
53.0	0.55
57.0	0.57

The effects of the Ag ad-atoms towards the electrochemical oxidation of HCOOH are qualitatively identical to those exerted by the Tl ad-atoms. Therefore, no figure is shown for the case involving the Ag ad-atoms. The peak currents of Peak A obtained during the positive potential scan are enhanced by the presence of the Ag ad-atoms. Peak D, obtained during the negative scan, is broadened and E_p shifts to the more negative values in the presence of the Ag ad-atoms. The values of $I_{p,A}$, $I_{p,D}$, EF_A and EF_D as a function of the concentration of Ag(I) are

tabulated in Table III-8 and plotted in Figures III-16, III-17, III-18 and III-19, respectively.

Table III-8. Dependence of $I_{p,A}$, $I_{p,D}$, EF_A and EF_D on the concentration of Ag(I) during the electrochemical oxidation of 0.25 M HCOOH on the Pt-RDE in 0.50 M H_2SO_4

[Ag(I)] (μM)	$I_{p,A}$ (μA)	$I_{p,D}$ (μA)	EF_A	EF_D
0.0	275	4000	1.0	1.0
1.0	650	4000	2.4	1.0
2.0	825	4000	3.0	1.0
4.0	850	3550	3.1	0.9
8.0	725	3480	2.6	0.9
12.0	475	3450	1.7	0.9
14.0	400	3450	1.5	0.9
20.0	300	3400	1.1	0.9
28.0	250	3350	0.9	0.8
36.0	200	3250	0.7	0.8
44.0	125	3100	0.5	0.8

According to the data presented in Table III-8, the maximum enhancement factor for Peak A occurs at approximately 4.0 μM Ag(I), which corresponds to θ_{Ag} of 0.04. It is not clear why the optimal values of θ_{Ag} is so small.

d. Pb ad-atoms The deposition of Pb ad-atoms on the Pt-RDE has been discussed previously in this section. The dependence of θ_{Pb} on the concentration of Pb(II) as calculated by the method of adsorption substitution, is tabulated in Table III-9 and plotted in Figure III-14.

Table III-9. Dependence of θ_{Pb} on the concentration of Pb(II)

[Pb(II)] (μM)	θ_{Pb}
0.0	0.00
4.0	0.08
6.0	0.12
10.0	0.20
18.0	0.35
22.0	0.39
26.0	0.45
30.0	0.50
34.0	0.51
38.0	0.63
42.0	0.64
46.0	0.65
50.0	0.65

The Pb ad-atoms are found to have tremendous effects on the electrochemical oxidation of HCOOH (see Figure III-23). They enhance the peak currents associated with Peak A 26X over that obtained in the absence of the Pb ad-atoms. The value of $I_{p,D}$ obtained during negative potential scan is not enhanced to a very large extent, but Peak D is slightly broadened in the presence of the Pb ad-atoms. The potential for Peaks A and D is shifted in a negative direction and a tentative conclusion is made that the electrochemical oxidation of HCOOH is more reversible in the presence of the Pb ad-atoms.

The values of $I_{p,A}$, $I_{p,D}$, EF_A and EF_D as a function of the concentration of Pb(II) are tabulated in Table III-10 and plotted in Figures III-16, III-17, III-19 and III-19, respectively.

Figure III-23. I-E curves of the Pt-RDE in a solution of 0.25 M HCOOH and 0.50 M H_2SO_4 in the absence and presence of Pb(II)

Electrode rotation speed (W): 400 rev min^{-1}

Potential scan rate (ϕ): 6 V min^{-1}

A, B, C and D: anodic peaks

——— 0.00 M Pb(II)

------- 3.2×10^{-6} M Pb(II)

····· 8.2×10^{-6} M Pb(II)

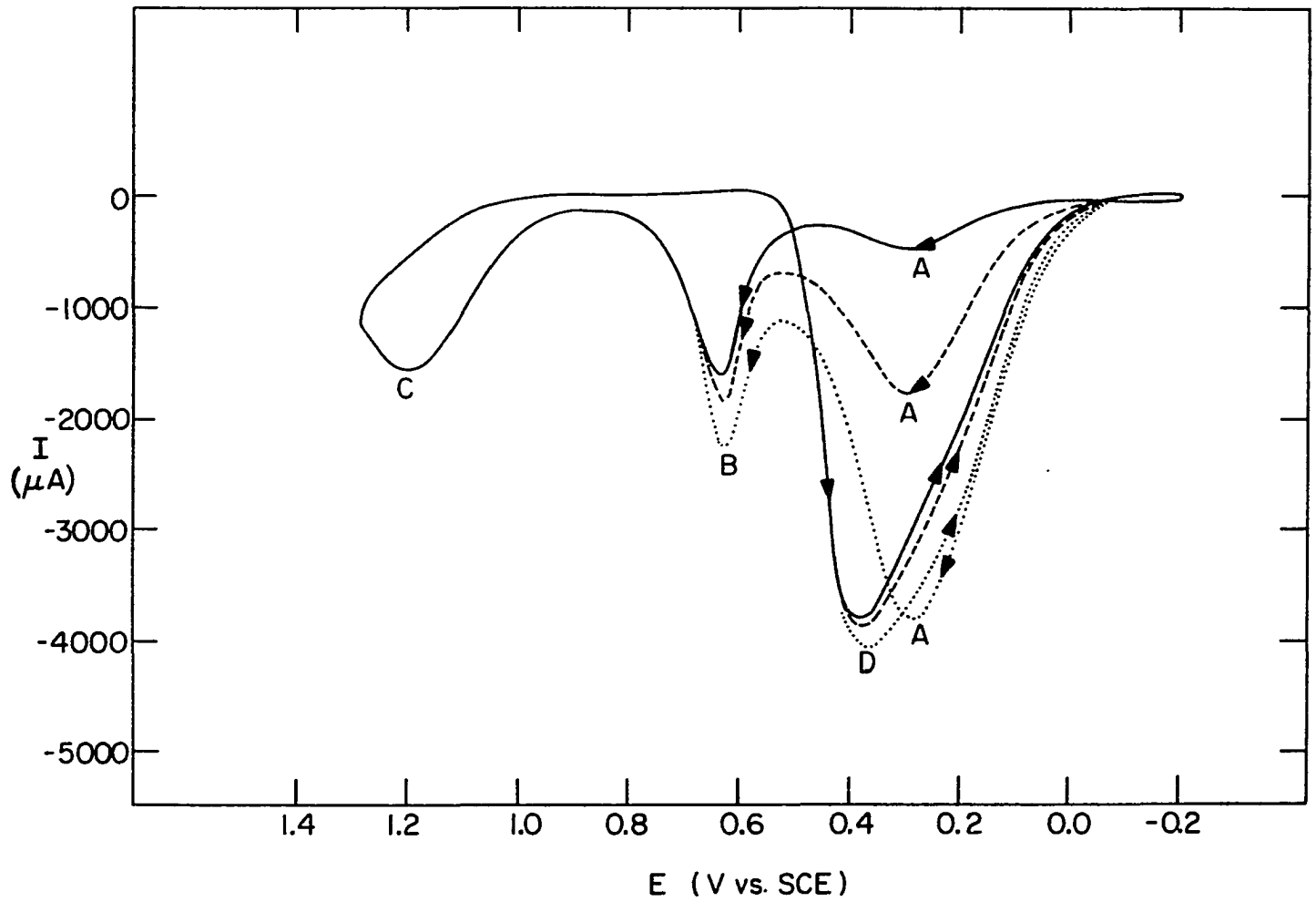
0
-1000
-2000
I
(μA)
-3000
-4000
-5000
1.4
1.2
1.0
0.8
0.6
0.4
0.2
0.0
-0.2
E (V vs. SCE)
A
A
A
B
C
D

Table III-10. Dependence of $I_{p,A}$, $I_{p,D}$, EF_A and EF_D on the concentration of Pb(II) during the electrochemical oxidation of 0.25 M HCOOH on the Pt-RDE in 0.50 M H_2SO_4

[Pb(II)] (μM)	$I_{p,A}$ (μA)	$I_{p,D}$ (μA)	EF_A	EF_D
0.0	500	3850	1.0	1.0
5.0	2350	3930	4.7	1.0
10.0	4450	4220	8.9	1.1
20.0	5750	4700	11.5	1.2
32.0	7550	5870	15.1	1.5
40.0	8950	6850	17.9	1.8
52.0	10700	8250	21.4	2.1
68.0	11800	9200	23.6	2.4
80.0	12500	9950	25.0	2.6
88.0	12800	10300	25.6	2.7

e. Cd ad-atoms The deposition and stripping of Cd ad-atoms has been discussed previously in this section. The dependence of θ_{Cd} on the concentration of Cd(II) is shown in Table III-11.

Table III-11. Dependence of θ_{Cd} on the concentration of Cd(II)

Cd(II) (μM)	θ_{Cd}
0.0	0.00
2.0	0.04
4.0	0.04
6.0	0.04
8.0	0.04
10.0	0.05
14.0	0.06
18.0	0.07
26.0	0.10
34.0	0.13
42.0	0.14
50.0	0.18

The effect of the Cd ad-atoms on the electrochemical oxidation of HCOOH is rather slight when compared to that of most of the other ad-atoms studied and the I-E curves are not shown. Peak A obtained during the positive potential scan is enhanced slightly by the Cd ad-atoms, but Peak D obtained during the negative potential scan is not affected. The dependence of the catalyzed peak-currents and the enhancement factors on the concentration of Cd(II) is shown in Table III-12 and Figures III-16, III-17, III-18 and III-19, respectively.

Table III-12. Dependence of $I_{p,A}$, $I_{p,D}$, EF_A and EF_D on the concentration of Cd(II) during the electrochemical oxidation of 0.25 M HCOOH on the Pt-RDE in 0.50 M H_2SO_4

[Cd(II)] (μM)	$I_{p,A}$ (μA)	$I_{p,D}$ (μA)	EF_A	EF_D
0.0	500	3550	1.0	1.0
2.0	925	3530	1.9	1.0
6.0	1350	3530	2.7	1.0
10.8	1580	3600	3.2	1.1
15.6	1630	3600	3.3	1.1
18.0	1650	3600	3.3	1.1
23.6	1700	3600	3.4	1.1

D. Summary and Conclusions

The enhancement effects of seven metal ad-atoms on the electrochemical oxidation of HCOOH were studied on the Pt-RDE. Of these metals, Tl, Bi, Pb and Hg were found to exert strong enhancement effects. Ag and Cd showed weak enhancement effects and Cu showed an inhibiting effect. Of the two procedures employed to control Θ_M,

Procedure B involving the standard addition of metal ions was found to be more advantageous than Procedure A involving deposition at a fixed potential because Procedure B afforded more reproducible control of Θ_M.

The trends in the maximum enhancement factor afforded by Pb, Tl, Bi, Cd and Ag for Peak A ($EF_{A,max}$) and Peak D ($EF_{D,max}$) are compared in Table III-13. Also given is a comparison of the trends in the values of Θ_M at a fixed concentration of the metal ions with the peak potential for the electrochemical stripping of the metal ad-atoms ($E_{p,strip}$).

Table III-13. Comparison of $E_{p,strip}$, Θ_M, $EF_{A,max}$ and $EF_{D,max}$ for Pb, Tl, Bi, Cd and Ag

$E_{p,strip}$	Ag > Tl > Bi > Pb > Cd
Θ_M	Tl > Pb > Bi > Ag > Cd
$EF_{A,max}$	Pb > Tl > Bi > Cd > Ag
$EF_{D,max}$	Bi > Pb > Tl > Cd > Ag

Comparisons of $E_{p,strip}$ and Θ_M reveal that, except for the case involving Ag, the metal ad-atoms with the most positive value of $E_{p,strip}$ tend to be more extensively deposited on the Pt substrate. This correlation is easily explained by the fact that deposition can occur for a longer portion of the cyclic sweep as the value of $E_{p,strip}$ increases. The anomaly of the Ag ad-atoms may have resulted from the fact that the method of adsorption substitution used for calculating Θ_M

may not be applicable to the Ag ad-atoms. Adzic et al. (67) reported that Ag ad-atoms do not appreciably suppress the adsorption of H-atoms on Pd until the surface of the Pd substrate has been almost saturated with respect to the Ag ad-atoms. This phenomenon is also observed in the deposition of the Ag ad-atoms on the Pt-RDE and is probably due to the preferential aggregation of the deposited Ag atoms leading to localized formations of bulk (stacked) layers of deposited Ag even before a monolayer of the Ag ad-atoms has been formed. This will lead to the low results for θ_{Ag} obtained by using the method of adsorption substitution, a method which is based on the assumption that each metal ad-atom deposited is responsible for blocking a Pt site which would otherwise be occupied by a H-atom.

Unfortunately, there is no direct correlation between the extent of surface coverage of the Pt-RDE by the metal ad-atoms (θ_M) and $EF_{A,max}$ or $EF_{D,max}$. This is probably due to the fact that the third body effect is not the only operable mechanism that leads to the enhancements observed. Each of the metals apparently has some specific catalytic activity towards the electrochemical oxidation of HCOOH since $EF_{A,max}$ and $EF_{D,max}$ are different for the different metals investigated.

The optimal coverages of the electrode by the metal ad-atoms that lead to maximum enhancement of Peak A and Peak D, $\theta_{M,A}$ and $\theta_{M,D}$, respectively, are shown in Table III-14. It is acknowledged here that the values of the optimal coverages given are estimates at best. Several difficulties preclude more accurate determination of the values of $\theta_{M,A}$ and $\theta_{M,D}$. First, these values are estimated by comparing the

plot of θ_M vs. $[M^{+n}]$ with the plot of EF_A or EF_D vs. $[M^{+n}]$. The former type of plot is obtained in the absence of HCOOH while the latter type of plot is obtained in the presence of HCOOH. The values of the optimal coverage thus obtained are valid only if HCOOH does not in any way interfere with the deposition of the ad-atoms. Secondly, because θ_M is potential dependent, it is extremely difficult to know the exact coverage of the electrode surface with respect to the metal ad-atoms at the peak potential of Peak A or Peak D.

Table III-14. Optimal coverage of the electrode, $\theta_{M,A}$ and $\theta_{M,D}$ corresponding to the maximum enhancement of Peak A and Peak D obtained during the electrochemical oxidation of HCOOH

Metal species	$\theta_{M,A}$	$\theta_{M,D}$
Pb	>0.75	>0.75
Tl	>0.75	0.75
Bi	0.40	>0.80
Cd	0.05	does not apply
Ag	0.05	does not apply

In most cases where the metal ad-atoms show enhancement effects towards the electrochemical oxidation of HCOOH, the optimal coverage of the electrode by the metal ad-atoms is greater than 0.5, the value which has been reported frequently by Adzic et al.

In several cases, such as Ag, Tl and Hg, where $E_{p,strip}$ for the metals is relatively positive, the enhancement effect of the metal ad-atoms is lost as soon as the potential of the electrode is scanned to a region where the formation of PtO commences, even though the metal ad-atoms are still present. This illustrates the importance of the Pt substrate in the electrochemical oxidation of HCOOH: the catalysts can exert their effects only when they co-exist with metallic Pt.

Several metals, including Bi, Pb and Tl which significantly enhance the anodic peaks obtained during the electrochemical oxidation of HCOOH, also appear to increase the reversibility of the oxidation processes that give rise to these peaks. This is a tentative conclusion based on the shift of the peak potential towards the negative values in the presence of the ad-atoms.

IV. EFFECTS OF METAL AD-ATOMS ON THE ELECTROCHEMICAL OXIDATION OF DEXTROSE ON PLATINUM AND GOLD ELECTRODES

A. Introduction

The electrochemical oxidation of dextrose (D-glucose) has been investigated by several workers (56, 57, 58, 59, 60) using Pt as the electrode material. However, the electrochemical oxidation of dextrose has apparently not been investigated on other electrode materials, and the effects of metal ad-atoms on the electrochemical oxidation of dextrose has never been studied. Such fundamental investigations are expected to contribute to the development of implantable biological fuel cells which are less prone to the loss of efficiency due to the fouling of the electrode material by the adsorbed products of glucose oxidation.

The purpose of this research is the examination of the electrochemical oxidation of dextrose on Pt and Au rotating-disc electrodes (RDE) in alkaline solutions. The effects of metal ad-atoms deposited at underpotential on the electrochemical oxidation of dextrose were investigated. The electroanalytical techniques applied to these studies included amperometry at constant potential and linear-sweep cyclic voltammetry. An adaptation of the latter, called "time-dependent voltammetry", was used to study slow changes in electrochemical response. All investigations were performed with NaOH as the supporting electrolyte because the electrochemical oxidation of dextrose was found not to occur in acidic media.

B. Experimental

1. Instrumentation

Several items were used in addition to those described in Section III.B. They included a Fisher Scientific combination pH electrode and a Corning 112 Research pH meter. A Heath-Schlumberger SR-225 strip-chart recorder was used to record amperometric and time-dependent voltammetric data. The Au-RDE (0.43 cm^2) was from Pine Instrument Co., Grove City, PA. The Pt-RDE was described in Section III.B.

2. Chemicals

Solutions of 0.35 M NaOH were prepared by dissolving reagent-grade NaOH pellets in triply distilled water. Stock solutions containing 1.00×10^{-3} M each of Tl(I), Pb(II) and Bi(III) were prepared from the corresponding nitrates as described in Section III.B. A 0.40 M stock solution of dextrose was prepared by dissolving 72 g ℓ^{-1} of reagent-grade dextrose in triply distilled water. The dextrose solution was then sterilized by boiling and stored in a refrigerator at 6°C. The stock solutions were prepared fresh every two weeks. Buffer solutions at pH 4.00 and pH 7.00 from Fisher Scientific Co. were used for calibration of the pH meter. Solutions of 0.35 M and 5.0 M NaOH, or concentrated and 0.35 M HNO_3 were used for pH adjustments in the studies involving variations of pH.

3. Procedures

Three techniques were used in the study of the electrochemical oxidation of dextrose on the Pt-RDE and the Au-RDE. They are described in the following sections. The batch-type electrochemical cell described in Section III.B was used in these experiments and all solutions were deaerated with N_2 as described in Section III.B.

a. Cyclic voltammetry This technique was used to perform fundamental studies on the electrochemical oxidation of dextrose and to characterize the effects of various metal ad-atoms on the electrochemical oxidation of this compound. The coverage of the Pt-RDE and the Au-RDE by the metal ad-atoms (θ_M) was controlled by standard additions of the corresponding metal ions to the solutions of dextrose in 0.10 M or 0.35 M NaOH. Other experimental parameters, including concentration of dextrose in solution, rotation speed (W) of the electrode, positive scan limit (E_+) and negative scan limit (E_-), were also varied for cases involving selected metal ad-atoms and their effects on the electrochemical oxidation of dextrose were observed.

b. Amperometry The current obtained during the electrochemical oxidation of dextrose in the presence and absence of Bi ad-atoms was measured at an applied potential maintained constant at the value corresponding to E_p of the anodic peak for dextrose observed on the positive potential sweep. Experimental parameters such as W, concentration of dextrose and Bi(III) were varied and their effects on the electrochemical oxidation of dextrose studied. Bi ad-atoms have a strong tendency to remain adsorbed on the surface of the electrode in an

alkaline medium, so the Pt electrode was immersed in concentrated HNO_3 before each run. The concentrated HNO_3 served to oxidatively desorb the Bi ad-atoms from the surface of the electrode.

c. Time-dependent voltammetry This is a technique devised for this research which is intermediate between linear-sweep cyclic voltammetry and amperometry. The potential of the electrode was continuously scanned in a cyclic fashion as in linear-sweep cyclic voltammetry. However, the I-E curves obtained were recorded on a strip-chart recorder instead of a x-y recorder. This is a convenient method to monitor the rates of changes in the peak currents for a large number of cyclic scans when the I-E curves vary slowly with time. When the chart speed on the strip-chart recorder was relatively slow, e.g., 1 in min^{-1}, and the rate of potential scan was relatively fast, e.g., 5-10 V min^{-1}, the peak currents of the peak-shaped I-E curves were recorded on the strip-chart recorder as a series of closely spaced repetitive current spikes. The anodic and cathodic current spikes that corresponded to the anodic and cathodic peaks of the original I-E curves were easily distinguishable from each other because they were recorded on different sides of the zero current axis. In the cases where more than one anodic or cathodic peaks were present, the current spikes showed up as repetitive doublets and triplets, etc. The relative separations between the individual spikes in the set depended on the separations of the peaks in the original I-E curve. Since it was unlikely that the spikes would be of equal height all through a particular recording, the individual spikes in the set were easily distinguishable.

Time-dependent voltammetry was used to study the electrochemical oxidation of dextrose in the absence and presence of Bi ad-atoms. Some of the experiments involved deposition of the Bi ad-atoms from solutions which contained Bi(III) in the presence of dextrose. In other experiments, the RDE was precoated with submonolayer amounts of Bi ad-atoms from a Bi(III) solution prior to being transferred to dextrose solutions. Experimental parameters such as W and the concentration of dextrose and Bi(III) were also varied in these experiments and the time-dependent change of peak currents observed.

4. Solubility of heavy metal ions in 0.10 M and 0.35 M NaOH

The solubility product constants (k_{sp}) of most heavy-metal hydroxides are very small. For example, the k_{sp} of $Pb(OH)_{2(s)}$ is 2.5×10^{-16}, and the solubility of $Pb(OH)_{2(s)}$ calculated from this value of k_{sp} is 2.5×10^{-14} M and 2.0×10^{-15} M in 0.10 and 0.35 M NaOH, respectively. However, the precipitation of Pb(II) as $Pb(OH)_{2(s)}$ was not observed visually for the alkaline supporting electrolyte even when the formal concentration of Pb(II) exceeded 1.00×10^{-5} M. The same observation was made for Tl(I), Cd(II) and Bi(III). Although the solubility of TlOH in 0.10 M and 0.35 M NaOH is 13.46 M and 3.85 M, respectively, as calculated on the basis of k_{sp}, the fact that Pb(II), Cd(II) and Bi(III) did not precipitate in 0.10 M or 0.35 M NaOH cannot be explained on the basis of the k_{sp} value of the individual hydroxides. However, $Pb(OH)_{2(s)}$, for example, undergoes complexometric reaction with additional OH^- to form the soluble species $Pb(OH)_3^-$, as described by Equation IV-1.

$$Pb(OH)_{2(s)} + OH^-_{(aq)} \rightleftharpoons Pb(OH)_3^-{}_{(aq)} \qquad \text{(IV-1)}$$

$$K_1 = \frac{[Pb(OH)_3^-]_{(aq)}}{[OH^-]_{(aq)}} = 5.0 \times 10^{-2} \qquad \text{(IV-2)}$$

Calculations based on the formation constant K_1 yielded the values of 5.0×10^{-3} M and 1.8×10^{-2} M for the formal solutions of Pb(II) in 0.10 M and 0.35 M NaOH, respectively. This is in agreement with the experimental observation that Pb(II) did not undergo precipitation as $Pb(OH)_2$ even when the formal concentration of Pb(II) exceeded 1.00×10^{-5} M. The absence in the literature of values for the formation constants (K_1) for the complexometric reactions between Bi(III) and Cd(II) with OH^- made impossible any attempts to calculate their solubilities in NaOH. However, it can be assumed that the complexometric reactions prevented the precipitation of Bi(III) and Cd(II) as the insoluble hydroxides under the experimental conditions employed.

C. Electrochemical Oxidation of Dextrose on the Pt-RDE in 0.35 M NaOH: Effects of Pb, Tl and Bi Ad-atoms Investigated Using Cyclic Voltammetry

1. Residual current-potential (I-E) curve

The general shape of the residual I-E curve obtained for the Pt-RDE in 0.35 M NaOH is virtually identical to that obtained in 0.10 M H_2SO_4 (see Figure III-1). However, the magnitudes of the currents obtained

in the alkaline medium are one-half or less than those obtained for the corresponding electrochemical processes in acidic media under identical conditions.

The available potential range of the Pt-RDE in 0.35 M NaOH, limited by the oxidation of H_2O and the reduction of H^+ on the positive and negative potential scan limits, respectively, is approximately 0.6V to -1.0V vs. SCE. This represents a -0.7V shift from the potential range of the Pt-RDE obtained in 0.10 M H_2SO_4.

2. The effect of pH on the electrochemical oxidation of dextrose

Initial studies of the electrochemical behavior of dextrose were performed with 0.10 M H_2SO_4 as the supporting electrolyte. However, no faradaic current attributable to the electrochemical oxidation of dextrose is obtained in 0.10 M H_2SO_4, i.e., the I-E curve of the Pt-RDE is the same in the absence as well as the presence of dextrose.

The electrochemical oxidation of dextrose was then investigated under different conditions of pH. The pH of a solution containing 5 mM dextrose in 0.10 M H_2SO_4 was raised progressively by the addition of aliquots of 0.35 M NaOH. The I-E curves of the Pt-RDE was recorded after each addition of NaOH. The settings of the scan limits (E_+ and E_-) on the potentiostat were shifted progressively more negative after each pH adjustment. The potential range, i.e., $E_+ - E_-$, was kept at a constant value of 1.5V throughout this set of experiments.

There is no well-defined anodic peak associated with the electrochemical oxidation of dextrose on the Pt-RDE below pH 10. An anodic peak, A, shown in Figure IV-1, at a potential coincidental with the

commencement of PtO formation is observed during the positive potential sweep as the pH of the solution is raised above a value of 10. The height of Peak A increases and a second peak, B, emerges at electrode potentials slightly more negative than Peak A as the pH of the solution is further raised. Anodic peaks C and D are also observed during the negative potential sweep. Subsequent investigations were performed with NaOH as the supporting electrolyte because well-defined anodic peaks for the electrochemical oxidation could be obtained only in an alkaline medium.

3. Deposition of metal ad-atoms on the Pt-RDE in 0.35 M NaOH

The deposition behavior of many metal species, including Tl, Bi and Cd in 0.35 M NaOH, were found to differ from those observed for 0.10 M H_2SO_4. Equilibrium between the metal ad-atoms on the electrode and the metal ions in solution is observed to be established very quickly for a fixed concentration of the metal ions when 0.10 M H_2SO_4 is used as the supporting electrolyte. This is reflected in the fact that the peak currents for the stripping peaks ($I_{p,strip}$) associated with the oxidation of the metal ad-atoms are observed to be well-established even after only one cycle of the potential-sweep between the scan limits and remain constant throughout subsequent scans. On the other hand, $I_{p,strip}$ for Bi, Tl and Cd in 0.35 M NaOH increases progressively towards some limiting value with each subsequent potential scan. In general, 10 cycles or more of the potential sweep are required to attain the limiting value of the peak currents. The I-E curves obtained for the Pt-RDE in alkaline solutions of Bi(III),

Figure IV-1. I-E curve of the Pt-RDE in 0.35 M NaOH containing 0.25 M dextrose

Electrode rotation speed (W): 400 rev min^{-1}

Potential scan rate (ϕ): 6 V min^{-1}

A, B, C, D and E: anodic peaks

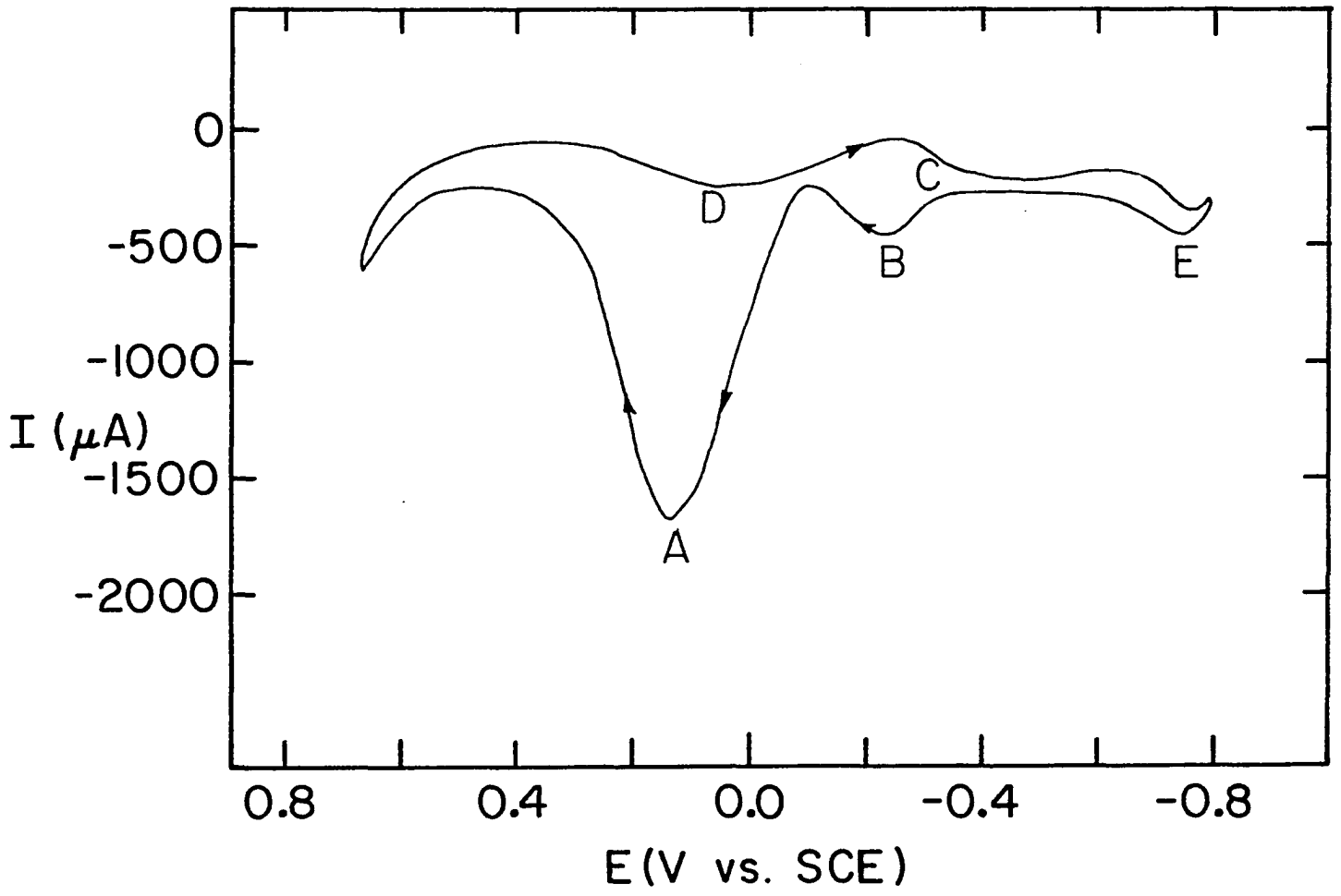
0
-500
-1000
-1500
-2000
I (μA)
A
B
C
D
E
0.8
0.4
0.0
-0.4
-0.8
E(V vs. SCE)

Tl(I), Cd(II) and Pb(II) are shown in Figures IV-2, IV-3, IV-4 and IV-5, respectively. In the cases of Bi(III), Tl(I) and Cd(II), the direction of the arrows in the corresponding figures indicates the direction of changes in the current values with increasing number of scans. In each of these cases, Peak P associated with the reduction of PtO increases in a synchronous manner with the increases in $I_{p,strip}$ of Peak S. A well-defined wave, W, is obtained in the case involving Tl (see Figure IV-3) between 0.1V and 0.25V vs. SCE during the negative potential sweep. The peaks associated with the adsorption and desorption of hydrogen atoms between -0.6V and -0.8V vs. SCE decrease progressively in height with each additional cycle.

The phenomenon described above points to the fact that the coverage of the Pt-RDE by the metal ad-atoms increases with time at a fixed concentration of the metal ions even when the potential of the electrode is cycled in a reproducible manner. This can be explained by the speculation that the metal ad-atoms are not desorbed from the surface of the electrode after they have been oxidized. The metal ad-atoms are probably oxidized to an insoluble hydroxide or oxide film, such as Bi_2O_3, Tl_2O or CdO. The insoluble oxide-films can be reduced back to the metal ad-atoms upon reversal of the direction of the potential scan to more negative potentials. This probably is the cause for the cathode wave W in the case of Tl. For Bi and Cd, the cathode currents associated with the reduction of the corresponding oxides are superimposed on Peak P, associated with the reduction of PtO, resulting in an increase in the value of $I_{p,P}$.

Figure IV-2. I-E curve of the Pt-RDE in 0.35 M NaOH containing 4.00×10^{-7} M Bi(III)

Electrode rotation speed (W): 400 rev min^{-1}

Potential scan rate (ϕ): 6 V min^{-1}

S: Bi oxidation peak

P: Pt oxide reduction peak

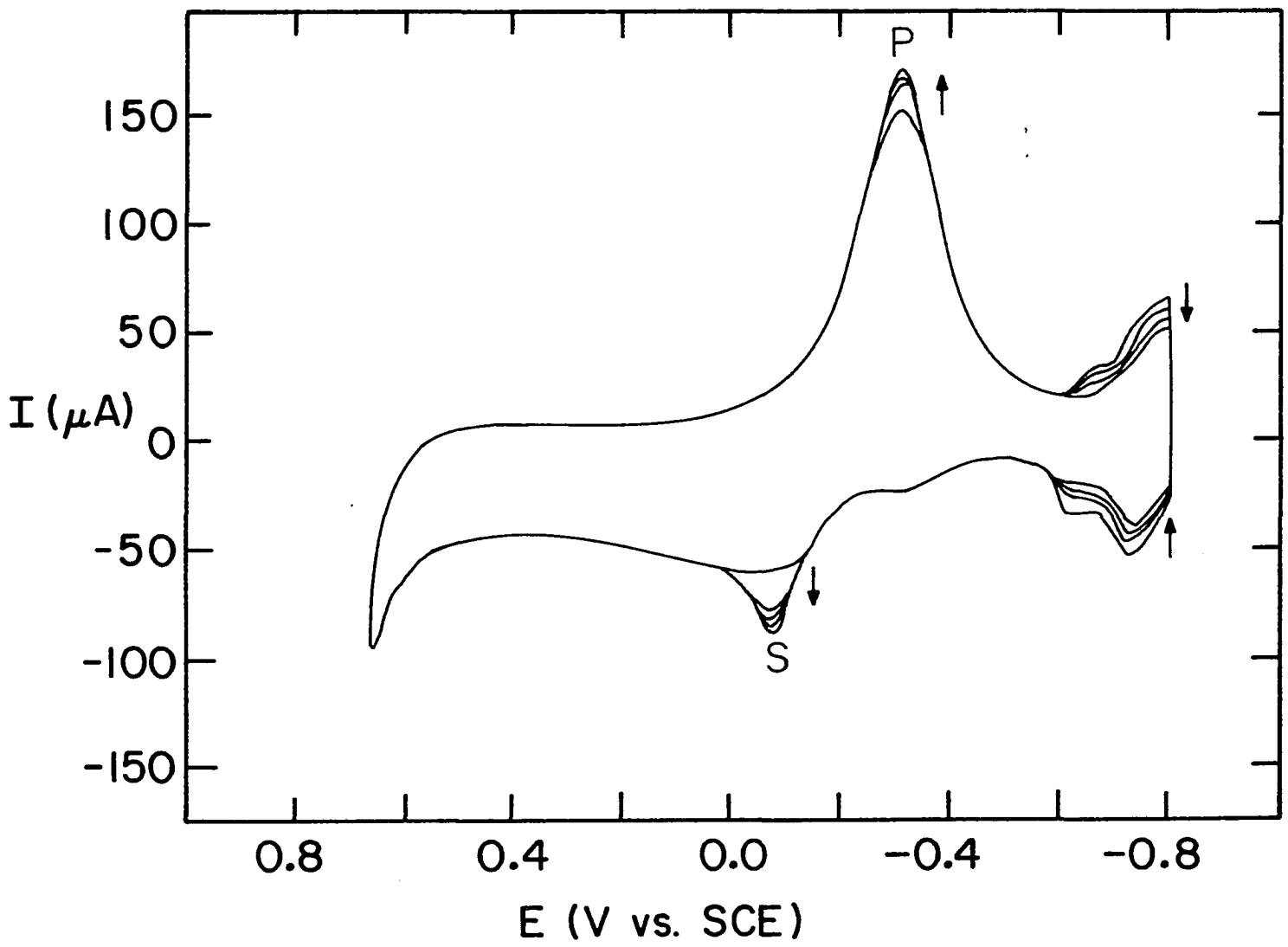
P
S
150
100
50
0
-50
-100
-150
I (μA)
0.8
0.4
0.0
-0.4
-0.8
E (V vs. SCE)

Figure IV-3. I-E curve of the Pt-RDE in 0.35 M NaOH containing 8.00×10^{-7} M Tl(I)

Electrode rotation speed (W): 400 rev min^{-1}

Potential scan rate (ϕ): 6 V min^{-1}

P: Pt oxide reduction peak

W: Tl oxide reduction wave

S: Tl oxidation peak

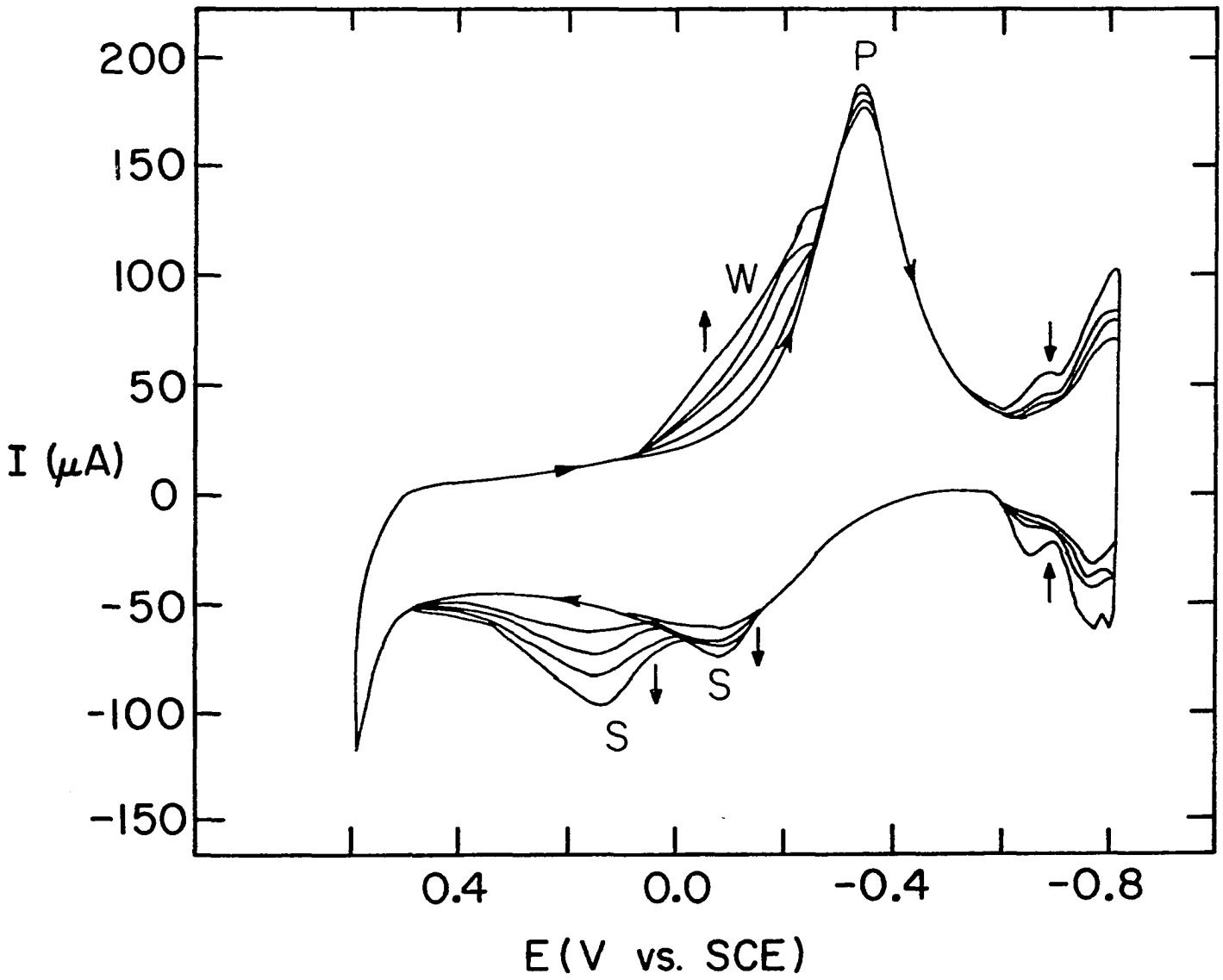
200
150
100
50
0
-50
-100
-150
I (μA)
P
W
S
S
0.4
0.0
-0.4
-0.8
E(V vs. SCE)

Figure IV-4. I-E curve of the Pt-RDE in 0.35 M NaOH containing 4.00×10^{-7} M Cd(II)

Electrode rotation speed (W): 400 rev min^{-1}

Potential scan rate (ϕ): 6 V min^{-1}

P: Pt oxide reduction peak

S: Cd oxidation peak

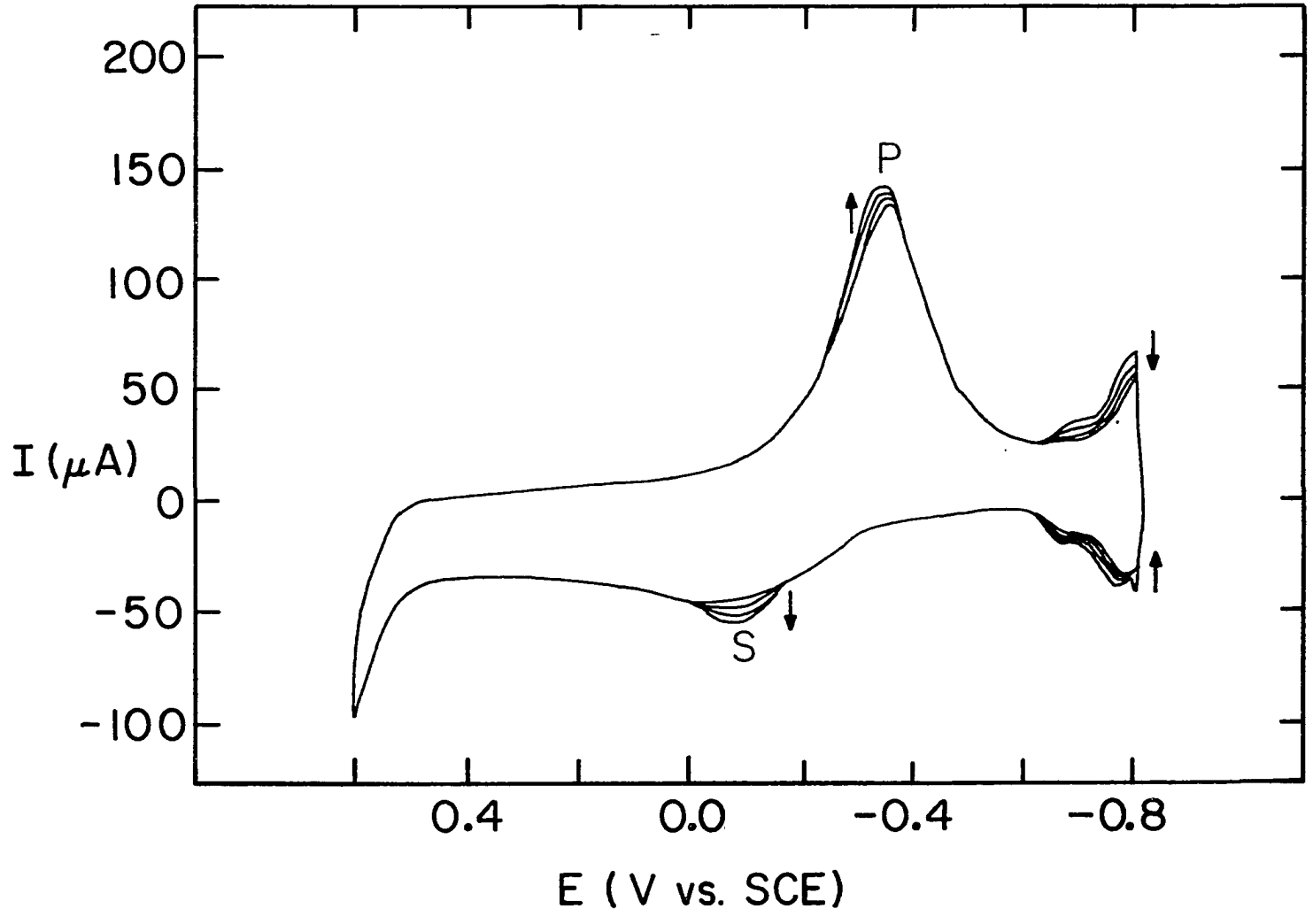
200
150
100
50
0
-50
-100
I (μA)
P
S
0.4
0.0
-0.4
-0.8
E (V vs. SCE)

Figure IV-5. I-E curve of the Pt-RDE in 0.35 M NaOH in the absence and the presence of Pb(II)

Electrode rotation speed (W): 400 rev min^{-1}

Potential scan rate (ϕ): 6 V min^{-1}

P: Pt oxide reduction peak

S: Pb oxidation peak

——— 0.0 M Pb(II)

------- 6.0×10^{-6} M Pb(II)

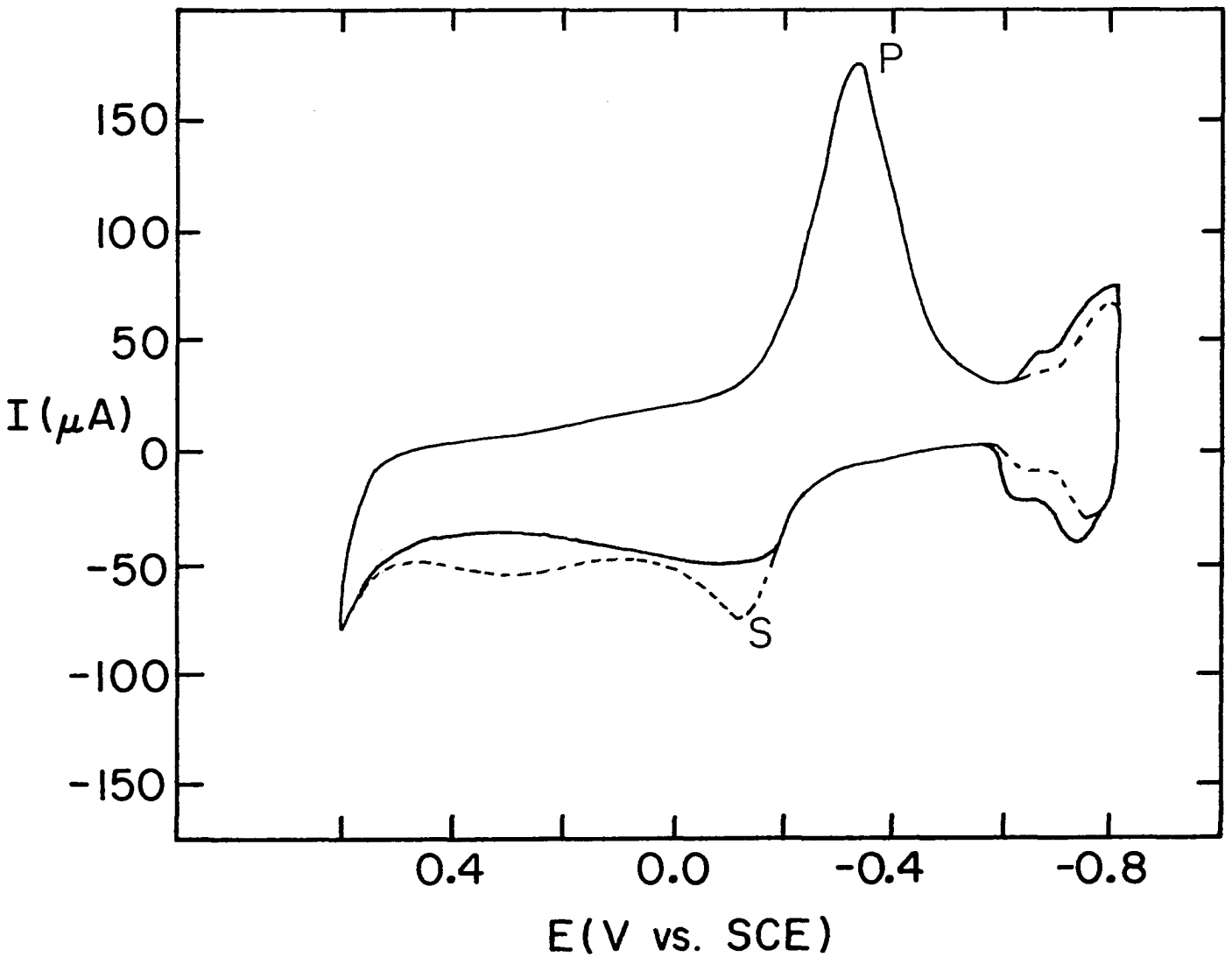
P
S
150
100
50
0
-50
-100
-150
I(μA)
0.4
0.0
-0.4
-0.8
E(V vs. SCE)

The deposition of additional amounts of metal ad-atoms occurs during each successive cycle of potential sweep when the potential of the electrode is in a region sufficiently negative for the deposition of the metal ad-atoms to occur. Therefore, the metal ad-atoms continue to accumulate until a maximum value of θ_M is achieved, as dictated by the equilibrium between the metal ad-atoms on the surface of the electrode and the metal ions in solution, after which further accumulation of the metal ad-atoms does not occur. If the concentration of metal ions in the solution is increased, the values of the peak currents is, likewise, increased with successive potential cycles until reaching a new constant value for which equilibrium is re-established.

The fact that the metal ad-atoms are not completely desorbed from the surface of the electrode following the stripping process was proven by an experiment which involved the precoating of the Pt-RDE with Bi ad-atoms in the absence of dextrose. After a reproducible coverage was achieved, the electrode was removed from the plating solution, rinsed thoroughly with deionized water and placed in a Bi(III)-free solution of 0.35 M NaOH. I-E curves were then obtained for which the stripping peak of the Bi ad-atoms was observed to decrease slowly in height during subsequent cycling of the electrode potential. At least 50% of the original amount of Bi ad-atoms was still present on the electrode surface after 20 min of potential scanning, during which the potential of the electrode had been cycled approximately 120 times.

The continuous accumulation of metal ad-atoms in an alkaline solution is not observed for Pb. The I-E curve for Pb(II) does not change with time in 0.35 M NaOH after the first cyclic scan.

4. The dependence of θ_M on the concentration of the metal ions in 0.35 M NaOH

The coverage of the Pt-RDE by metal ad-atoms (θ_M) was determined for Cd, Tl, Bi and Pb at various concentrations of the corresponding metal ions, using the method of adsorption substitution as described in Section III.C.4. The dependence of θ_M on the concentration of the metal ions is shown in Tables IV-1, IV-2, IV-3 and IV-4, and plotted in Figure IV-6.

Table IV-1. Dependence of θ_{Bi} on the concentration of Bi(III) in 0.35 M NaOH

[Bi(III)] (μM)	θ_{Bi}
0.00	0.00
0.50	0.08
1.00	0.19
1.50	0.25
2.00	0.44
3.00	0.65
3.50	0.77

Table IV-2. Dependence of θ_{Tl} on the concentration of Tl(I) in 0.35 M NaOH

[Tl(I)] (μM)	θ_{Tl}
0.00	0.00
0.40	0.13
0.80	0.36
1.20	0.52
1.60	0.64
2.40	0.73
3.20	0.75
4.60	0.80

Table IV-3. Dependence of θ_{Cd} on the concentration of Cd(II) in 0.35 M NaOH

[Cd(II)] (μM)	θ_{Cd}
0.00	0.00
0.40	0.23
0.80	0.23
1.20	0.26
2.00	0.29
2.80	0.31
5.20	0.34

Table IV-4. Dependence of θ_{Pb} on the concentration of Pb(II) in 0.35 M NaOH

[Pb(II)] (μM)	θ_{Pb}
0.00	0.00
1.20	0.05
3.20	0.13
6.00	0.22
8.00	0.26
10.60	0.38
12.00	0.39
14.80	0.46
16.00	0.48
17.20	0.52
20.80	0.58
23.20	0.61

Comparison of the data presented in Figure IV-6 with those in Figure III-14 reveals that, for identical concentration of the metal ions, the surface coverage of the electrode with respect to the metal ad-atoms is much more extensive for 0.35 M NaOH than for 0.10 M H_2SO_4. This is especially true for Tl, Bi and Cd, which are not completely removed from the electrode by the stripping process. For example, at a concentration of 4.0 μM Tl(I), θ_{Tl} is 0.10 for 0.10 M H_2SO_4 and 0.80 for 0.35 M NaOH. The value of θ_M for Pb, which does not accumulate on the electrode surface, is approximately 0.15 for a solution of 0.35 M NaOH containing 4.0 μM Pb(II).

Figure IV-6. Dependence of θ_M on $[M^{+n}]$ for the electrodeposition of metal ad-atoms on the Pt-RDE

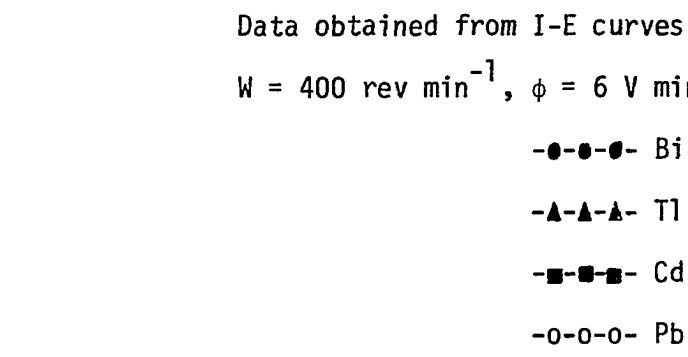

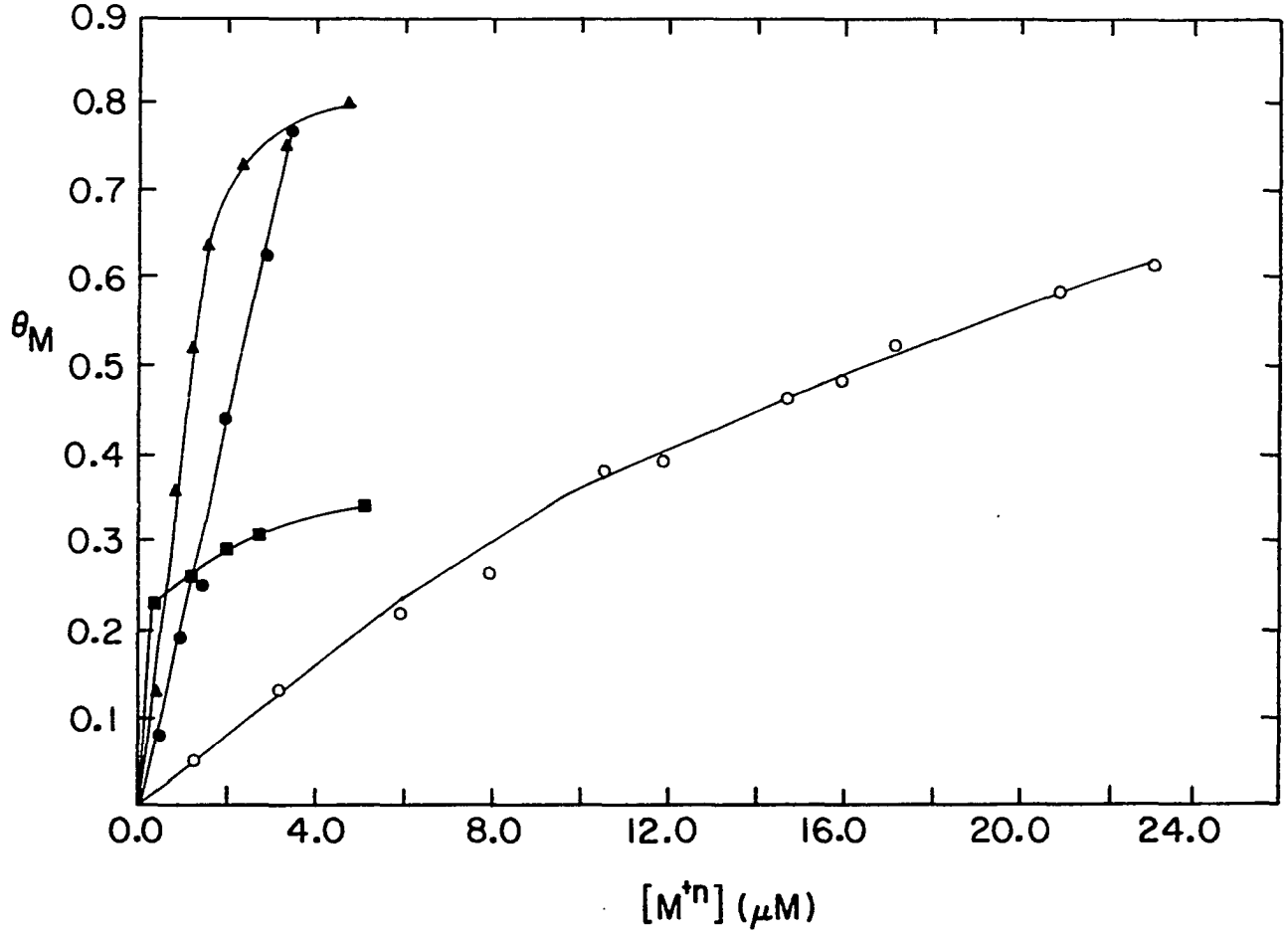
0.9
0.8
0.7
0.6
0.5
0.4
0.3
0.2
0.1
θ_M
0.0
4.0
8.0
12.0
16.0
20.0
24.0
$[M^{+n}]$ (μM)

5. The effects of Bi, Pb and Tl on the electrochemical oxidation of 0.25 M dextrose on the Pt-RDE in 0.35 M NaOH

The effects of Bi, Pb and Tl on the electrochemical oxidation of 0.25 M dextrose was investigated in 0.35 M NaOH. θ_M was controlled by standard addition of the corresponding metal ions to the solution of 0.25 M dextrose. The effects of the metal ad-atoms were expected to increase with time for a fixed concentration of the metal ions because Bi, Tl and Cd had been found to accumulate on the electrode surface. This was observed experimentally and, therefore, the I-E curves were recorded only after they had become reproducible following each addition of the metal ions.

Six anodic peaks are observed in the electrochemical oxidation of dextrose in the potential range between 0.6V and -0.8V vs. SCE, as shown in Figure IV-1. Peaks A and B, both obtained during the positive potential sweep, are significantly larger than the remaining peaks. Substantial anodic current is also observed in the potential region more positive than 0.4V vs. SCE in the presence of dextrose. The qualitative aspects of the effects of Bi, Pb, Tl and Cd on the electrochemical oxidation of dextrose are discussed in the following sections.

a. Bi ad-atoms The effect of Bi ad-atoms on the electrochemical oxidation of dextrose is shown in Figure IV-7. The values of $I_{p,B}$ and $I_{p,C}$ are both increased by the presence of the Bi ad-atoms. On the other hand, $I_{p,A}$ obtained during the positive scan is decreased. $E_{p,B}$ is shifted in a negative direction in the presence of the Bi ad-atoms. The anodic current obtained during positive potential scan

Figure IV-7. I-E curve of the Pt-RDE in 0.35 M NaOH containing 0.25 M dextrose and various concentrations of Bi(III)

Electrode rotation speed (W): 400 rev min^{-1}

Potential scan rate (ϕ): 6 V min^{-1}

A, B, C, D and E: anodic peaks

——— 0.0 μM Bi(III)

------- 2.0 μM Bi(III)

····· 4.0 μM Bi(III)

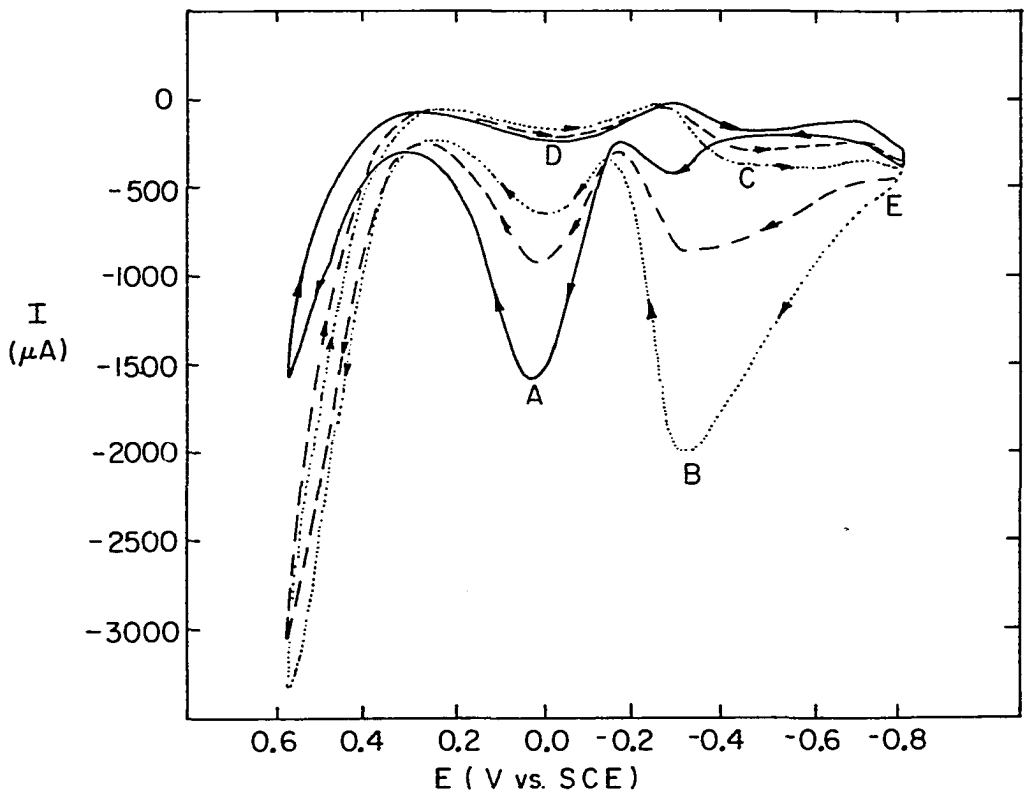
0
-500
-1000
-1500
-2000
-2500
-3000
I
(μA)
A
B
C
D
E
0.6
0.4
0.2
0.0
-0.2
-0.4
-0.6
-0.8
E (V vs. SCE)

in the region between -0.8V and $E_{p,B}$ also increases more rapidly with increasing potential as the concentration of Bi(III) is raised. This indicates clearly that the Bi ad-atoms have increased the rate of the anodic process associated with Peak B.

The role of the metal ad-atoms in decreasing the amount of adsorbed poisonous species formed during the oxidation of HCOOH has been discussed in previous sections. Poisons are also formed during the electrochemical oxidation of dextrose and it is likely that the Bi ad-atoms either suppress the formation of the poisons or increase the rate of desorption of the poisons. It can be speculated that Peak B is associated with the main oxidation process of surface-adsorbed dextrose to products of higher oxidation states which are then desorbed from the electrodes. Peak A is associated with the oxidation of the strongly bound poisons adsorbed on the surface of the Pt-RDE. Because the Bi ad-atoms decrease the loss of electrode activity resulting from poisons adsorbed on the electrode surface, Peak A associated with the electrochemical removal of the poisons decreases in size with increases in the fractional coverage of the electrode surface by the Bi ad-atoms.

The current of Peak B decreases sharply during the positive potential scan after passing $E_{p,B}$, even when Bi ad-atoms are present. The fall-off of the current of Peak B is essentially complete at -0.1V *vs.* SCE. Inspection of Figure IV-2 reveals that the fall-off of the current of Peak B coincides with the oxidation of the Bi ad-atoms to the insoluble oxide (perhaps Bi_2O_3) and the oxidation of the Pt substrate to PtO. It is concluded that the Bi species must exist as

the metal ad-atoms on a reduced Pt substrate in order to exert the enhancement effects observed during the electrochemical oxidation of dextrose.

The anodic peak C obtained during the negative potential scan is enhanced slightly with increases in the concentration of Bi(III) up to 60 μM. As the concentration of Bi(III) is raised above 60 μM, a very sharp peak suddenly appears in the potential region of Peak C. The height of this peak remains unchanged as the Bi(III) concentration is increased further.

b. Pb ad-atoms The effects of Pb ad-atoms on the electrochemical oxidation of dextrose are qualitatively identical to those observed with the Bi ad-atoms described in the previous section. The enhancement of $I_{p,B}$ and decrease of $I_{p,A}$ with increases in the concentration of Pb(II) are observed at low concentrations of Pb(II), while a decrease in $I_{p,B}$ is observed at high concentrations of Pb(II). Peak B is shifted slightly in the negative direction along the potential axis in the presence of the Pb ad-atoms.

c. Tl ad-atoms The effects of the Tl ad-atoms on the electrochemical oxidation of dextrose are qualitatively identical to those observed with Pb and Bi ad-atoms and will not be discussed here.

d. Other metal ad-atoms Cd, Cu and Zn ad-atoms were also investigated for their effects on the electrochemical oxidation of dextrose. All these metal species were found to inhibit the oxidation and no further study was performed with these metals.

6. Dependence of the enhancement obtained during the electrochemical oxidation of dextrose on the concentration of the metal ions

The enhancement effect of the metal ad-atoms on the electrochemical oxidation of dextrose was characterized quantitatively by two methods. The first method, A, involved the plotting of the enhancement factor, EF, versus the concentration of the metal ions. The second method, B, involved the plotting of the coulombic enhancement factor, QEF, versus the concentration of the metal ions. QEF is defined as the ratio of the charge under the catalyzed peak to the charge under the uncatalyzed peak, i.e., $QEF_B = Q_{catalyzed}/Q_{uncatalyzed}$. The values of Q were obtained by integration of the areas under the anodic peaks. Methods A and B were applied to the characterization of the effects of the metal ad-atoms on the anodic peak B obtained in the positive potential scan.

a. Method A The enhancement factor (EF) and the value of $I_{p,B}$ are shown in Tables IV-5, IV-6, IV-7 and Figure IV-8 as a function of the concentration of Bi(III), Pb(II) and Tl(I).

Table IV-5. Dependence of $I_{p,B}$ and EF_B on [Bi(III)] obtained during the electrochemical oxidation of 0.25 M dextrose on the Pt-RDE in 0.35 M NaOH

[Bi(III)] (μM)	$I_{p,B}$ (μA)	EF_B
0.00	188	1.0
1.00	363	1.9
2.50	788	4.2
4.00	1750	9.3
5.00	2580	13.7

Table IV-5. (Continued)

[Bi(III)] (μM)	$I_{p,B}$ (μA)	EF_B
6.00	3700	19.7
7.00	5100	27.1
8.00	6750	35.9
9.00	8500	45.2
10.00	11350	60.4
12.00	13000	69.2
14.00	15400	81.7
16.00	17000	90.4
18.00	18300	97.1
20.00	19000	101.1
26.00	19800	105.1
30.00	19800	105.1
38.00	19000	101.1
55.00	17000	90.4
65.00	15100	80.5
75.00	13900	73.8
90.00	13000	69.2

Table IV-6. Dependence of $I_{p,B}$ and EF_B on [Pb(II)] obtained during the electrochemical oxidation of 0.25 M dextrose on the Pt-RDE in 0.35 M NaOH

[Pb(II)] (μM)	$I_{p,B}$ (μA)	EF_B
0.00	188	1.0
2.00	575	3.1
3.00	1430	7.6
5.50	3400	18.1
6.50	5250	27.9
7.50	5750	30.6
8.50	6750	35.9
10.50	8050	42.8
14.50	9350	49.7
16.00	9450	50.0
22.00	9000	47.9
30.00	7550	40.2
38.00	6150	32.7

Table IV-7. Dependence of $I_{p,B}$ and EF_B on [Tl(I)] obtained during the electrochemical oxidation of 0.25 M dextrose on the Pt-RDE in 0.35 M NaOH

[Tl(I)] (μM)	$I_{p,B}$ (μA)	EF_B
0.00	250	1.0
1.00	688	2.8
2.00	2230	8.9
2.50	3250	13.0
3.00	4400	17.6
3.50	5500	22.0
4.00	6350	25.4
5.00	7000	28.0
6.00	6700	26.8
7.00	5700	22.8
8.00	4700	18.8
9.00	3800	15.2
11.00	2400	9.6

Examination of Tables IV-5 to IV-7 and Figure IV-8 reveals that the maximum enhancement effect of the metal ad-atoms decreases in the order Bi > Pb > Tl, ranging from 105 for Bi to 28 for Tl. The concentrations of the metal ions that produce the maximum enhancement are 26 μM, 16 μM and 5 μM for Bi(III), Pb(II) and Tl(I), respectively.

b. Method B The coulombic enhancement factor, QEF_B, and the charge under Peak B, Q_B, are given in Tables IV-8, IV-9, IV-10 and Figure IV-9 as a function of the concentration of the metal ions.

Figure IV-8. Dependence of EF_B on the concentration of metal ions for the electrochemical oxidation of dextrose

Electrode: Pt-RDE

Supporting electrolyte: 0.35 M NaOH

[dextrose]: 0.25 M

Electrode rotation speed (W): 400 rev min^{-1}

Potential scan rate (ϕ): 6 V min^{-1}

-●-●-●- Bi(III)

-▲-▲-▲- Pb(II)

-■-■-■- Tl(I)

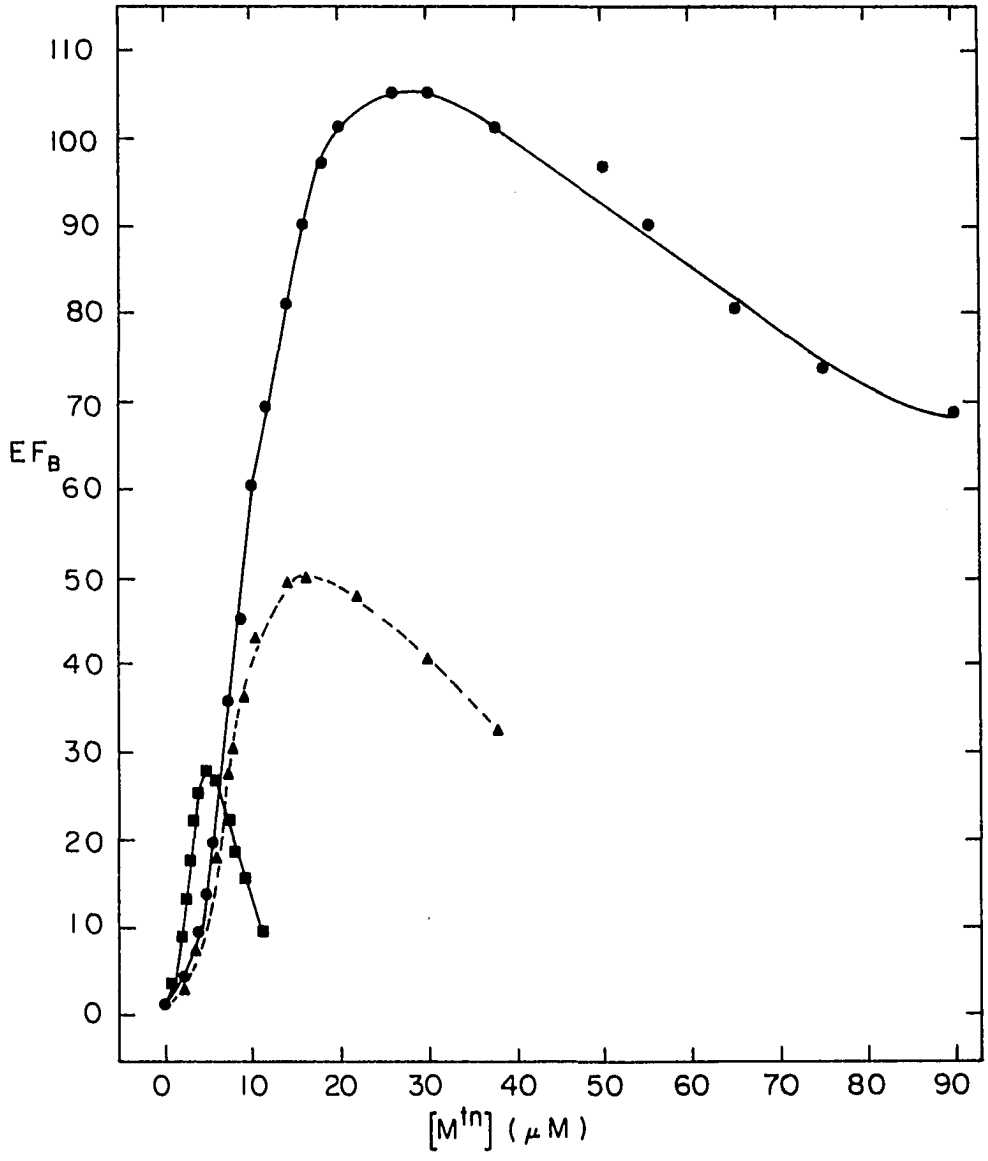
110
100
90
80
70
EF$_B$
60
50
40
30
20
10
0
0
10
20
30
40
50
60
70
80
90
[M^{tn}] (μM)

Table IV-8. Dependence of Q_B and QEF_B on the concentration of Bi(III), obtained during the electrochemical oxidation of 0.25 M dextrose on the Pt-RDE in 0.35 M NaOH

[Bi(III)] (μM)	Q_B (μ coulombs)	QEF_B
0.00	240	1.0
2.50	2790	11.5
5.00	7550	31.2
7.00	14100	58.2
9.00	23900	98.7
10.00	33800	140.8
12.06	43500	181.3
14.00	51200	213.3
16.00	63900	266.3
18.00	67600	281.7
20.00	72600	302.5
26.00	83000	345.8
30.00	83300	347.1
38.00	79400	330.8
51.00	70600	294.2
53.00	63100	262.9
55.00	60700	252.9
65.00	49000	204.2
75.00	43700	182.1
90.00	39300	163.8

Table 9. Dependence of Q_B and QEF_B on the concentration of Pb(II), obtained during the electrochemical oxidation of 0.25 M dextrose on the Pt-RDE in 0.35 M NaOH

[Pb(II)] (μM)	Q_B (μ coulombs)	QEF_B
0.00	338	1.0
2.00	2140	6.3
3.00	5160	15.3
4.50	9480	28.0
5.50	12600	37.3
10.50	24400	72.2
14.50	29300	86.7
16.00	31100	92.0
22.00	28000	82.8
30.00	21300	63.0
38.00	15600	46.2

Table IV-10. Dependence of Q_B and QEF_B on the concentration of Tl(I), obtained during the electrochemical oxidation of 0.25 M dextrose on the Pt-RDE in 0.35 M NaOH

[Tl(I)] (μM)	Q_B (μ coulombs)	QEF_B
0.00	372	1.0
2.00	7770	20.9
3.00	16100	43.3
5.00	26300	70.7
6.00	22100	59.4
7.00	18000	48.4
8.00	13600	36.6
9.00	10400	28.0
11.00	5420	14.6

Figure IV-9. Dependence of QEF_B on the concentration of metal ions for the electrochemical oxidation of dextrose

Electrode: Pt-RDE

Supporting electrolyte: 0.35 M NaOH

[dextrose]: 0.25 M

Electrode rotation speed (W): 400 rev min^{-1}

Potential scan rate (ϕ): 6 V min^{-1}

-●-●-●- Bi(III)

-▲-▲-▲- Pb(II)

-■-■-■- Tl(I)

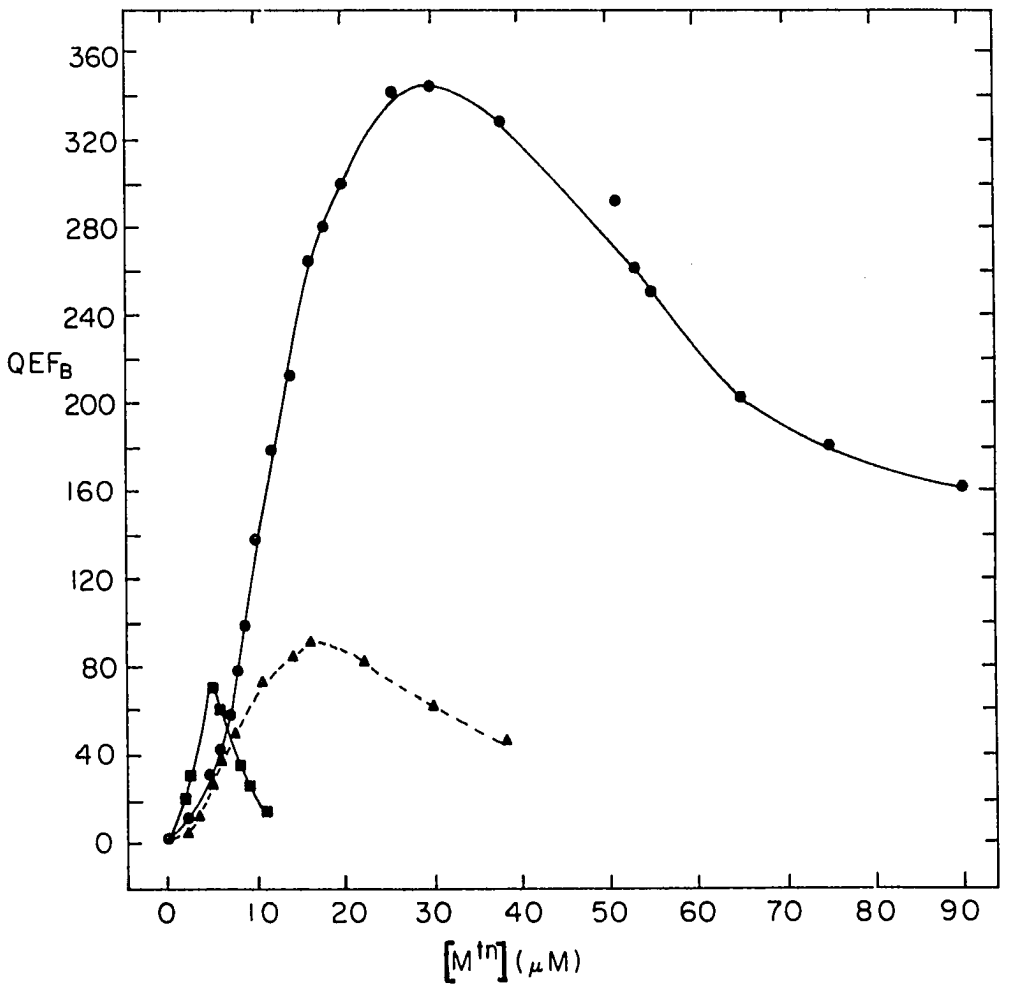
360
320
280
240
QEF$_B$
200
160
120
80
40
0
0
10
20
30
40
50
60
70
80
90
[M^{tn}] (μM)

The maximum value of QEF_B, as in the cases for EF_B, decreases in the order Bi > Pb > Tl. In each case, the maximum value of QEF_B is much larger than the corresponding value of EF_B. For example, the maximum QEF_B for Bi is 344, while the maximum EF_B is only 105. This is tentatively attributed to the fact that the metal ad-atoms enhance as well as catalyze the oxidation process associated with Peak B.

7. Dependence of $I_{p,B}$ on $W^{1/2}$ for the electrochemical oxidation of dextrose on the Bi-coated Pt-RDE

Of all the metal species investigated, Bi ad-atoms produced the greatest enhancement towards the electrochemical oxidation of dextrose, increasing the area of Peak B obtained on the positive scan some three hundred and forty fold. Because of the tremendous enhancement exerted by the Bi ad-atoms, a series of experiments was conducted to test whether the Bi ad-atoms increase the heterogeneous rate constant of the reaction associated with Peak B to the point where the electrochemical oxidation of dextrose becomes mass transport limited, i.e., $I_{p,B}$ is linearly dependent on $W^{1/2}$ as predicted by the Levich Equation (see Equation III-8). It was determined that $I_{p,B}$ had no dependence on W in the absence of the metal ad-atoms.

Values of $I_{p,B}$ obtained for the electrochemical oxidation of dextrose in the presence of 1.00×10^{-5} M Bi(III) are shown in Table IV-11 and Figure IV-10 as a function of $W^{1/2}$ for several concentrations of dextrose. The plots of $I_{p,B}$ vs. $W^{1/2}$ are linear in those cases where the concentration of dextrose is less than 5 mM. Nonlinearity is

observed at high values of $W^{1/2}$ in those cases where the concentration of dextrose exceeds 5 mM.

Table IV-11. Dependence of $I_{p,B}$ on $W^{1/2}$ in the presence of 1.00×10^{-5} M Bi(III) for the electrochemical oxidation of dextrose on the Pt-RDE

[dextrose] (mM)	$W^{1/2}$ ($rev^{1/2}$ $min^{-1/2}$)	$I_{p,B}$ (μA)
1.0	20	600
	30	690
	40	750
	50	800
	60	840
3.0	20	1430
	30	1550
	40	1680
	50	1780
	60	1880
5.0	20	2200
	30	2450
	40	2480
	50	2580
	60	2580
10.0	20	3050
	30	4000
	40	4350
	50	4350
	60	4350
20.0	20	3600
	30	5530
	40	6500
	50	6750
	60	6750

Figure IV-10. Dependence of $I_{p,B}$ on $W^{1/2}$ for the electrochemical oxidation of dextrose in the presence of Bi(III)

Electrode: Pt-RDE

Supporting electrolyte: 0.35 M NaOH

[Bi(III)]: 1.00×10^{-5} M

Potential scan rate (ϕ): 6 V min^{-1}

-●-●-●- 1.0 mM dextrose

-▲-▲-▲- 3.0 mM dextrose

-■-■-■- 5.0 mM dextrose

-o-o-o- 10.0 mM dextrose

-Δ-Δ-Δ- 20.0 mM dextrose

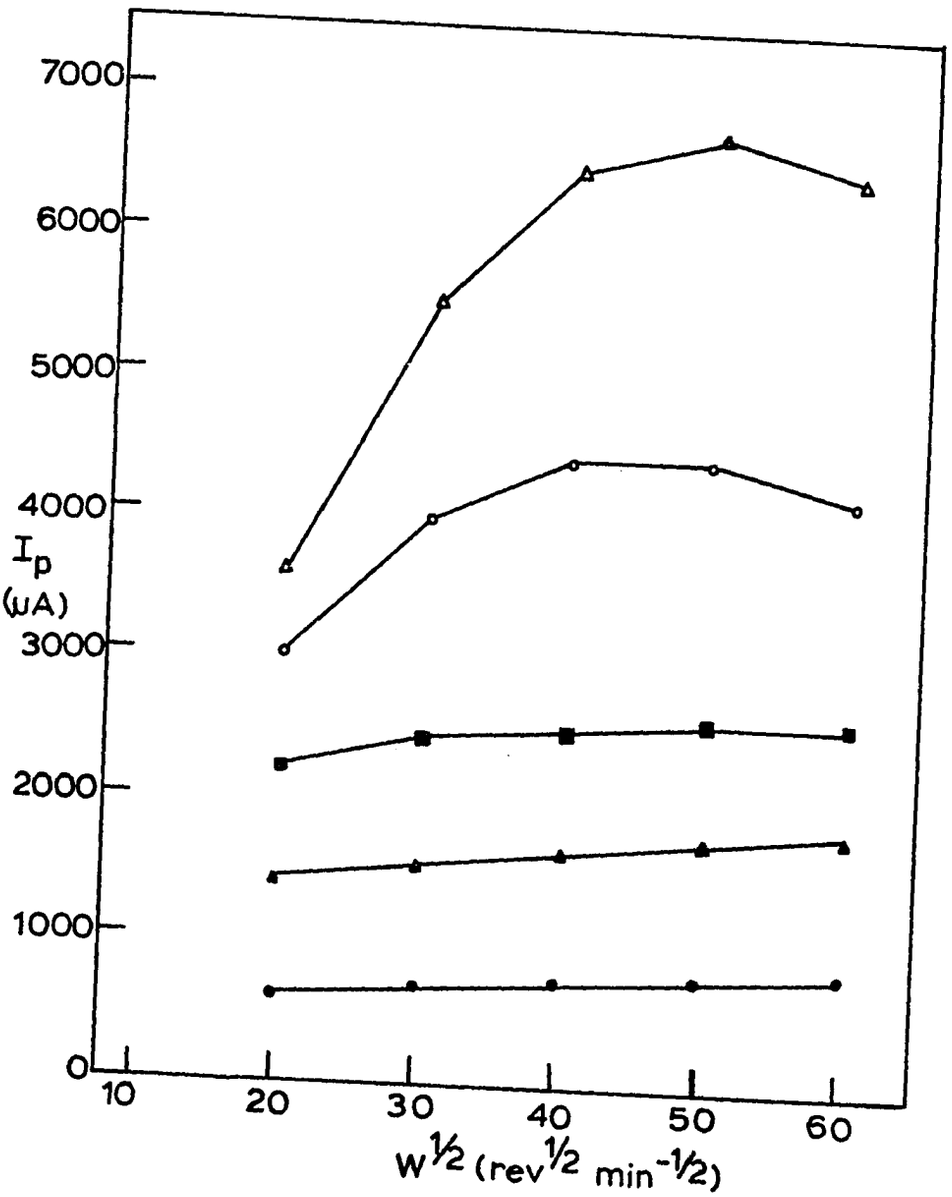
7000
6000
5000
4000
I_p
(μA)
3000
2000
1000
0
10
20
30
40
50
60
$w^{1/2}$ (rev$^{1/2}$ min$^{-1/2}$)

The theoretical slope of the plot of $I_{p,B}$ vs. $W^{1/2}$ can be calculated from the Levich Equation provided that n, the stoichiometric number of electrons transferred in the oxidation reaction, is known. Assuming that, in the relatively negative potential region where Peak B is observed, dextrose is oxidized only to gluconic acid (57), n is equal

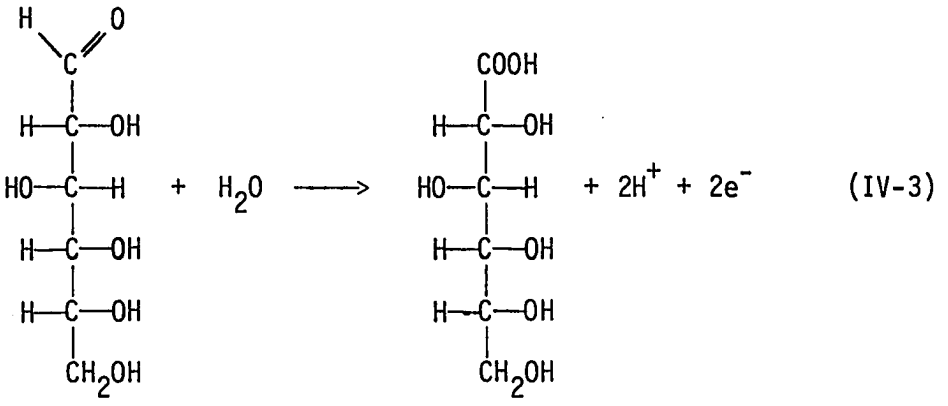

(IV-3)

to 2. Substituting n = 2, F = 96487 coulombs/eq, A = 0.43 cm^2, D = 1 x 10^{-5} cm^2 sec^{-1} (an estimated value), ν = 0.01 cm^2 sec^{-1} into the Levich Equation,

$$I_{p,B}\ (\mu A) = 20000\ C^b\ (M)\ W^{1/2}\ (rev^{1/2}\ min^{-1/2}) \qquad \text{(IV-4)}$$

Therefore, the slope of the plot of $I_{p,B}$ vs. $W^{1/2}$ is predicted to be 20,000 C^b μA $rev^{-1/2}$ $min^{1/2}$.

The slopes of the plots of $I_{p,B}$ vs. $W^{1/2}$ for the different concentrations of dextrose are compared in Table IV-12 with the theoretical slopes calculated from the Levich Equation. The calculated slopes are approximately 3 to 7X larger than the experimentally observed value for the different concentrations of dextrose.

Table IV-12. Comparison of the slopes of experimental $I_{p,B}$-$W^{1/2}$ plots at low $W^{1/2}$ with the theoretical slopes calculated from the Levich Equation

Dextrose (mM)	Experimental slope ($\mu A\ rev^{-1/2}\ min^{1/2}$)	Calculated (Eq. IV-4) slope ($\mu A\ rev^{-1/2}\ min^{1/2}$)
1	6.0	20
3	9.3	50
5	12.7	90
10	65.0	200
20	145.0	300

8. Dependence of $I_{p,B}$ on ϕ for the electrochemical oxidation of dextrose on the Bi-coated Pt-RDE

Since $I_{p,B}$ obtained in the presence of the Bi ad-atoms was determined to be a linear function of $W^{1/2}$ for small values of $W^{1/2}$, $I_{p,B}$ was investigated as a function of the rate of potential scan, ϕ. The current associated with a mass-transport limited reaction has no dependence on ϕ. On the other hand, the dependence for a surface-controlled process is a linear function of ϕ.

Preliminary studies which involved the variation of ϕ at a constant value of W equal to 400 rev min^{-1}, for a solution of 0.35 M NaOH containing 5 mM dextrose and 30 μM Bi(III), produced unsatisfactory results.

The amount of Bi ad-atoms deposited on the Pt-RDE varied inversely with ϕ due to the fact that the amount of time for which $E_{dep} < E$ was greater for smaller values of ϕ. Since $I_{p,B}$ depends on θ_{Bi}, an inverse dependence of $I_{p,B}$ on ϕ was observed.

To eliminate the complications arising from the dependence of θ_{Bi} on ϕ, the Pt-RDE was precoated with Bi ad-atoms from a solution of 0.35 M NaOH containing 30 μM Bi(III) until a reproducible coverage was obtained. The electrode was then transferred to a Bi(III)-free solution of 5 mM dextrose in 0.35 M NaOH and the variation of ϕ performed. The positive scan limit (E_+) was restricted to 0.0V vs. SCE to minimize the loss of the Bi ad-atoms with increasing scan number. The value of $I_{p,B}$ obtained was found to be completely independent of ϕ. This is in agreement with the results obtained in Section IV.C.6 in which it was concluded that the Bi-catalyzed reaction is mass transport limited. The value of W chosen for this set of ϕ studies was 400 rev min^{-1}, which was in the region where $I_{p,B}$ was found to be a linear function of $W^{1/2}$ and should, therefore, have little dependence on ϕ. Based on this result, it is confirmed that the anodic reaction in the presence of Bi ad-atoms produces an electrode current which is less than the mass-transport limited value which would be obtained for a fully active electrode, i.e., based on A = 0.43 cm^2 and the assumed values of n and D.

9. Effects of the potential scan limits on the electrochemical oxidation of dextrose on the Pt-RDE and the Bi-coated Pt-RDE

The scan limits employed in the cyclic voltammetric studies of the electrochemical oxidation of dextrose was 0.6V and -0.8V vs. SCE for

data described above. These limits are approximately the maximum values available for the Pt-RDE in 0.35 M NaOH without extensive decomposition of the solvent. It is quite possible that such a potential range may not be the optimal value for the oxidation of dextrose, whether in the absence or the presence of the metal ad-atoms. A series of experiments was performed which involved variation of the positive and negative scan limits. The effects of the potential limits on the anodic peaks, especially Peak B, were compared.

a. Effects of the positive and negative potential limits for the Pt-RDE The effect of varying the positive scan limit (E_+) with a constant negative limit (E_-) is shown in Figure IV-11. The anodic peaks E, B and A obtained during the positive potential scan are all increased in height as E_+ is moved progressively more positive from an initial value of 0.0V vs. SCE to a final value of 0.6V vs. SCE. The height of Peak C obtained on the negative potential scan is also increased as E_+ is moved in the positive direction. These observations are attributed to the fact that the poisons formed during the electrochemical oxidation of dextrose are more efficiently removed from the surface of the electrode as the potential of the electrode is allowed to scan to more positive values. It was suggested previously in Section IV.C.5.a that Peak A is attributable to the process involving the electrochemical oxidation of the poisonous species on the surface of the electrode. The data presented in Figure IV-11 support this view. As E_+ is moved from 0.0V to 0.3V vs. SCE, the peak heights of both Peak E and Peak B increase toward a limiting value. Increasing E_+ to

Figure IV-11. The effect of the positive potential limit (E_+) on the electrochemical oxidation of dextrose on the Pt-RDE

Supporting electrolyte: 0.35 M NaOH

[dextrose]; 5 mM

Electrode rotation speed (W): 400 rev min^{-1}

Potential scan rate (ϕ): 6 V min^{-1}

A, B, C, D and D: anodic peaks

——— E_+ = 0.0V vs. SCE

------- E_+ = 0.3V vs. SCE

····· E_+ = 0.5V vs. SCE

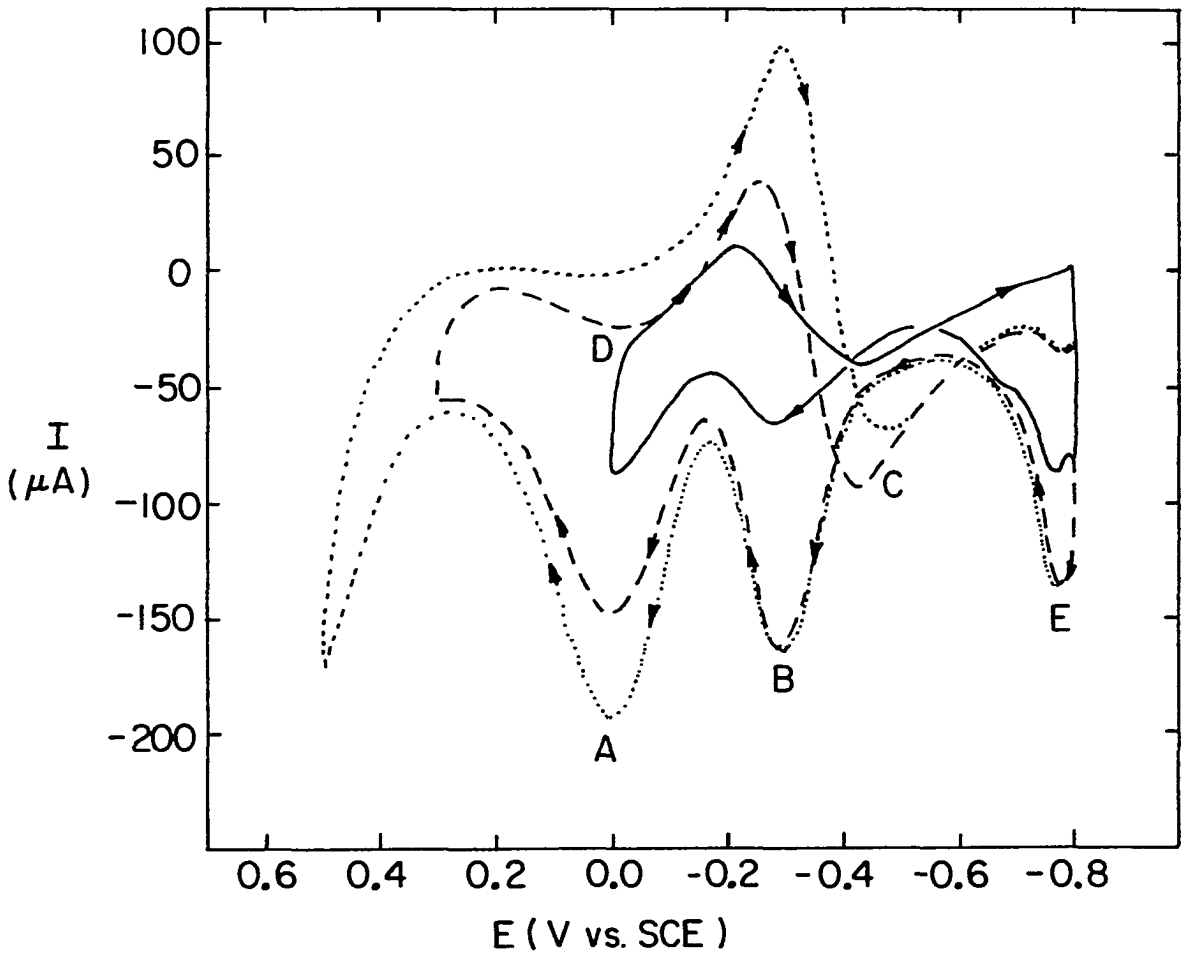
100
50
0
-50
-100
-150
-200
I
(μA)
A
B
C
D
E
0.6
0.4
0.2
0.0
-0.2
-0.4
-0.6
-0.8
E (V vs. SCE)

values above 0.3V vs. SCE produces no further increase in the heights of either Peak E or Peak B. This is concluded to result because all the poison is oxidized from the surface of the electrode when the potential is allowed to scan to the region more positive than Peak A.

The effect of the variation of E_- on the anodic peaks obtained during the electrochemical oxidation of dextrose is shown in Figure IV-12. The heights of the anodic peaks E, B and A obtained during the positive potential scan are increased as E_- is set at progressively more negative values ranging down to -0.95V vs. SCE. This phenomenon can be explained by the conclusion that the amount of dextrose that can undergo surface-controlled dehydrogenation is increased as E_- is made more negative. Hence, more surface adsorbed dextrose is available for oxidation during the subsequent positive scan. This results in increases in the heights of Peaks B and A. The height of Peak E is also increased as E_- is made more negative because this peak, located at the potential value where surface-adsorbed hydrogen atoms are oxidized in the absence of dextrose, can be attributed to the oxidation of the hydrogen atoms formed during the dehydrogenation of dextrose.

b. Effects of the positive and negative potential limits for the Bi-coated Pt-RDE The anodic peaks B and C obtained during the positive and negative scans, respectively, are increased in height as E_- is made more negative during the electrochemical oxidation of dextrose in a solution containing 20 μM Bi(III). The increase in $I_{p,B}$ with decreasing E_- is greater than the case when Bi ad-atoms are absent and can be attributed to the fact that the amount of Bi ad-atoms deposited on the Pt-RDE is greater as E_- is made more negative.

Figure IV-12. The effect of the negative potential limit (E_-) on the electrochemical oxidation of dextrose on the Pt-RDE

Supporting electrolyte: 0.35 M NaOH

[dextrose]: 5 mM

Electrode rotation speed (W): 400 rev min^{-1}

Potential scan rate (ϕ): 6 V min^{-1}

A, B, C, D and E: anodic peaks

——— E_- = -0.6V vs. SCE

------- E_- = -0.75V vs. SCE

····· E_- = -0.95V vs. SCE

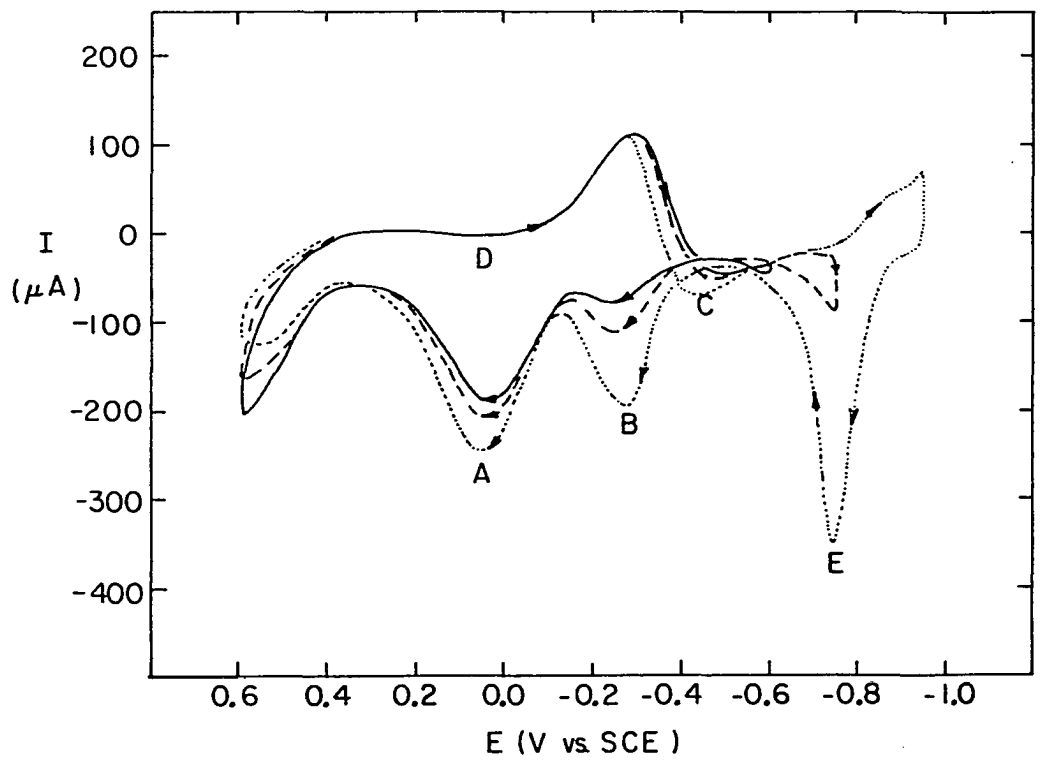
200
100
0
-100
-200
-300
-400
I
(μA)
D
C
B
A
E
0.6
0.4
0.2
0.0
-0.2
-0.4
-0.6
-0.8
-1.0
E (V vs. SCE)

The effect of varying E_+ in the presence of the Bi ad-atoms is exactly opposite to that obtained in the absence of the Bi ad-atoms, as shown in Figure IV-13. Whereas, the peak heights of Peaks B and C are increased as E_+ is adjusted to more positive values in the absence of the Bi ad-atoms (see Figure III-11), the peak heights actually decrease as E_+ is made more positive in the presence of the Bi ad-atoms. This can be explained by the conclusion that the amount of Bi ad-atoms maintained on the electrode surface for a fixed concentration of Bi(III) is larger when E_+ is restricted to the more negative potential region. Hence, the catalyzed currents of Peaks B and C increase as E_+ is made more negative. Peaks A and E are absent from the I-E curve when Bi ad-atoms are present.

In conclusion, the magnitude of the peak current of the anodic peaks in the absence of the Bi ad-atoms depends largely on the number of Pt sites not fouled by poisonous species. High values of E_+ favor the cleaning of the electrode surface and, hence, favor higher currents. In the presence of the Bi ad-atoms, the amount of poison formed during the electrochemical oxidation of dextrose is expected to be greatly decreased. Consequently, the peak currents depend more on the effective preservation of the surface Bi ad-atoms at the low values of E_+ rather than the cleaning effects achieved at high E_+. Hence, the same directional changes in E_+ produce exactly opposite effects on the electrochemical oxidation of dextrose in the absence and presence of the Bi ad-atoms.

Figure IV-13. The effect of the positive potential limit (E_+) on the electrochemical oxidation of dextrose on the Pt-RDE in the presence of Bi(III)

Supporting electrolyte: 0.35 M NaOH

[dextrose]: 5 mM

[Bi(III)]: 20 μM

Electrode rotation speed (W): 400 rev min^{-1}

Potential scan rate (ϕ): 6 V min^{-1}

B and C: anodic peaks

——— E_+ = 0.6V vs. SCE

------- E_+ = 0.0V vs. SCE

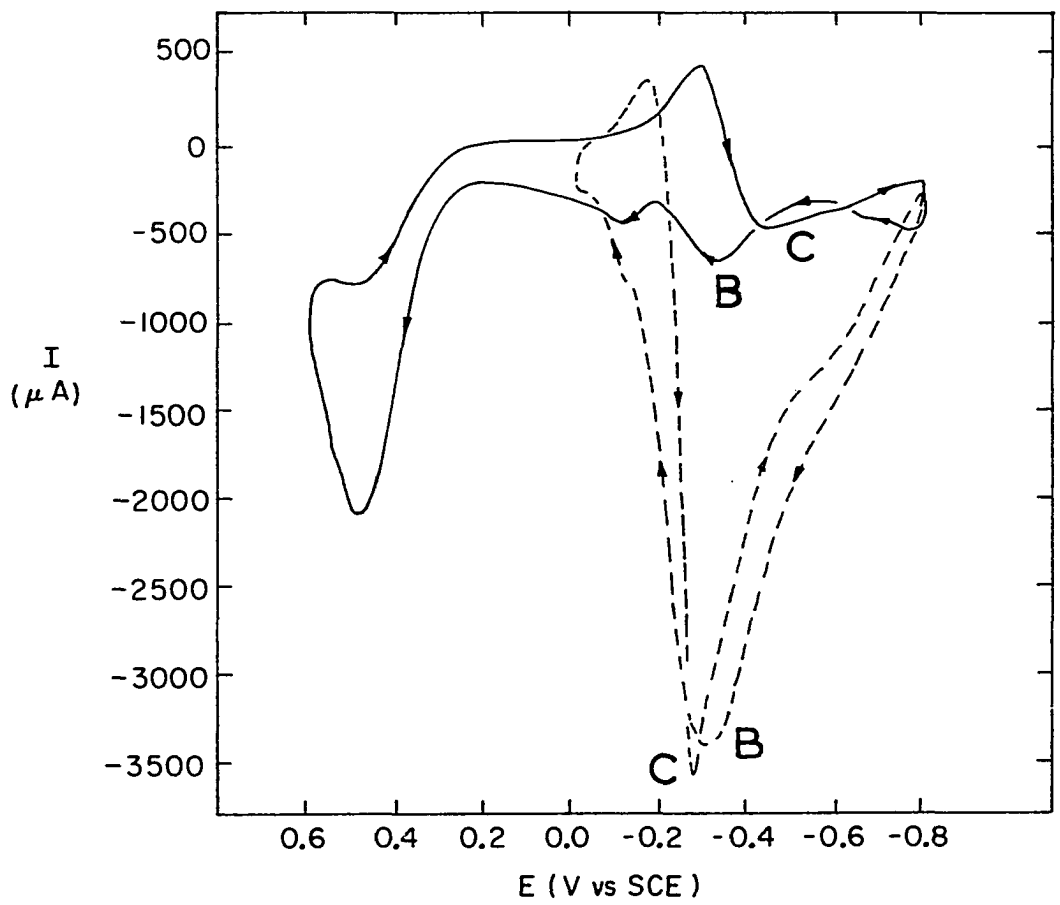
500
0
-500
-1000
-1500
-2000
-2500
-3000
-3500
I
(μA)
B
C
C
B
0.6
0.4
0.2
0.0
-0.2
-0.4
-0.6
-0.8
E (V vs SCE)

D. Amperometric Studies of the Effect of Bi Ad-atoms on the Electrochemical Oxidation of Dextrose on the Pt-RDE

The amperometric technique was employed to study the electrochemical oxidation of dextrose in 0.35 M NaOH in the presence of Bi ad-atoms. The anodic current obtained for the oxidation of dextrose was monitored at a fixed potential of -0.36V vs. SCE, which corresponds to $E_{p,B}$ (see Figure IV-1) obtained during positive potential scan. The value $E_{p,B}$ was chosen for the amperometric study because Peak B is most greatly enhanced by Bi ad-atoms.

The test solutions employed in this series of experiments contained both dextrose and Bi(III) at various concentrations. Bi ad-atoms are deposited at underpotential at -0.36V vs. SCE in 0.35 M NaOH, and, hence the deposition of the Bi ad-atom is concurrent with the electrochemical oxidation of dextrose. The Pt-RDE was removed from the test solution and immersed in concentrated HNO_3 between each run to remove the electrodeposited Bi ad-atoms and insoluble oxide which would otherwise be carried over into successive experiments.

The anodic current of Peak B was first monitored in the absence of any Bi ad-atoms. At the start of the experiment, the Pt-RDE was cleaned by immersion in reagent-grade concentrated HNO_3, rinsed thoroughly in triply distilled water, and then introduced under open-circuit conditions into a solution of 0.35 M NaOH containing 5 mM dextrose. The value of the applied potential was then adjusted to -0.36V vs. SCE and the circuit was closed. The anodic current was

monitored as a function of time on a strip-chart recorder. The anodic current was found to decay sharply towards a value of zero within 10 seconds in the absence of the Bi ad-atoms, and remained at zero thereafter as shown in Figure IV-14A. This is concluded to be the time period within which a clean Pt surface is completely fouled by the poisons formed during the electrochemical oxidation of dextrose at -0.36V vs. SCE.

Next, the anodic current was monitored at -0.36V vs. SCE in the presence of Bi(III) at various concentrations. Representative I-t curves are shown in Figure IV-14. At very low concentrations of Bi(III), e.g., 2.5×10^{-7} M, the anodic current decreases rapidly towards zero following the closing of the circuit. However, instead of remaining at zero, the anodic current slowly increases until a peak value ($I_{t,max}$) is reached, after which the current again decreases with time. Perhaps, the slow decrease occurs because the surface of the electrode becomes saturated with respect to the Bi ad-atoms. The time, τ_{max}, required for the anodic current to reach its maximum value is decreased as the concentration of Bi(III) is raised. The value of the slope, S, of the rising portion of the I-t curve, as well as the value of $I_{t,max}$ are both increased as the concentration of Bi(III) is increased. The values of S, $I_{t,max}$ and τ_{max} are shown in Table IV-13 as a function of Bi(III) concentration. The increase in S and decrease in τ_{max} with increases in the concentration of Bi(III) are concluded to result from the increased rate of deposition of the Bi ad-atoms as the concentration of Bi(III) is raised. At Bi(III) concentrations above

Figure IV-14. I-t curves of the Pt-RDE in 0.35 M NaOH containing 5 mM dextrose and various concentrations of Bi(III)

Electrode rotation speed (W): 400 rev min^{-1}

Current monitored at -0.36V *vs.* SCE

A 0.0 μM Bi(III)

B 1.5 μM Bi(III)

C 3.0 μM Bi(III)

D 5.0 μM Bi(III)

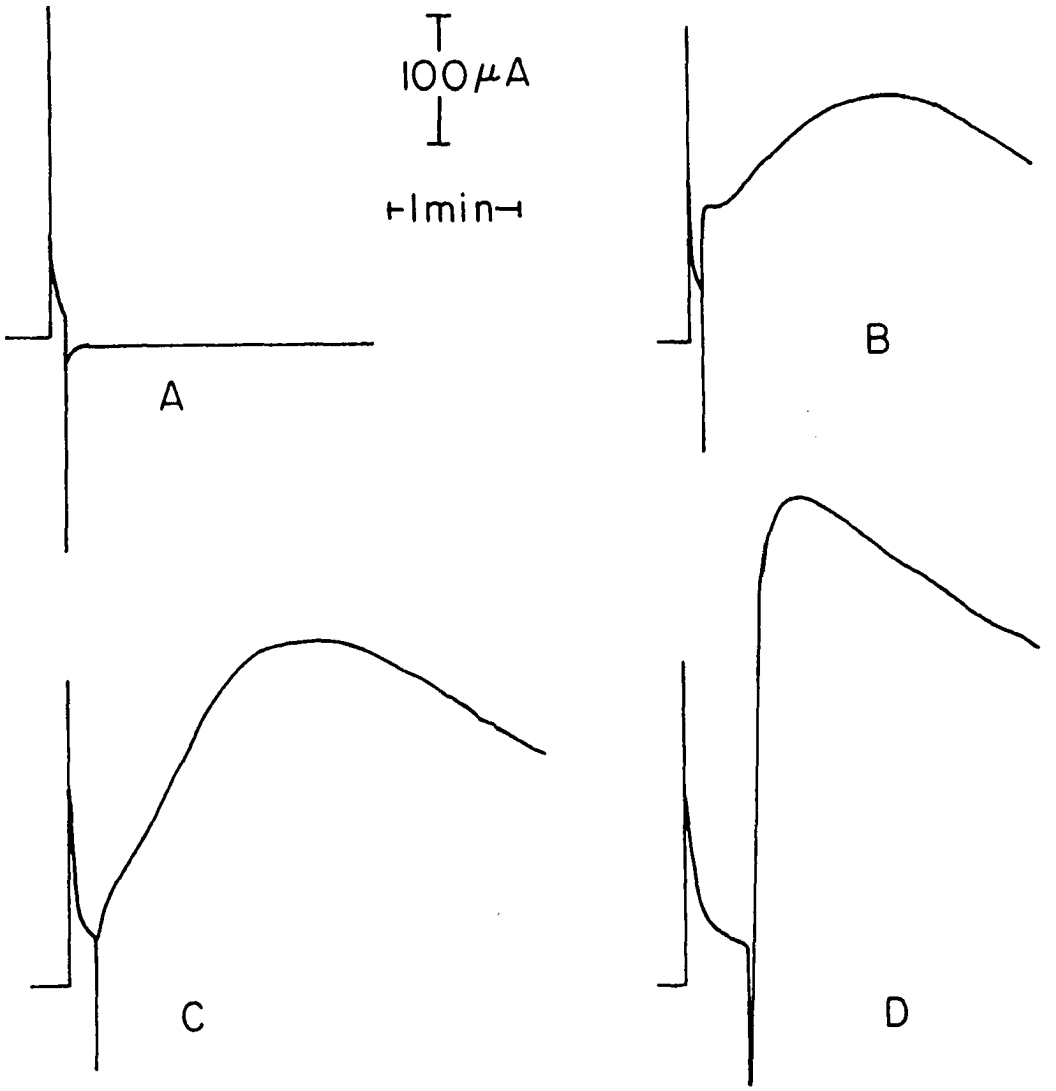
100μA
1min
A
B
C
D

Table IV-13. Dependence of S, $I_{t,max}$ and τ_{max} on the concentration of Bi(III)

Bi(III) (μM)	S ($\mu A\ min^{-1}$)	$I_{t,max}$ (μA)	τ_{max} (min)
0.00	0	0	∞
0.50	25	80	3.2
1.00	75	120	2.0
1.50	130	190	1.3
2.00	140	260	0.8
3.00	400	280	0.7
4.00	∞	360	0.0
5.00	∞	360	0.0
6.00	∞	360	0.0

4.00 μM, the rate of deposition of the Bi ad-atoms is so high that the maximum value of the anodic current ($I_{t,max}$) is achieved almost instantaneously after the circuit is closed, i.e., τ_{max} = 0.0 min. In such cases, the value of S is designated as ∞ in Table IV-13. $I_{t,max}$ also increases as the concentration of Bi(III) is increased, ultimately reaching a constant value independent of the concentration of Bi(III).

The value of S, $I_{t,max}$ and τ_{max} were also investigated as a function of the concentration of dextrose at a fixed concentration of Bi(III) equal to 1.00×10^{-6} M. The relatively low value of Bi(III) concentration was chosen for this experiment in order that S would not

become infinity. The results of this set of experiments are shown in Table IV-14.

Table IV-14. Dependence of S, $I_{t,max}$ and τ_{max} on the concentration of dextrose

[Dextrose] (mM)	S (A min^{-1})	$I_{t,max}$ (μA)	τ_{max} (min)
2.0	20	43	2.2
3.0	26	58	2.3
4.0	32	70	2.5
5.0	31	78	2.5
6.0	32	84	2.5
7.0	32	100	2.7
8.0	33	94	2.4
9.0	33	94	2.4
10.0	38	108	2.6

As shown in Table IV-14, the value of S and that of τ_{max} are fairly independent of the concentration of dextrose, confirming that the value of S and τ_{max} is solely dependent upon the rate of deposition of the Bi ad-atoms. $I_{t,max}$ increases with increases in the concentration of dextrose, but becomes independent of the concentration of dextrose at values above 6 mM.

E. Time-dependent Voltammetric Studies of the Effects of Bi Ad-atoms on the Electrochemical Oxidation of Dextrose on the Pt-RDE

Two techniques were used to electrodeposit the Bi ad-atoms onto the Pt-RDE during the time-dependent voltammetric studies of the effects of the ad-atoms on the electrochemical oxidation of dextrose. In the first, Technique A, the Bi ad-atoms were deposited concurrently with the electrochemical oxidation of dextrose, i.e., from a solution containing both Bi(III) and dextrose. In this technique, the anodic currents obtained for the oxidation of dextrose were monitored as the Bi ad-atoms were slowly accumulated onto the Pt-RDE during the successive cyclic scans. In the second method, Technique B, the Bi ad-atoms were deposited onto the Pt-RDE from a solution containing the Bi(III) ions in 0.35 M NaOH without dextrose. The precoated Pt-RDE was then transferred to a solution containing dextrose in the 0.35 M NaOH without Bi(III) and the change in the anodic peak currents for the electrochemical oxidation of dextrose was monitored by time-dependent voltammetry. The Pt-RDE which had been precoated with the Bi ad-atoms was immersed in concentrated HNO_3 between runs to remove the Bi ad-atoms.

1. Technique A

Typical time-dependent voltammetric (I-t) curves obtained for the Pt-RDE in a solution containing Bi(III) and 5 mM dextrose are shown in Figure IV-15. Two well-defined sets of anodic current spikes,

Figure IV-15. Time-dependent voltammetric curve of the Pt-RDE in 0.35 M NaOH containing 5 mM dextrose and Bi(III)

Potential scan rate (ϕ): 10 V min^{-1}

Electrode rotation speed (W): 400 rev min^{-1}

Positive scan limit (E_+): 0.0V *vs.* SCE

Negative scan limit (E_-): -0.9V *vs.* SCE

B and C: anodic spikes

I 0.5 μM Bi(III)

II 5.0 μM Bi(III)

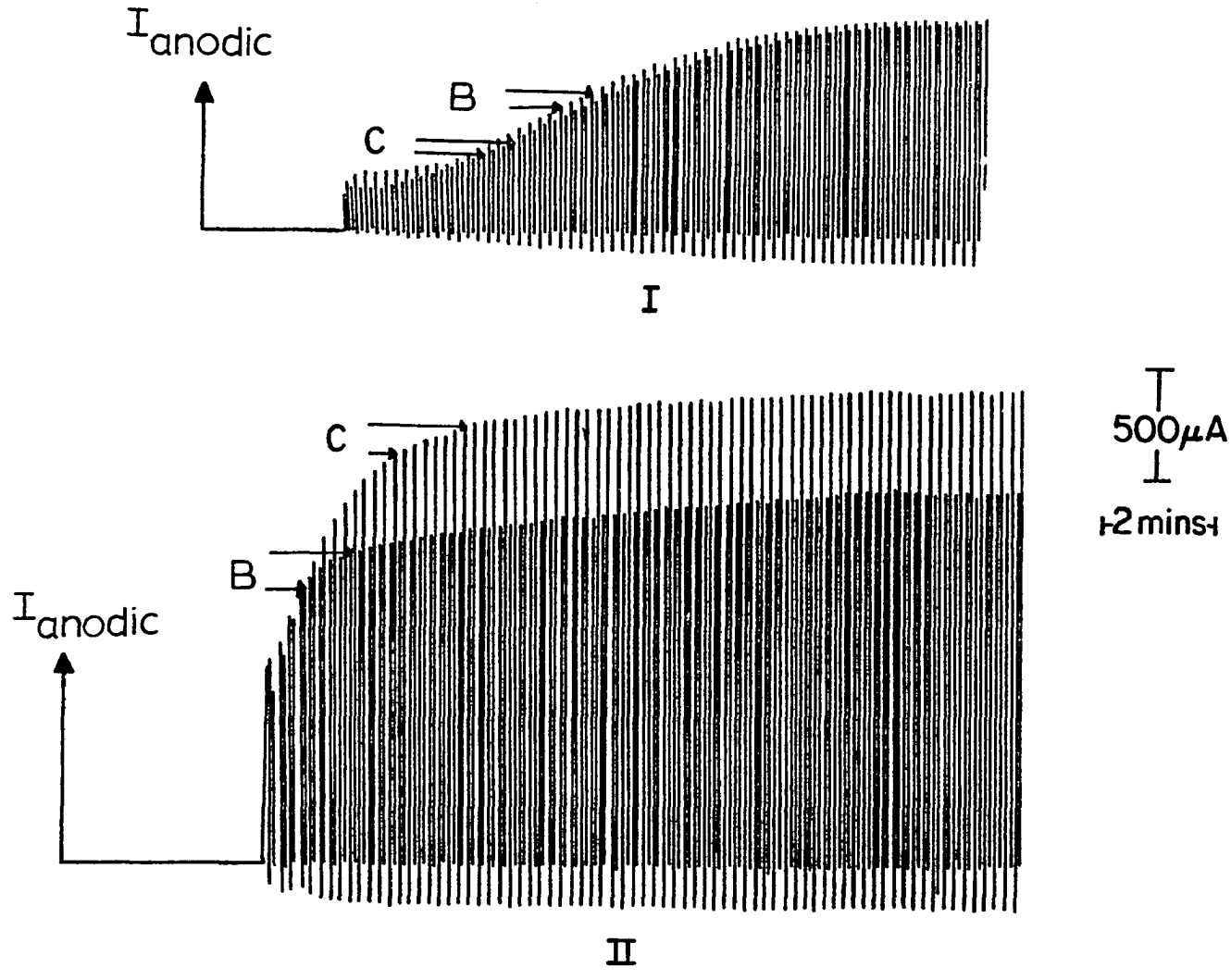
I anodic
B
C
I
C
B
I anodic
II
500μA
2 mins

designated as B and C, are apparent, which correspond to the anodic peaks B and C (see Figure IV-1) obtained during the positive and negative potential scans, respectively. $I_{p,B}$ and $I_{p,C}$ both increase with time as the Bi ad-atoms are deposited onto the Pt-RDE until a reproducible surface coverage is achieved, for which both $I_{p,B}$ and $I_{p,C}$ become constant with time. The maximum height achieved by Peaks B and C is, as expected, dependent on the concentration of Bi(III) in solution. The value of anodic current increases with increasing concentration of Bi(III) until the electrode becomes saturated with Bi ad-atoms for high concentration of Bi(III).

2. Technique B

The electrodeposition of Bi ad-atoms during the precoating of the Pt-RDE was monitored by time-dependent voltammetry in the plating solution. Such a time-dependent voltammetric curve is shown in Figure IV-16 for a solution of 0.35 M NaOH containing 5.0×10^{-7} M Bi(III). The anodic spikes, designated as A in Figure IV-16, correspond to the peak associated with the oxidation of the Bi ad-atoms to the insoluble oxides during the positive potential scan (see Figure IV-2). The insoluble oxides remain adsorbed on the electrode and the set of cathodic spikes, designated as C in Figure IV-16, corresponds to the concurrent reduction of the oxides of Pt and Bi during the negative potential scan. Both sets of spikes increase in height as additional Bi ad-atoms are accumulated on the electrode surface with successive cyclic sweeps of the electrode potential. The spikes become constant in height when the maximum amount of Bi ad-atoms, for a specific

Figure IV-16. Time-dependent voltammetric curve of the Pt-RDE in 0.35 M NaOH containing 5.00×10^{-7} M Bi(III)

Potential scan rate (ϕ): 10 V min^{-1}

Electrode rotation speed (W): 400 rev min^{-1}

Positive scan limit (E_+): 0.0V *vs.* SCE

Negative scan limit (E_-): -0.9V *vs.* SCE

A: anodic spike

C: cathodic spike

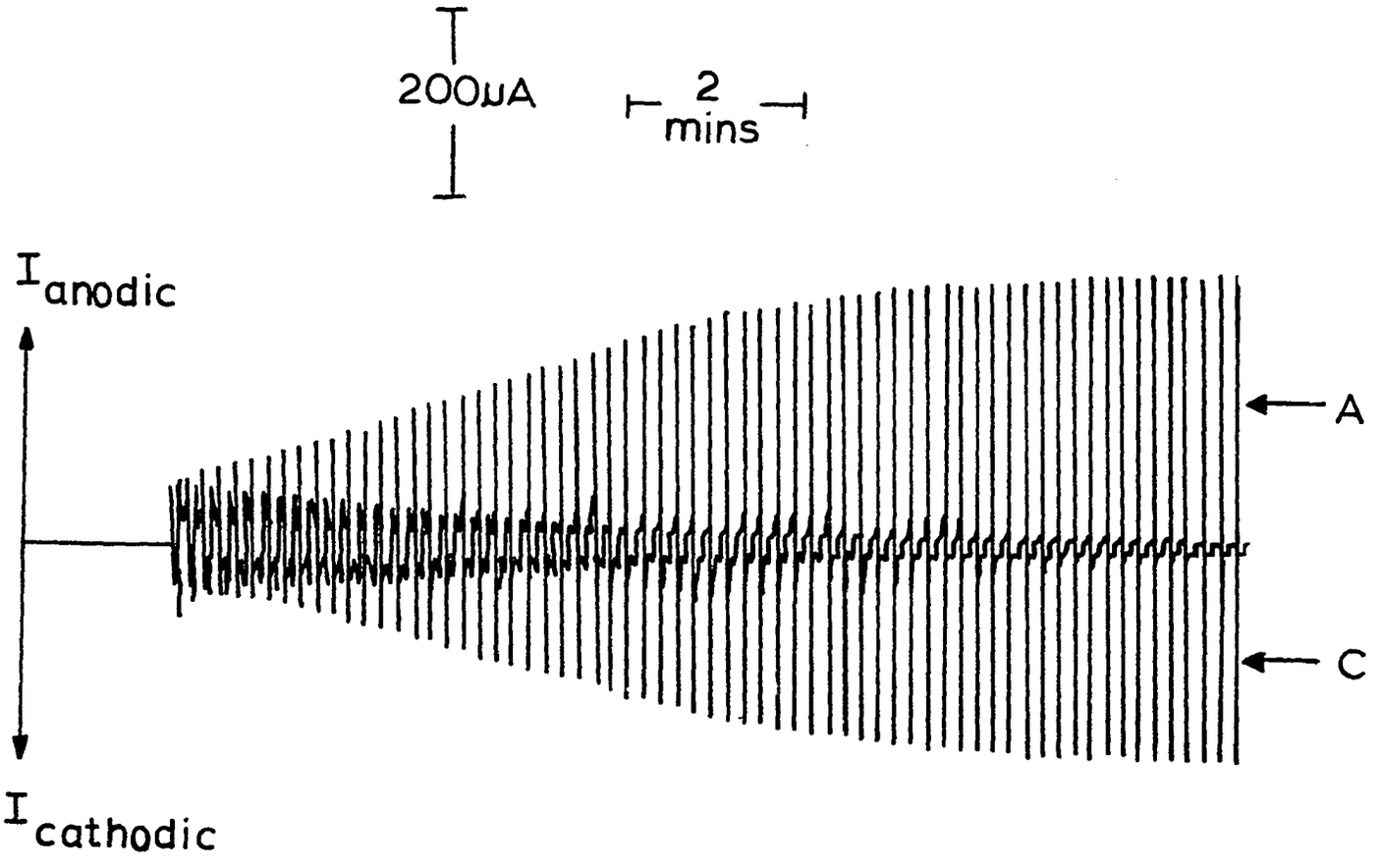
200μA
2
mins
I anodic
A
C
I cathodic

concentration of Bi(III) in solution, has been deposited. Therefore, the constant height of the anodic spikes was taken as an indication that the Pt-RDE had been precoated to a reproducible extent under the experimental conditions. The electrode was then transferred to the solution containing dextrose in 0.35 M NaOH.

A typical time-dependent voltammetric curve for a Bi-precoated Pt-RDE in a solution of dextrose is shown in Figure IV-17. Again, two well-defined sets of current spikes, designated as B and C, are observed which correspond to the anodic peaks B and C (see Figure IV-1) observed during the positive and negative potential scans, respectively. However, in sharp contrast to the case where Bi(III) is present in the solution, the magnitude of the anodic current spikes observed in this Bi(III)-free solution is initially high, but decreases with time in an exponential fashion.

A series of such time-dependent voltammetric curves was obtained as a function of the rotation speed, W, of the Pt-RDE for 5 mM dextrose. The Pt-RDE was precoated with Bi ad-atoms from a solution containing 5.00×10^{-7} M Bi(III) at the start of each experiment. The rate of the exponential decrease of the anodic current spikes B and C was observed to increase as W was increased. Spike B of each time-dependent voltammetric curve was fitted to the equation

$$I_t = I_o e^{-bt} \qquad \text{(IV-5)}$$

where I_t is the experimentally observed peak height at time t, and I_o is the initial peak height of Peak B. The constant b is the exponential decay constant of the time-dependent voltammetric curve. Since the

Figure IV-17. Time-dependent voltammetry of the Bi precoated Pt-RDE in 0.35 M NaOH containing 5 mM dextrose

Electrode rotation speed (W): 400 rev min^{-1}

Potential scan rate (ϕ): 10 V min^{-1}

Positive scan limit (E_+): 0.0V *vs.* SCE

Negative scan limit (E_-): -0.9V *vs.* SCE

B and C: anodic spikes

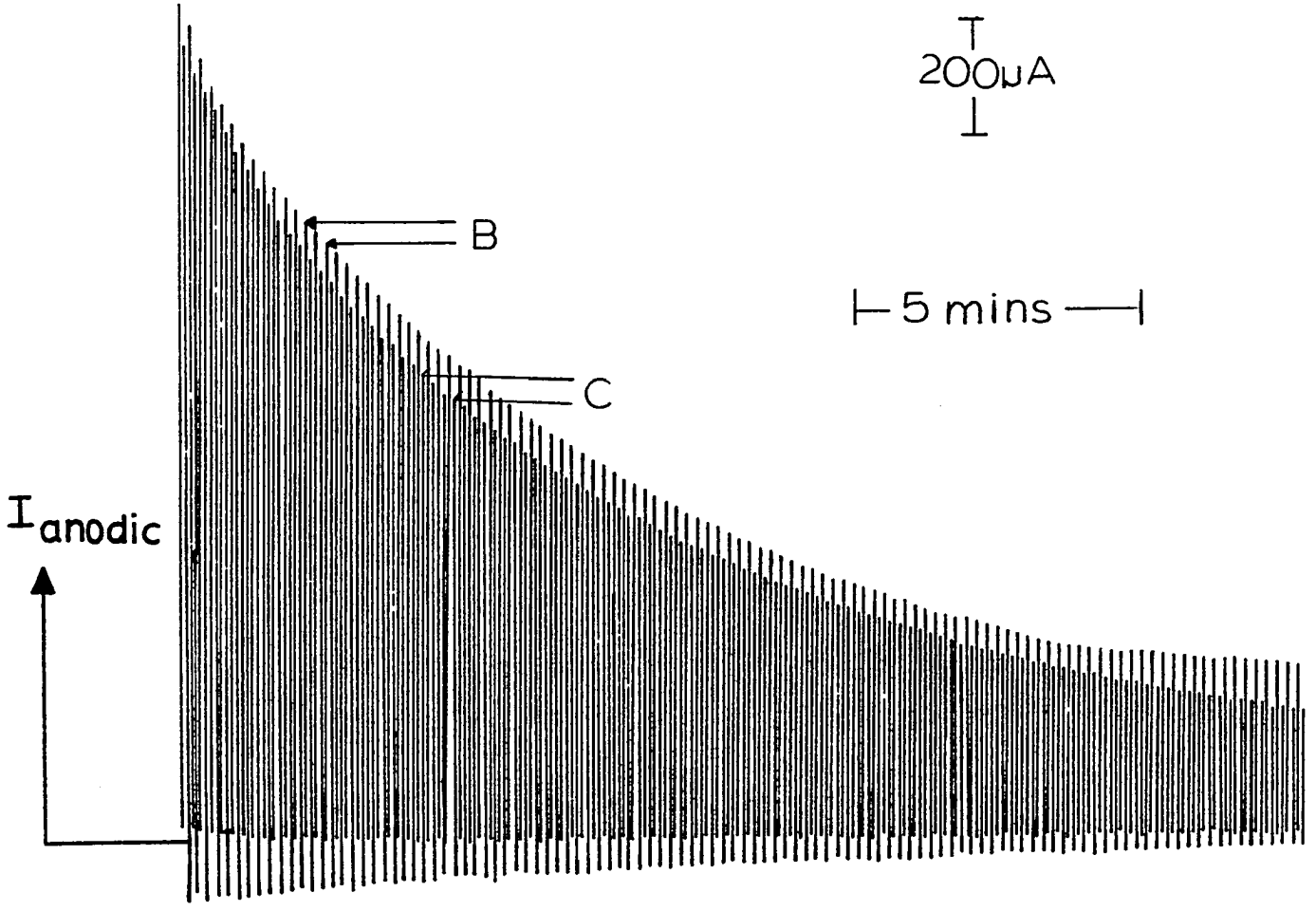
200μA
B
5 mins
C
I anodic

rate of the exponential decay was observed upon inspection of the time-dependent voltammetric curves to increase with increases in $W^{1/2}$, the value of b was expected to increase also with increases in W. The dependence of b on $W^{1/2}$ is shown in Table IV-15 and plotted in Figure IV-18. The dependence of I_o on $W^{1/2}$ is also shown in Table IV-15. The plot of b vs. $W^{1/2}$ is linear.

Table IV-15. Dependence of b and I_o on $W^{1/2}$

$W^{1/2}$ ($rev^{1/2}$ $min^{-1/2}$)	b x 10^3 (sec^{-1})	I_o (μA)
0	0.7	320
20	1.5	1230
30	2.0	1530
40	2.4	1750
50	3.8	2340
60	3.8	2350
70	4.1	2350

A second series of time-dependent voltammetric curves was obtained as a function of the concentration of dextrose at a fixed value of W equal to 400 rev min^{-1} for the precoated Pt-RDE. The dependence of b and I_o of spike B on the concentration of dextrose is shown in Table IV-16. The dependence of b on the concentration of dextrose is also plotted in Figure IV-19 and is found to be linear.

Figure IV-18. Dependence of b on $W^{1/2}$

Electrode: Bi-precoated Pt-RDE

[Dextrose: 5 mM

Supporting electrolyte: 0.35 M NaOH

Potential scan rate (ϕ): 10 V min^{-1}

Electrode rotation speed: 400 rev min^{-1}

Positive potential limit (E_+): 0.0V vs. SCE

Negative potential limit (E_-): -0.9V vs. SCE

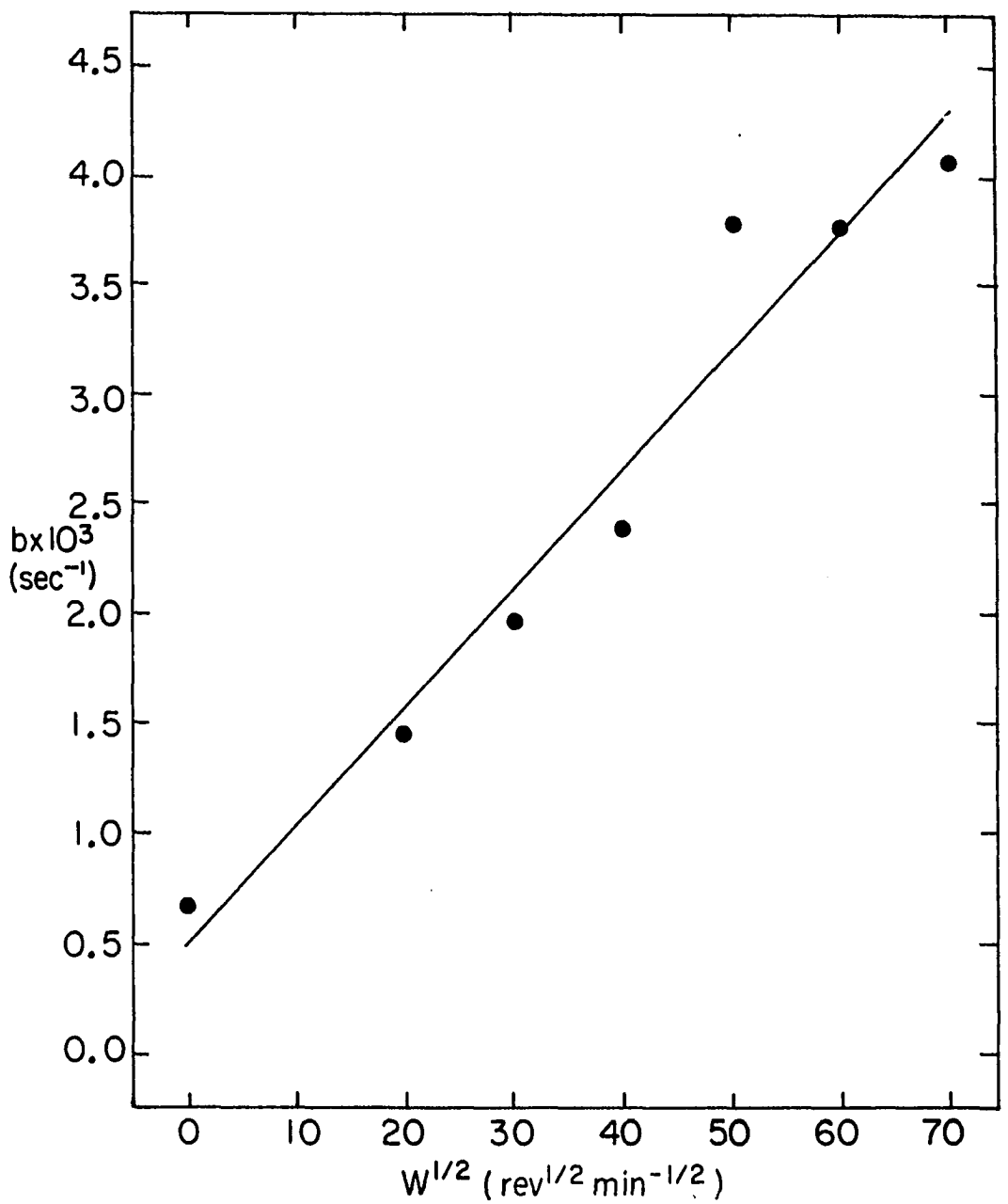
4.5
4.0
3.5
3.0
2.5
2.0
1.5
1.0
0.5
0.0
bx10³
(sec⁻¹)
0
10
20
30
40
50
60
70
W^1/2 (rev^1/2 min^-1/2)

Table IV-16. Dependence of b and I_o on the concentration of dextrose

[Dextrose] (mM)	b x 10^3 (sec^{-1})	I_o (μA)
0.5	0.3	260
2.0	0.7	620
4.0	1.0	1080
5.0	1.1	1210
6.0	1.3	1460

Because the rate constant, b, of the exponential decay had a linear dependence on both $W^{1/2}$ and the concentration of dextrose, it was suspected that the dextrose molecules may be attacking the Bi ad-atoms deposited on the Pt substrate, causing them to be desorbed from the surface of the electrode. When either W or the concentration of dextrose is increased, the flux of the dextrose molecules towards the surface of the electrode is increased and the rate of attack on the Bi ad-atoms is also increased as a consequence. This leads to an increase in the rate at which the anodic current peaks decrease with time, and consequently an increase of b.

Experiments were conducted to test the assumption that the pre-coated Bi ad-atoms were removed from the surface of the electrode by the dextrose molecules or by the products of dextrose oxidation. The Pt-RDE was reproducibly precoated with Bi ad-atoms from a solution of

Figure IV-19. Dependence of b on the concentration of dextrose

Electrode: Bi-precoated Pt-RDE

Supporting electrolyte: 0.35 M NaOH

Potential scan rate (ϕ): 10 V min^{-1}

Electrode rotation speed (W): 400 rev min^{-1}

Positive potential limit (E_+): 0.0V *vs.* SCE

Negative potential limit (E_-): -0.9V *vs.* SCE

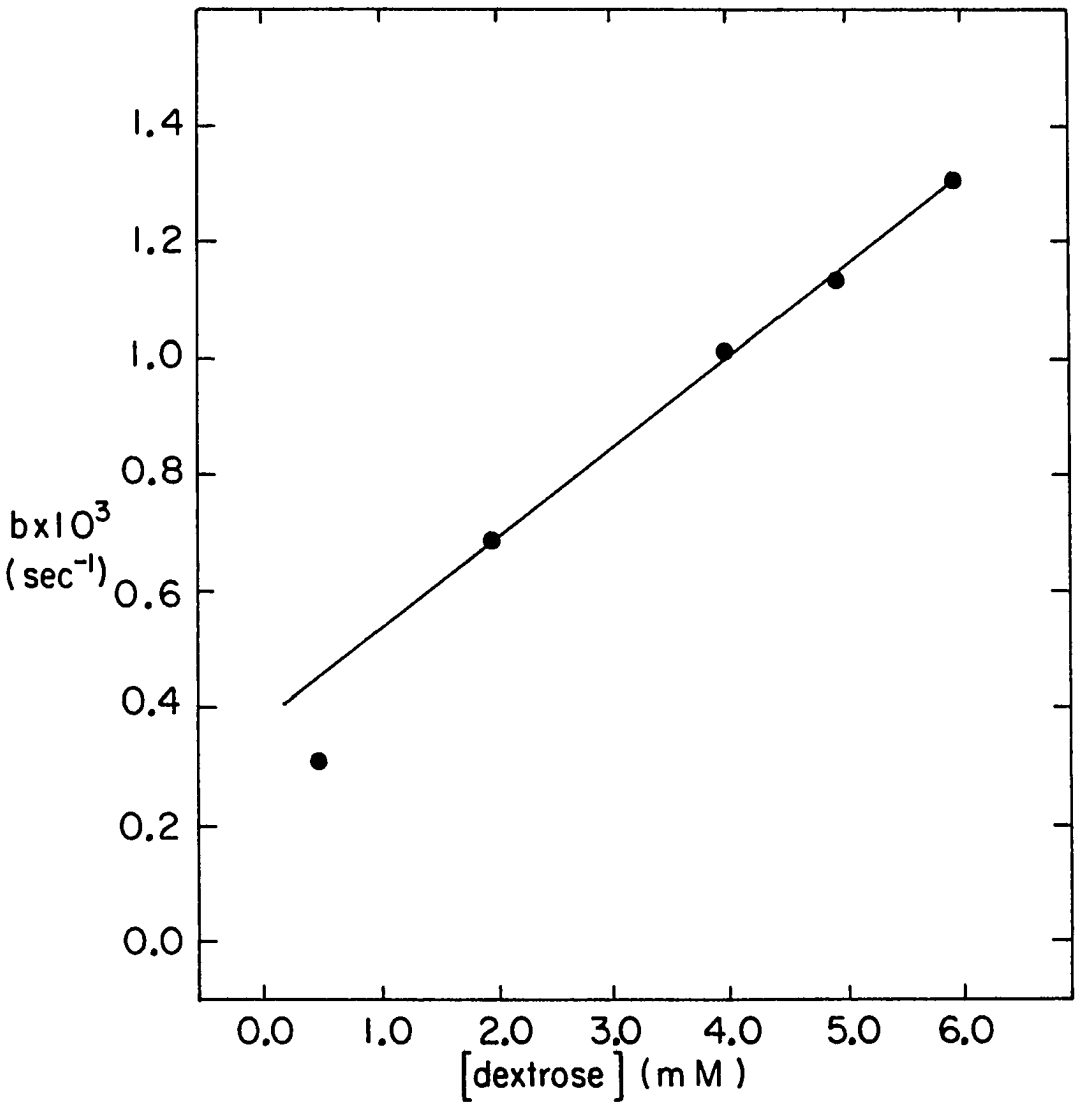
1.4
1.2
1.0
0.8
0.6
0.4
0.2
0.0
b x 10^3
(sec^-1)
0.0
1.0
2.0
3.0
4.0
5.0
6.0
[dextrose] (m M)

5.00×10^{-7} M Bi(III) and the time-dependent voltammetric curves (see Figure IV-18) were monitored until the maximum amount of Bi ad-atoms had been deposited, as indicated by the constant height of the current spikes. The Bi-coated Pt-RDE was then transferred to a 5 mM dextrose solution and the time-dependent voltammetric curves for this solution were monitored for 8 min, during which the anodic current spikes associated with the oxidation of dextrose were observed to decrease to about 25% of the original value. The Pt-RDE was then transferred to a solution of 0.35 M NaOH. The magnitude of the current spikes associated with the oxidation of Bi to the insoluble oxide in this solution, when compared to those observed during the precoating of the Pt-RDE with Bi, indicated that approximately 40% of the original amount of the Bi ad-atoms had been removed while the electrode was immersed in the dextrose solution. A similar experiment, conducted under open circuit conditions while the Bi-precoated Pt-RDE was immersed in the dextrose solution, revealed that under conditions for which the products of dextrose oxidation were absent, about 25% of the Bi ad-atoms were lost after 8 min. A control experiment conducted in the absence of dextrose indicated that only 4% of the Bi ad-atoms would have been lost in the supporting electrolyte alone. Hence, the dextrose molecules and/or the products of dextrose oxidation are concluded to cause removal of the Bi ad-atoms from the precoated electrode.

F. Effects of Metal Ad-atoms on the Electrochemical Oxidation of Dextrose on the Au-RDE

The electrochemical oxidation of dextrose has not been investigated at noble-metal electrodes other than the Pt-electrode. Therefore, the electrochemical behavior of dextrose was investigated at a Au-RDE, both in the absence and the presence of metal ad-atoms which included Bi, Pb, Tl and Cd. An alkaline medium of 0.35 M NaOH was also employed as the supporting electrolyte in these studies.

The residual I-E curve of the Au-RDE in 0.35 M NaOH is shown in Figure IV-20. The accessible potential range of the Au-RDE, which extends from 0.6V vs. SCE to -1.4V vs. SCE, is considerably larger than that of the Pt-RDE, which is from 0.6V vs. SCE to -0.8V vs. SCE. Anodic and cathodic currents associated with the formation and reduction of the oxide layer on the Au surface are also observed for the Au-RDE. However, peaks associated with the processes of hydrogen adsorption and desorption, which are observed in the residual I-E curve of the Pt-RDE, are completely absent for the Au-RDE.

Bi was chosen as the metal to illustrate the deposition of ad-atoms on the Au-RDE. The I-E curve of the Au-RDE in the presence of Bi(III) is shown in Figure IV-21. The electrodeposition and stripping of Bi ad-atoms on the Au-RDE occur in a potential region more negative than Peaks D and E, which are associated respectively with the formation and the subsequent reduction of oxide on the Au surface. The groupings of anodic (A,B,C) and cathodic (A',B',C') peaks are associated

Figure IV-20. I-E curve of the Au-RDE in 0.35 M NaOH

Electrode rotation speed (W): 400 rev min^{-1}

Potential scan rate (ϕ): 6 V min^{-1}

D: Au oxidation peak

E: Au oxide reduction peak

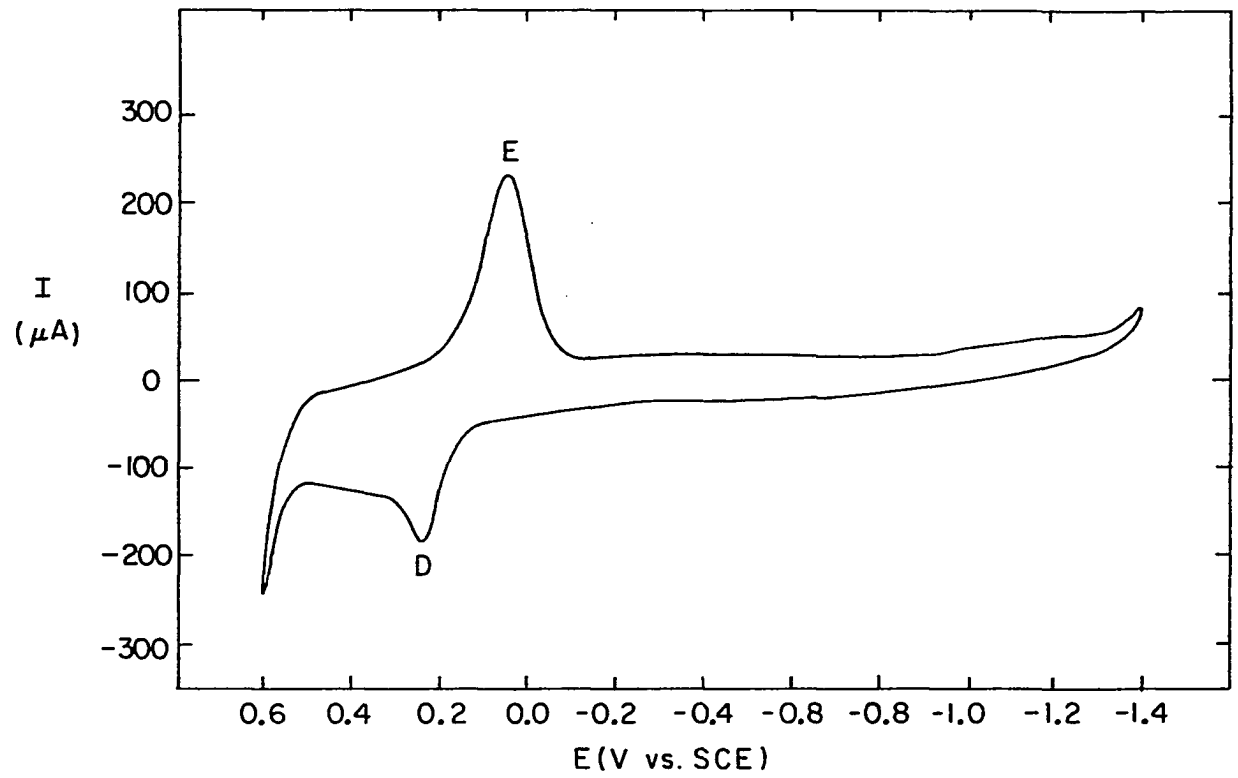
300
200
100
0
-100
-200
-300
I
(μA)
E
D
0.6
0.4
0.2
0.0
-0.2
-0.4
-0.8
-0.8
-1.0
-1.2
-1.4
E(V vs. SCE)

Figure IV-21. I-E curves of the Au-RDE in 0.35 M NaOH containing various concentrations of Bi(III)

Electrode rotation speed (W): 400 rev min^{-1}

Potential scan rate (ϕ): 6 V min^{-1}

A, B and C: Bi oxidation peaks

A', B' and C': Bi oxide reduction peaks

D: Au oxidation peak

E: Au oxide reduction peak

——— 0.25 μM Bi(III)

------- 2.0 μM Bi(III)

••••••• 19.0 μM Bi(III)

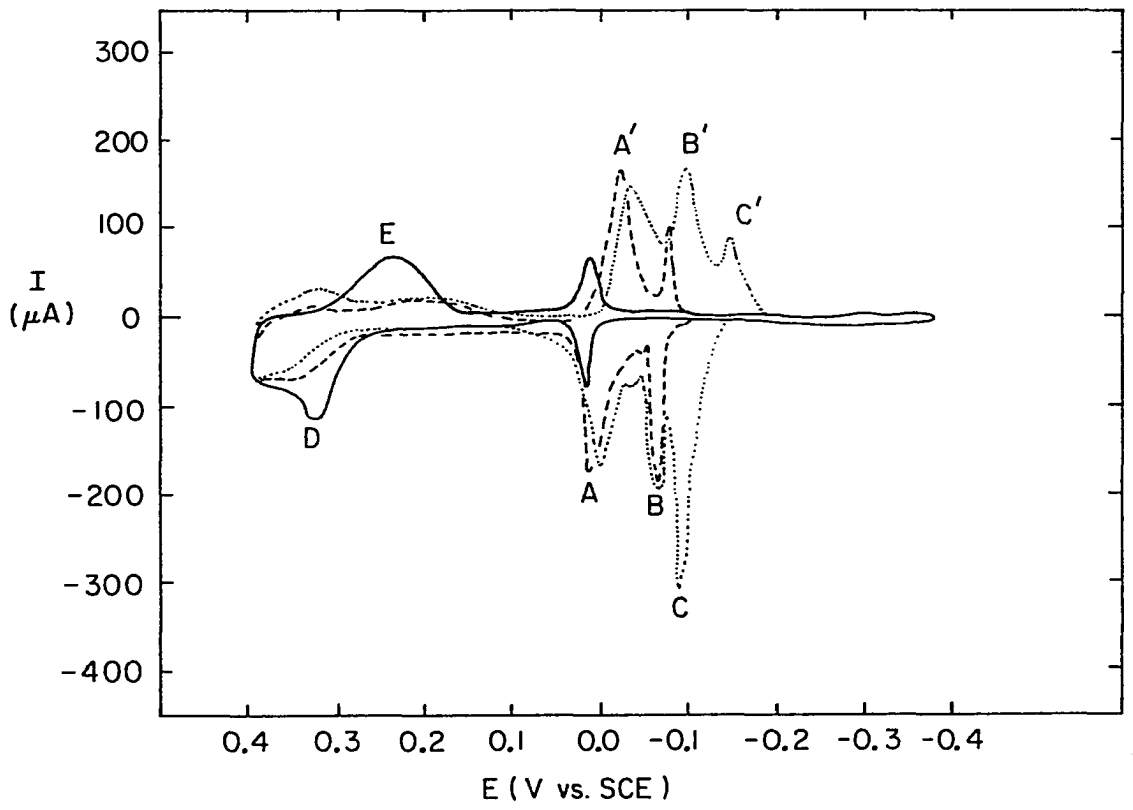
300
200
100
0
-100
-200
-300
-400
I
(μA)
A′
B′
C′
E
D
A
B
C
0.4
0.3
0.2
0.1
0.0
-0.1
-0.2
-0.3
-0.4
E (V vs. SCE)

respectively with the oxidation of the deposited Bi to the insoluble oxide and the subsequent reduction of that oxide to Bi. Hence, the Bi ad-atoms are oxidized on the positive potential sweep before the substrate Au metal is oxidized. The observation that as many as three peaks are observed for both the oxidation of Bi and the reduction of the insoluble oxide is the basis for concluding that, at high concentrations of Bi(III), the ad-atoms are deposited in three different states of activity on the Au-RDE. Perhaps, they are deposited first as isolated ad-atoms without significant Bi-Bi interactions, then as aggregates of ad-atoms, and finally as the bulk metal. Peaks C and C' are the only ones observed to continuously increase with increases in the concentration of Bi(III) and they are concluded to be associated with bulk Bi atoms, i.e., unit activity. The oxidized state of the Bi ad-atoms interferes with the formation of Au oxide, as indicated by the decrease in both Peak D and Peak E observed after the Bi has been deposited.

The I-E curve for the electrochemical oxidation of 0.025 M dextrose on the Au-RDE is shown in Figure IV-22. The behavior of dextrose on the Au-RDE is very different from that on the Pt-RDE. Two overlapping anodic peaks, A and B, are obtained during the negative potential scan while two similar anodic peaks, C and D, are obtained during the positive scan. Peaks A and D and Peaks B and C, although obtained for opposite scan directions, have similar values of E_p and I_p. Integration of the total area under the anodic peaks of the I-E curve shown in Figure IV-22 yielded 0.19 and 0.23 coulombs for the peaks obtained on the negative and positive scans, respectively. The

Figure IV-22. I-E curve of the Au-RDE in 0.35 M NaOH containing 0.025 M dextrose

Electrode rotation speed (W): 400 rev min^{-1}

Potential scan rate (ϕ): 6 V min^{-1}

A, B, C and D: anodic peaks

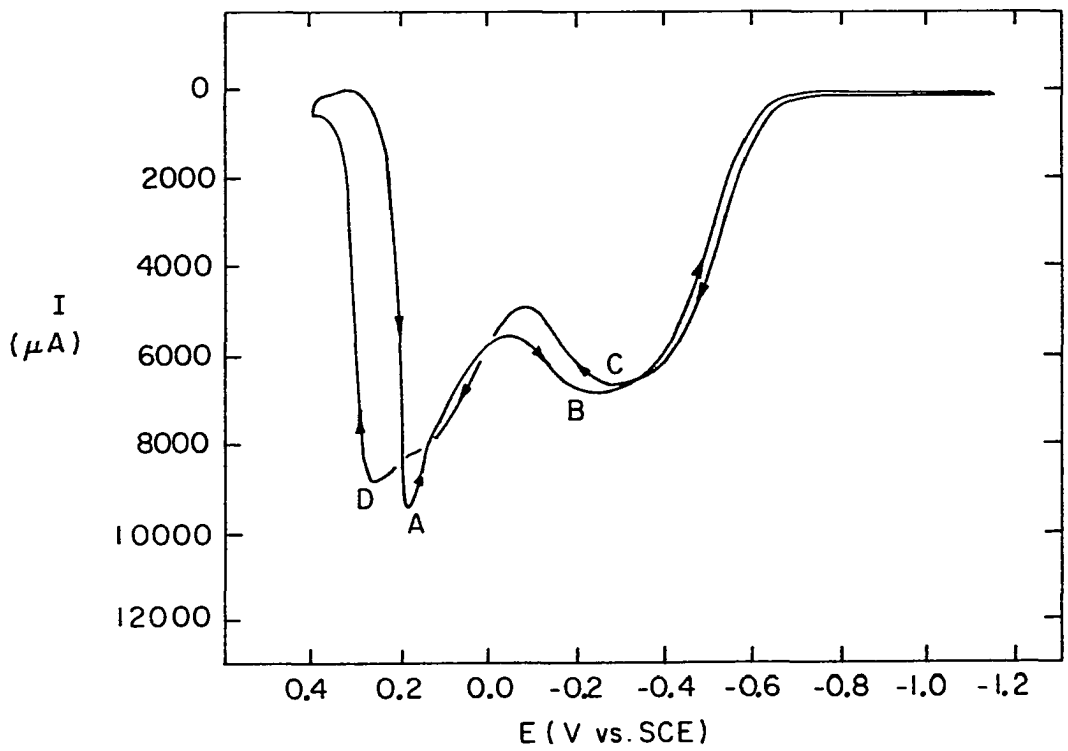
I
(μA)
0
2000
4000
6000
8000
10000
12000
0.4
0.2
0.0
-0.2
-0.4
-0.6
-0.8
-1.0
-1.2
E (V vs. SCE)
A
B
C
D

total charge under these peaks, obtained when the positive scan limit was restricted to 0.2V vs. SCE so that the Au substrate was not oxidized, were equal to each other with a value of 0.19 coulombs. The equivalency of charge is concluded to indicate that an equal number of surface sites is available for the oxidation of dextrose on the positive and negative scans. Furthermore, the fact that an equal number of sites is available, even when E_+ is restricted to 0.20V vs. SCE to minimize the cleaning effects accompanying the oxidation of the Au substrate, suggests that little or no poisonous species are formed on the Au surface during the electrochemical oxidation of dextrose.

The effect of Bi, Pb, Tl and Cd on the electrochemical oxidation of dextrose on the Au-RDE is shown in Figure IV-23. In all the cases, the presence of the metal ad-atoms drastically decreases the current of all the anodic peaks for the oxidation of dextrose. The greatest effect is exerted by Tl and Cd. Although the values of I_p are drastically decreased by the metal ad-atoms, the values of E_p are not greatly affected. This is concluded to occur because little or no poisons are formed on the Au-RDE during the anodic reactions of dextrose. The metal ad-atoms simply block the surface of the Au-RDE and thereby decrease the number of sites available for the electrochemical oxidation of dextrose.

The currents observed during the electrochemical oxidation of dextrose for the Au-RDE in the absence of any metal ad-atoms are much larger than those obtained under similar experimental conditions for the Pt-RDE. Therefore, a series of I-E curves for the Au-RDE in

Figure IV-23. I-E curves of Au-RDE in 0.35 M NaOH containing 0.025 M dextrose and various concentrations of Bi(III), Pb(II), Tl(I) and Cd(II)

Electrode rotation speed (W): 400 rev min^{-1}

Potential scan rate (ϕ): 6 V min^{-1}

A, B, C and D: anodic peaks

I ——— 0.0 μM Bi(III)

------- 6.0 μM Bi(III)

II ——— 0.0 μM Pb(II)

------- 6.0 μM Pb(II)

III ——— 0.0 μM Tl(I)

------- 2.0 μM Tl(I)

IV ——— 0.0 μM Cd(II)

------- 2.0 μM Cd(II)

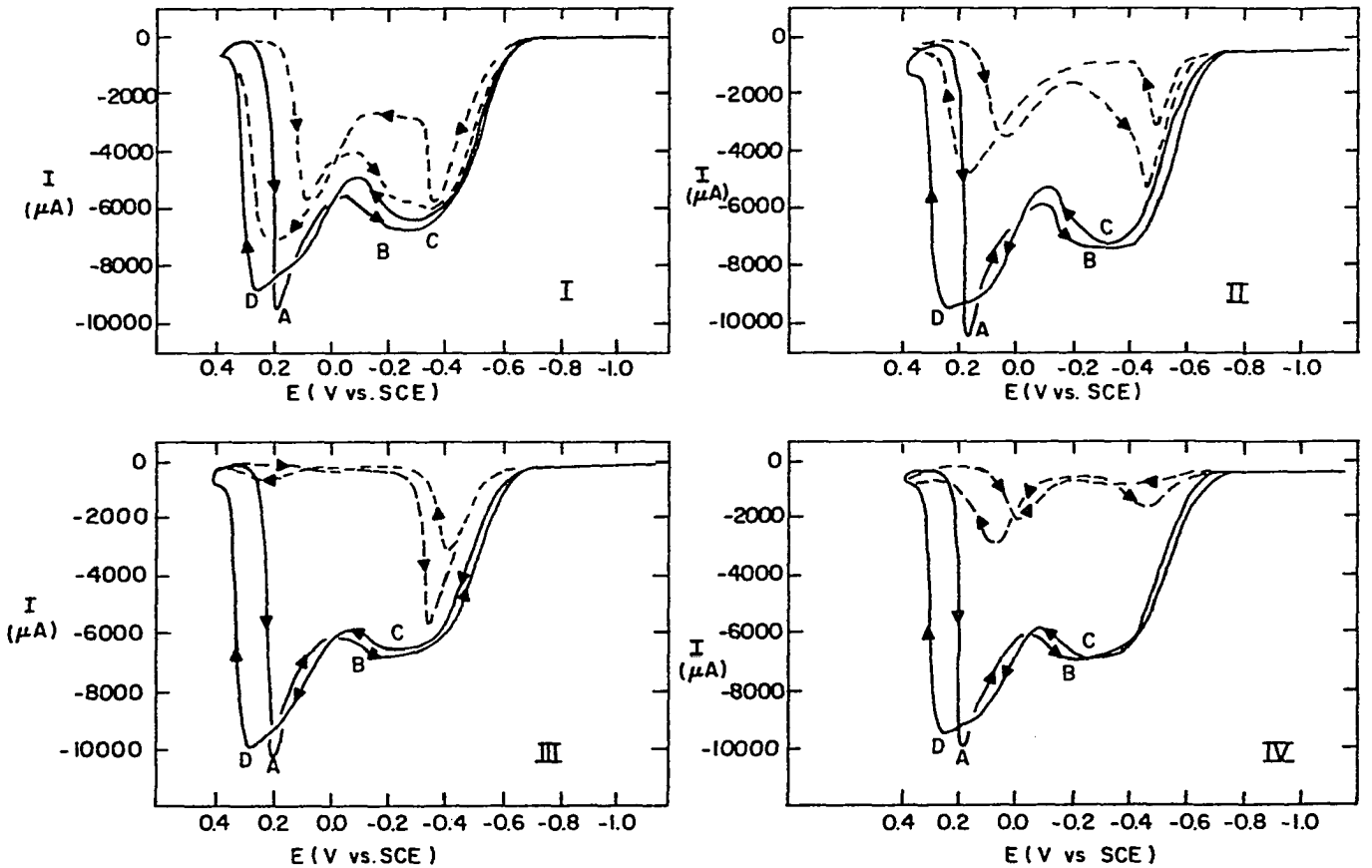
I
(μA)
0
-2000
-4000
-6000
-8000
-10000
A
B
C
D
I
0.4 0.2 0.0 -0.2 -0.4 -0.6 -0.8 -1.0
E (V vs. SCE)
II
III
IV
E (V vs SCE)

0.35 M NaOH containing dextrose was obtained as a function of W for several concentrations of dextrose. This was done to investigate whether the observed anodic currents approached the theoretical values predicted by the Levich Equation (see Section III-8) for a mass transport-limited process. $I_{p,C}$ was chosen for this analysis. It was assumed that gluconic acid is the sole product of the oxidation, i.e., n = 2. Values of the other parameter of the Levich Equation used for the estimation were as follows:

$F = 96487$ coulomb eq^{-1}

$A = 0.43$ cm^2

$D = 1 \times 10^{-5}$ cm^2 sec^{-1} (an estimate)

$v = 0.01$ cm^2, sec^{-1}

The observed and the predicted values of $I_{p,C}$ are compared in Table IV-17 for several concentrations of dextrose.

Table IV-17. Observed and predicted values of $I_{p,B}$ for the electrochemical oxidation of dextrose on the Au-RDE

[Dextrose] (mM)	$W^{1/2}$ ($rev^{1/2}$ $min^{-1/2}$)	$I_{p,C,predicted}$ (μA)	$I_{p,C,observed}$ (μA)
0.8	20	264	175
	30	396	250
	40	528	300
	50	660	375
	60	792	438
5.0	20	1656	1400
	30	2484	1800
	40	3312	2200
	50	4140	2550
	60	4968	3000

Table IV-17. (Continued)

[Dextrose] (mM)	$W^{1/2}$ ($rev^{1/2}$ $min^{-1/2}$)	$I_{p,C,predicted}$ (μA)	$I_{p,C,observed}$ (μA)
8.0	20	2650	1850
	30	3975	2500
	40	5300	3100
	50	6625	3700
	60	7950	4250
12.0	20	3974	2600
	30	5961	3600
	40	7948	4550
	50	9935	5450
	60	11922	6300

The observed and predicted values are plotted in Figure IV-24 as a function of $W^{1/2}$ for 0.8 mM and 8 mM dextrose. In all cases, the slope of the plot of $I_{p,C,predicted}$ *vs.* $W^{1/2}$ is twice that of the plot of $I_{p,C,observed}$ *vs.* $W^{1/2}$. This is probably due to an incorrect choice of the value of n = 2. Although the slopes of the predicted and observed plots are not identical, the linearity of the plot of $I_{p,observed}$ *vs.* $W^{1/2}$ supports the conclusion that the electrochemical process associated with Peak C is mass transport limited, *i.e.*, the heterogeneous rate constant for the electron transfer step is large.

The anodic processes associated with Peaks A and D are dependent on the rate of potential scan ϕ, increasing with increases in ϕ. Peaks B and C are, however, independent of ϕ. Peaks A and D are also

Figure IV-24. Comparison of the observed and predicted values of $I_{p,C}$ obtained during the electrochemical oxidation of dextrose on the Au-RDE

Supporting electrolyte: 0.35 M NaOH

Potential scan rate (ϕ): 6 V min^{-1}

-●-●-●- observed $I_{p,C}$ at 0.8 mM dextrose

-o-o-o- predicted $I_{p,C}$ at 0.8 mM dextrose

-▲-▲-▲- observed $I_{p,C}$ at 8 mM dextrose

-Δ-Δ-Δ- predicted $I_{p,C}$ at 8 mM dextrose

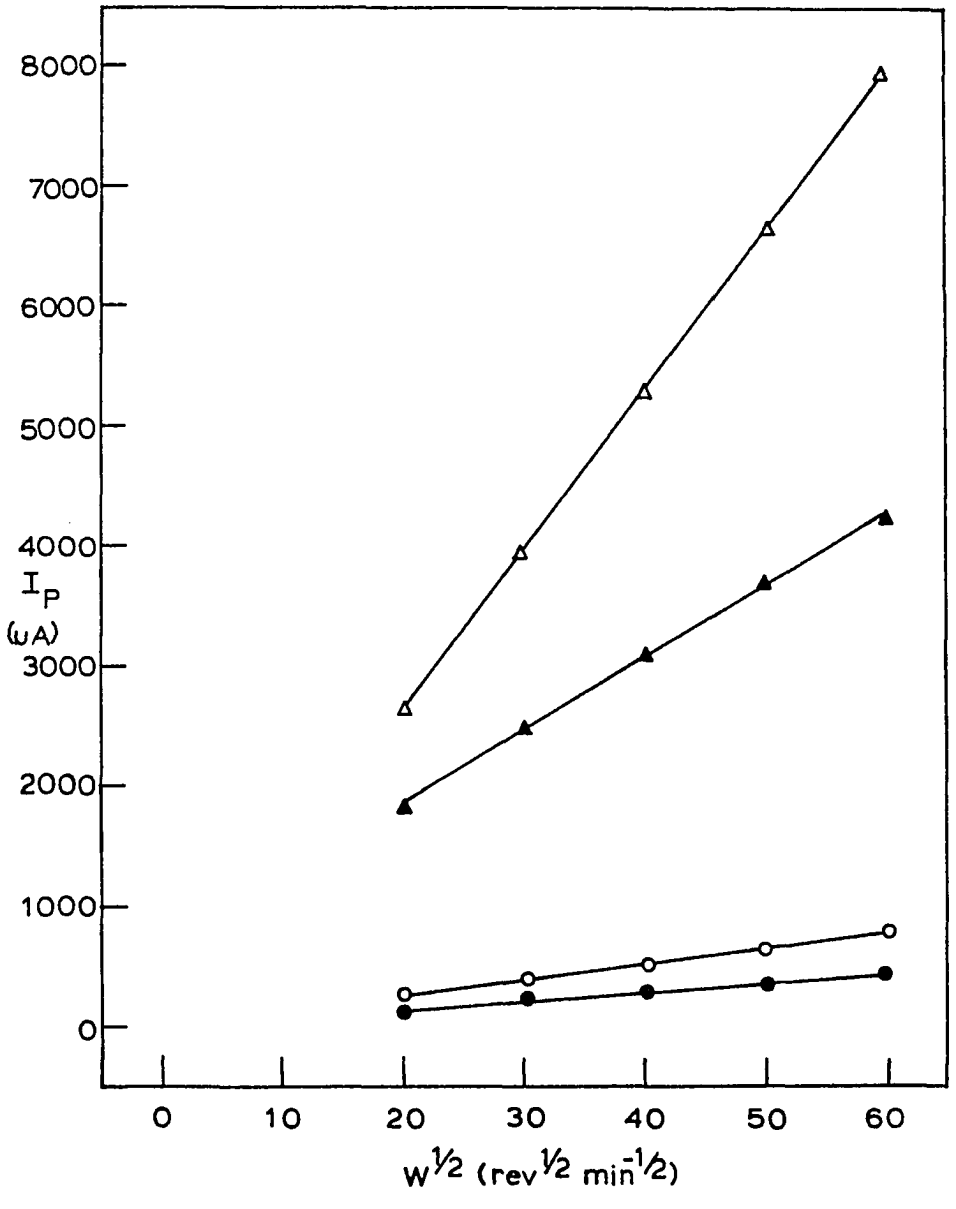
8000
7000
6000
5000
4000
I_P
(μA)
3000
2000
1000
0
0
10
20
30
40
50
60
$w^{1/2}$ (rev$^{1/2}$ min$^{-1/2}$)

dependent on E_-, decreasing as E_- is moved positive. Peaks B and C show no dependence on E_-. From studies of the effects of W, ϕ and E_- on the I-E curves, it is concluded that Peaks B and C represent the same electrochemical process while Peaks A and D represent a different process. A summary of the results obtained for variations of W, ϕ and E_- is given in Table IV-18.

Table IV-18. Summary of W, ϕ and E_- studies for the electrochemical oxidation of dextrose on the Au-RDE

Peak	A	B	C	D
W dependency	Yes	Yes	Yes	Yes
ϕ dependency	Yes	No	No	Yes
E_- dependency	Yes	No	No	Yes

The summary presented in Table IV-18 indicates that Peaks A and D are associated with a mixed mass transport limited and surface-controlled process while Peaks B and C are associated with a totally mass transport-limited process.

Amperometric studies involving the oxidation of dextrose on the Au-RDE also support this conclusion. When E was held in the potential region of Peaks A and D following potential scanning, the peak current immediately decreased from 9 mA to a steady-state value (I_{ss}) on the order of 1.5 mA for a solution containing 0.025 M dextrose with

$W = 400$ rev min^{-1}. When E was held in the potential region of Peaks B or C, the value of I_{ss} was almost equal to $I_{p,B}$ and $I_{p,C}$, being on the order of 6 mA for over 10 minutes.

Perhaps, Peak A and Peak D represent the oxidation of dextrose on the AuO surface. This would explain the dependence of $I_{p,A}$ and $I_{p,D}$ on ϕ because each is the sum of two I values. $I_{p,dextrose}$ is

$$I_p = I_{p,dextrose} + I_{p,AuO} \qquad \text{(IV-6)}$$

independent of ϕ but $I_{p,AuO}$, which is associated with the surface-controlled oxidation of Au to AuO, is dependent on ϕ. Peaks B and C represent the mass transport-limited oxidation of dextrose on metallic Au, and are, therefore, independent of ϕ.

G. Comparisons of the Anodic Peak Currents Obtained During Voltammetric Studies of the Electrochemical Oxidation of Dextrose on the Au-RDE and the Bi-coated Pt-RDE

The Au-RDE is concluded to be free from poisons during the electrochemical oxidation of dextrose. Hence, much higher anodic currents are obtained for the electrochemical oxidation of dextrose on the Au-RDE than on the Pt-RDE. However, a Pt-RDE that has been precoated to an optimal coverage by Bi ad-atoms should also be effectively protected from poisons. A comparison of the maximum anodic peak currents obtained for dextrose on the Au-RDE and the Bi-coated Pt-RDE would reveal whether poisoning was indeed completely prevented on the Bi-coated Pt-RDE. The value of $I_{max}/C^b \cdot N_{act}$, where I_{max} is the maximum anodic current, C^b is

the concentration of dextrose, and N_{act} is the number of active sites, is used as the basis for the comparison. I_{max} was obtained for $W = 400$ rev min^{-1} and $\phi = 6$ V min^{-1}. Peak C, obtained at -0.3V vs. SCE (see Figure IV-22) during the oxidation of dextrose on the Au-RDE, and Peak B, obtained at -0.3V vs. SCE (see Figure IV-7) during the electrochemical oxidation of dextrose on the Bi-coated Pt-RDE, were chosen for the comparison.

The total number of sites (N_{tot}) on the Au-RDE and the Pt-RDE, both 0.43 cm^2 in geometric area, can be calculated simply from the Au-Au and Pt-Pt interatomic distance, χ, which are 2.88 Å and 2.74 Å, respectively. Assuming a roughness factor of unity for both the Au-RDE and the Pt-RDE surface, the total number of sites (N_{tot}) on the surface of the Au-RDE and Pt-RDE are estimated to be 6.58×10^{14} and 7.26×10^{14}, respectively, by substituting the appropriate values of the parameter into the equation

$$N_{tot} = \frac{0.43}{\pi\,(\chi/2)^2} \qquad \text{(IV-7)}$$

The number of active sites (N_{act}) on the Au-RDE, i.e., sites where electron transfer actually occur during the oxidation of dextrose, is equal to N_{tot}. However, N_{act} is less than N_{tot} for the Bi-coated Pt-RDE since the Bi-sites are assumed not to be involved in the electron transfer process. Comparison of Table IV-5 with Table IV-1 indicates that $\theta_{Bi} \approx 1$ for the optimal enhancement of dextrose oxidation on the Pt-RDE. It has been estimated experimentally that a single closely spaced layer of Bi ad-atoms occupies about 70% of the

active sites on the Pt-RDE. Hence, $N_{act} = 0.3\ N_{tot}$, or 2.18×10^{14} sites, for the Pt-RDE. The appropriate parameters that were used for calculating $I_{max}/C^b \cdot N_{act}$ for the oxidation of dextrose are shown in Table IV-19. $I_{max}/C^b \cdot N_{act}$ estimated for the oxidation of dextrose on

Table IV-19. Values of the parameters used in calculating $I_{max}/C^b \cdot N_{act}$ for the oxidation of dextrose on the Au-RDE and Pt-RDE

Electrode	Au-RDE	Bi-coated Pt-RDE
I_{max}	6600 μA	20000 μA
C^b dextrose	0.025 M	0.25 M
N_{act}	6.58×10^{14} sites	2.18×10^{14} sites

the Au-RDE and the Bi-coated Pt-RDE are 4.02×10^{-10} μA mole^{-1} ℓ site^{-1} and 3.70×10^{-10} μA mole^{-1} ℓ site^{-1}, respectively. Because these values are quite close to each other, the conclusion is made that almost no poisoning species are formed on the Pt-RDE which has been optimally covered with the Bi ad-atoms. This is in agreement with the fact that the peak currents observed for the oxidation of dextrose on the Bi-coated Pt-RDE show no dependence on ϕ and do not decrease rapidly with time during amperometric studies (see Figure IV-14).

The question still remains as to why, if no poisons are formed on both the pure Au surface and the optimally Bi-coated Pt surface, is it that the oxidation of dextrose on the Au is close to mass transport-limited while that on the Pt-RDE is not. That is, why is the plot of I_p *vs.* $W^{1/2}$ linear for the Au-RDE, but nonlinear for the Pt-RDE? The solution may be arrived at by a consideration of the effective diffusion layer thickness, δ_{eff}, in the case of the Au-RDE and the Bi-coated Pt-RDE. The Levich Equation, which predicts that a plot of I_p *vs.* $W^{1/2}$ should be linear for a mass transport-limited process, is derived from the general expression which relates the mass transport-limited current on an electrochemical process to the bulk concentration of the electroactive species.

$$I_\ell = \frac{nFADC^b}{\delta_{theory}} \qquad \text{(IV-8)}$$

The theoretical diffusion layer thickness, δ_{theory}, is taken to be equivalent to the thickness of a stagnant layer of solution immediately adjacent to the surface of a RDE through which electroactive species must diffuse before reaching the surface of the electrode. δ_{theory} is proportional to $W^{-1/2}$, hence I_ℓ is proportional to $W^{1/2}$. Equation IV-8 as well as the Levich Equation apply only to a RDE whose surface is uniformly accessible to the incoming electroactive species. An electrode at which all surface sites can participate in the electrochemical reaction is considered to be uniformly accessible. Hence, the Au-RDE surface is uniformly accessible during the oxidation of dextrose, and the Levich Equation is valid for predicting the values

of the observed anodic currents as a function of $W^{1/2}$, i.e., plots of $I_{p,observed}$ vs. $W^{1/2}$ are linear. On the other hand, a Bi-coated Pt-RDE is not uniformly accessible to the incoming dextrose molecules, which only react on Pt sites but not on Bi ad-atoms, as illustrated by Figure IV-25. In this case, only the molecules diffusing along a path perpendicular to a Pt site travel a distance equal to δ_{theory}. Other molecules have to travel in a curved path to reach a Pt site, and therefore, δ_{eff}, the effective distance travelled by these species, is greater than δ_{theory}. δ_{eff} depends on the separation of the active sites and is not directly proportional to $W^{-1/2}$. Since $\delta_{eff} > \delta_{theory}$, $I_{p,observed} < I_{p,predicted}$. The difference between δ_{theory} and δ_{eff} for a particular electrode becomes larger with increases in W (see Figure IV-25). Hence, the negative deviation of the observed peak currents from the predicted values in the plots of I_p vs. $W^{1/2}$ becomes more evident at high values of $W^{1/2}$.

H. Summary and Conclusions

The effects of various metal ad-atoms, including Bi, Pb, Cd, Tl and Zn, on the oxidation of dextrose on the Pt-RDE and the Au-RDE were investigated. Although Cd and Zn inhibited the electrochemical oxidation of dextrose on the Pt-RDE, Bi, Pb and Tl greatly enhanced the oxidation of dextrose. For example, Bi, the most effective of the metal ad-atoms, increased the height of the anodic peak B for the oxidation of dextrose 100 X and the area of the same peak 340 X. The ordering of the effectiveness of the metal ad-atoms on the

Figure IV-25. A model of the diffusion path of the dextrose molecules towards a clean and a partially blocked surface

A low W

B high W

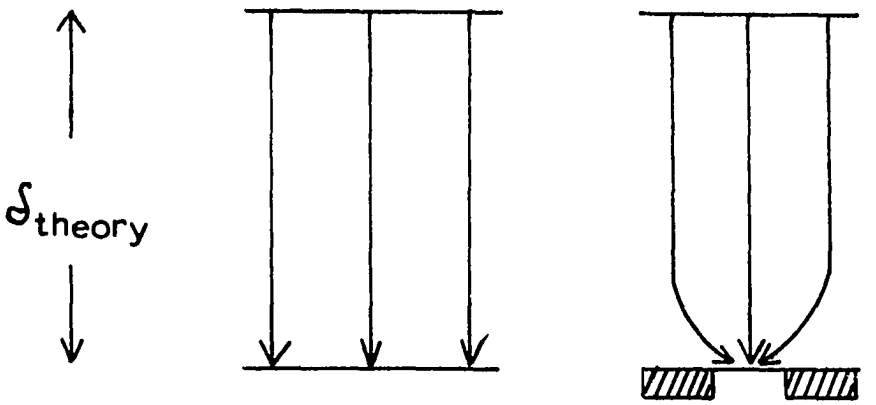

A

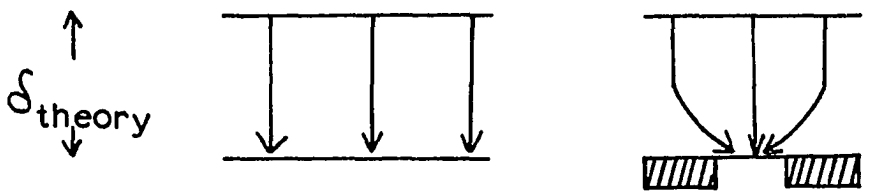

B

electrochemical oxidation of dextrose, as characterized by $QEF_{B,max}$, is correlated with the electron configuration of the metals in Table IV-20.

Table IV-20. Correlations between the electron configuration of the metal ad-atoms and their effects towards the electrochemical oxidation of dextrose on the Pt-RDE

Metal ad-atom	QEF_B	Electron configuration
Cu	inhibition	[Ar] $3d^{10}$ 4s
Zn	inhibition	[Ar] $3d^{10}$ $4s^2$
Cd	inhibition	[Kr] $4d^{10}$ 5s
Tl	70	[Xe] $4f^{14}$ $5d^{10}$ $6s^2$ 6p
Pb	90	[Xe] $4f^{14}$ $5d^{10}$ $6s^2$ $6p^2$
Bi	340	[Xe] $4f^{14}$ $5d^{10}$ $6s^2$ $6p^3$

As a group, the metal ad-atoms which enhance the electrochemical oxidation of dextrose all have electrons in the 6p-level and the effect of the metal ad-atoms increases as the number of 6p-electrons increases. The 6p-electrons of the metal ad-atoms may have an important role in increasing the extent of adsorption of the reacting molecules as the initial step in the course of the oxidation reaction. However, part of the enhancement effect may also be due to a decrease in the amount of adsorbed poisons on the Pt-RDE resulting from the ad-atoms.

The concentrations of the metal ions Bi(III) and Tl(I) required to reach the optimal enhancement of the oxidation of dextrose are much lower in an alkaline medium than in an acidic medium because these metals accumulated on the surface of the Pt-RDE on an alkaline medium. However, Bi ad-atoms precoated on the surface of the Pt-RDE were demonstrated to be partially removed by dextrose, leading to a decrease in the catalytic currents.

The peak currents for the oxidation of dextrose on the Pt-RDE show no dependence on $W^{1/2}$ in the absence of the metal ad-atoms. Some dependence on $W^{1/2}$ is observed for the peak currents in the presence of the ad-atoms. Plots of I_p *vs.* $W^{1/2}$ show negative deviation from linearity at high values of $W^{1/2}$ due to the fact that $\delta_{eff} > \delta_{theory}$ for the Pt-RDE which is partially blocked by metal ad-atoms.

The electrochemical oxidation of dextrose on the Au-RDE is close to a mass transport-limited process. Plots of I_p *vs.* $W^{1/2}$ show no deviation from linearity at high values of $W^{1/2}$ and the peak currents observed are quite close to those predicted by the Levich Equation. Anodic currents obtained at a fixed potential show little decrease with time, indicating that almost no poisons are formed on the Au-RDE during the electrochemical oxidation of dextrose. The metal ad-atoms prohibit the oxidation of dextrose on this electrode because they block some of the Au active sites from the dextrose molecules.

V. EVALUATION OF THE ACTIVATION ENERGY OF THE ELECTROCHEMICAL OXIDATION OF HCOOH ON THE Pt-RDE AND THE Bi-COATED Pt-RDE IN 0.50 M H_2SO_4

A. Introduction

The empirical activation energies of the electrochemical oxidation of HCOOH on the Pt-RDE and the Bi-coated Pt-RDE were obtained from analysis of the anodic peak currents as a function of temperature. These values of the activation energy are compared and conclusions made regarding the role of the Bi ad-atoms in the oxidation of HCOOH. Formic acid was chosen instead of dextrose for this investigation because dextrose was found to be unstable in dilute base at elevated temperatures.

A simplified empirical mechanism is given below for surface-catalyzed reactions where S represents the electrode surface, R the reactant molecules and P the product of the faradaic reaction. In this mechanistic model, P can remain adsorbed to the electrode surface, thereby poisoning the surface for further reaction. The actual mechanism corresponding to the anodic reactions at the Pt electrode

$$S + R \underset{k_{-1}}{\overset{k_1}{\rightleftharpoons}} S - R \qquad \text{(adsorption)} \qquad \text{(V-1)}$$

$$S - R \xrightarrow{k_2} S - P + ne \qquad \text{(faradaic reaction)} \qquad \text{(V-2)}$$

$$S - P \xrightarrow{k_3} S + P \qquad \text{(reactivation)} \qquad \text{(V-3)}$$

with and without the presence of Bi ad-atoms is undoubtedly more complex than the mechanism above. This simplified model is thought to be useful, however, for recognizing the critical steps in the overall process. There are similarities between the proposed mechanistic model and that for heterogeneous chain reactions. Adsorption is a pre-requisite for the anodic reaction and, therefore, is the "initiation" step of the mechanism. This case is unique in that the ultimate desired product, electrical current, is produced in the step which "terminates" the reaction sequence. Finally, the desorption of adsorbed P in Equation V-3 serves to renew the activity of the electrode and, therefore, constitutes sort of a "propagation" step.

The faradaic response for the solute, R, is proportional to the surface coverage of the electrode by R. It is observed that the

$$I \propto k_2 \theta_R \tag{V-4}$$

faradaic response is in the form of a peak. Since dI/dt is momentarily equal to zero at the peak potential, a steady-state approximation is made to evaluate θ_R. Furthermore, since $\theta_R + \theta_P \approx 1$ for a high

$$d\theta_R/dt = 0 = k_1 C_R(1 - \theta_R - \theta_P) - k_{-1}\theta_R - k_2\theta_R \tag{V-5}$$

concentration of HCOOH,

$$d\theta_P/dt = 0 = k_2\theta_R - k_3\theta_P \tag{V-6}$$

and

$$\theta_P = k_2\theta_R/k_3 \tag{V-7}$$

Combining Equations V-5 and V-7 and solving for θ_R yields

$$\theta_R = \frac{k_1 C_R}{k_1 C_R + k_1 k_2 C_R / k_3 + k_{-1} + k_2} \qquad \text{(V-8)}$$

The equilibrium constant for adsorption can be defined as $K = k_1/k_{-1}$. Hence,

$$\theta_R = \frac{KC_R}{KC_R + Kk_2 C_R / k_3 + 1 + k_2/k_{-1}} \qquad \text{(V-9)}$$

B. Experimental

The majority of the equipment and solutions have been described in Section III. The electrolysis cell was similar in design to the one described previously with the exception that a water jacket was provided for the temperature regulation of the cell's contents. A mixture of 50/50 H_2O and ethylene glycol at constant temperature was circulated through the water jacket from a Forma-Scientific Model 2095 temperature-regulating bath.

A 24 gauge Pt wire, 5 inches in length, was formed into a coil and used as the working electrode. This Pt coil electrode was used instead of the Teflon-sheathed Pt-RDE because it was feared that the latter would develop a leak at elevated temperatures.

Solutions of 0.50 M H_2SO_4 containing 0.25 M HCOOH, or 0.25 M HCOOH and 8 μM Bi(III), were thermostated at specific temperatures and the I-E curves of the Pt electrode obtained. The calculation of the apparent activation energy (ΔG^*_{app}) for the electrochemical oxidation

of HCOOH was based on plots of the logarithm of the peak current vs. 1/T.

C. Results and Discussion

I-E curves were obtained as a function of temperature for the Pt electrode and the Bi-coated Pt electrode in 0.25 M HCOOH. Examination of these curves revealed that while the values of I_p were increased with increases in temperature, the width of the anodic peaks and the position of the peaks along the potential axis were not affected by changes in temperature. It is concluded that variation in temperature does not affect the rate of electron transfer for the anodic reaction. This implies that the apparent energy of activation, ΔG^*_{app}, obtained in these experiments cannot be associated with the energy barrier for electron transfer.

Combination of Equations V-4 and V-9 yields

$$I_p \propto \frac{k_2 K C_R}{K C_R + k_2 K C_R / k_3 + 1 + k_2 / k_{-1}} \qquad \text{(V-10)}$$

For the large value of C_R (0.25 M) used in this work,

$$1 + k_2/k_{-1} << K C_R + k_2 K C_R / k_3 \qquad \text{(V-11)}$$

Hence, Equation V-10 reduces to

$$I_p \propto \frac{k_2}{1 + k_2/k_3} \qquad \text{(V-12)}$$

Since it was observed that E_p and peak shape was not influenced by variations of temperature, it is concluded that the rate of the electron transfer step is large (see Equation V-2). Hence, $k_2 >> k_3$. This reduces Equation V-12 to

$$I_p \propto k_3 \tag{V-13}$$

Equation V-13 implies that, based on the Arrehenius theory, the plots of ln I_p vs. 1/T are expected to yield values for the activation energy of the desorption step shown in Equation V-3

$$I_p = Z \exp\{-\Delta G_3^*/RT\} \tag{V-14}$$

$$\ln I_p = \ln Z - \Delta G_3^*/RT \tag{V-15}$$

ΔG_3^* can be evaluated from the slope of the plot of ln I_p vs. 1/T. Furthermore, the value of Z, obtained from the intercept of the plot, is a sort of frequency factor for the propagation step, and the term $\exp\{-\Delta G_3/RT\}$ is, therefore, the probability that one vibrational event will successfully result in the removal of the adsorbed poison as shown in Equation V-3.

The data used for the calculation of ΔG_3^*, based on $I_{p,D}$ and $I_{p,A}$ (see Figure III-2) as a function of T, are tabulated in Tables V-1 and V-2, respectively.

The plots of ln I_p vs. 1/T are shown in Figures V-1 and V-2 to be linear. The values of the slope, S, and the intercept, ln Z,

Table V-1. Data for the calculation of ΔG_3^*, based on Peak D obtained on the negative potential scan during the oxidation of 0.25 M HCOOH

	T (°K)	$1/T \times 10^3$ ($°K^{-1}$)	I_p (mA)	$\ln I_p$
Bi ad-atoms absent	283	3.53	31.5	3.45
	287	3.48	40.5	3.70
	292	3.42	53.5	3.98
	296	3.38	72.0	4.28
	303	3.30	116.0	4.75
	316	3.16	255.0	5.54
Bi ad-atoms present	283	3.53	25.5	3.24
	288	3.48	30.5	3.42
	296	3.38	50.5	3.92
	302	3.31	74.0	4.30
	307	3.26	125.0	4.83
	316	3.17	248.0	5.52

Table V-2. Data for the calculation of ΔG_3^*, based on Peak A obtained on the positive potential scan during the oxidation of 0.25 M HCOOH

	T (°K)	$1/T \times 10^3$ ($°K^{-1}$)	I_p (mA)	$\ln I_p$
Bi ad-atoms absent	283	3.53	9.0	2.20
	287	3.48	10.0	2.30
	292	3.42	11.6	2.45
	296	3.38	13.0	2.56
	303	3.30	16.0	2.77
Bi ad-atoms present	283	3.53	13.8	2.62
	288	3.48	16.0	2.77
	296	3.38	25.0	3.22
	302	3.31	34.0	3.53
	307	3.26	50.0	3.91
	316	3.17	86.0	4.45

Figure V-1. Plot of ln I_p *vs.* 1/T for Peak A obtained during the positive potential scan for the oxidation of HCOOH on the Pt electrode

Electrode rotation speed (W): 400 rev min^{-1}

Potential scan rate (ϕ): 6 V min^{-1}

Positive scan limit (E_+): 0.6V *vs.* SCE

Negative scan limit (E_-): -0.8V *vs.* SCE

Supporting electrolyte: 0.5 M H_2SO_4

[HCOOH]: 0.25 M

-o-o-o- Bi ad-atoms absent

-●-●-●- Bi ad-atoms present

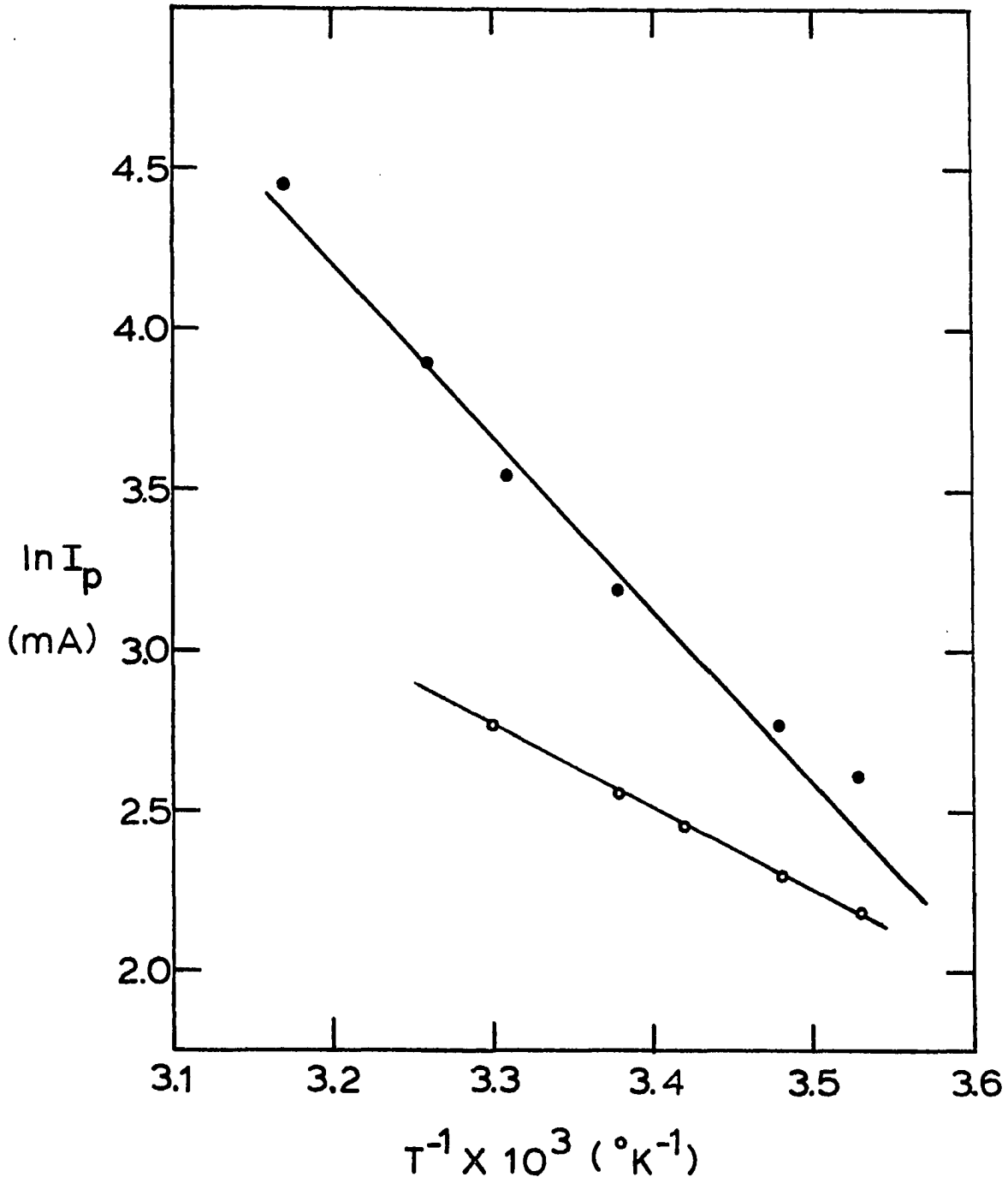
4.5
4.0
3.5
3.0
2.5
2.0
ln I_p
(mA)
3.1
3.2
3.3
3.4
3.5
3.6
$T^{-1} \times 10^3$ ($°K^{-1}$)

Figure V-2. Plot of ln I_p *vs.* 1/T for Peak D obtained during the negative potential scan for the oxidation of HCOOH on the Pt electrode

Supporting electrolyte: 0.5 M H_2SO_4

[HCOOH]: 0.25 M

Electrode rotation speed (W): 400 rev min^{-1}

Potential scan rate (ϕ): 6 V min^{-1}

Positive scan limit (E_+): 0.6V *vs.* SCE

Negative scan limit (E_-): -0.8V *vs.* SCE

-o-o-o- Bi ad-atoms absent

-●-●-●- Bi ad-atoms present

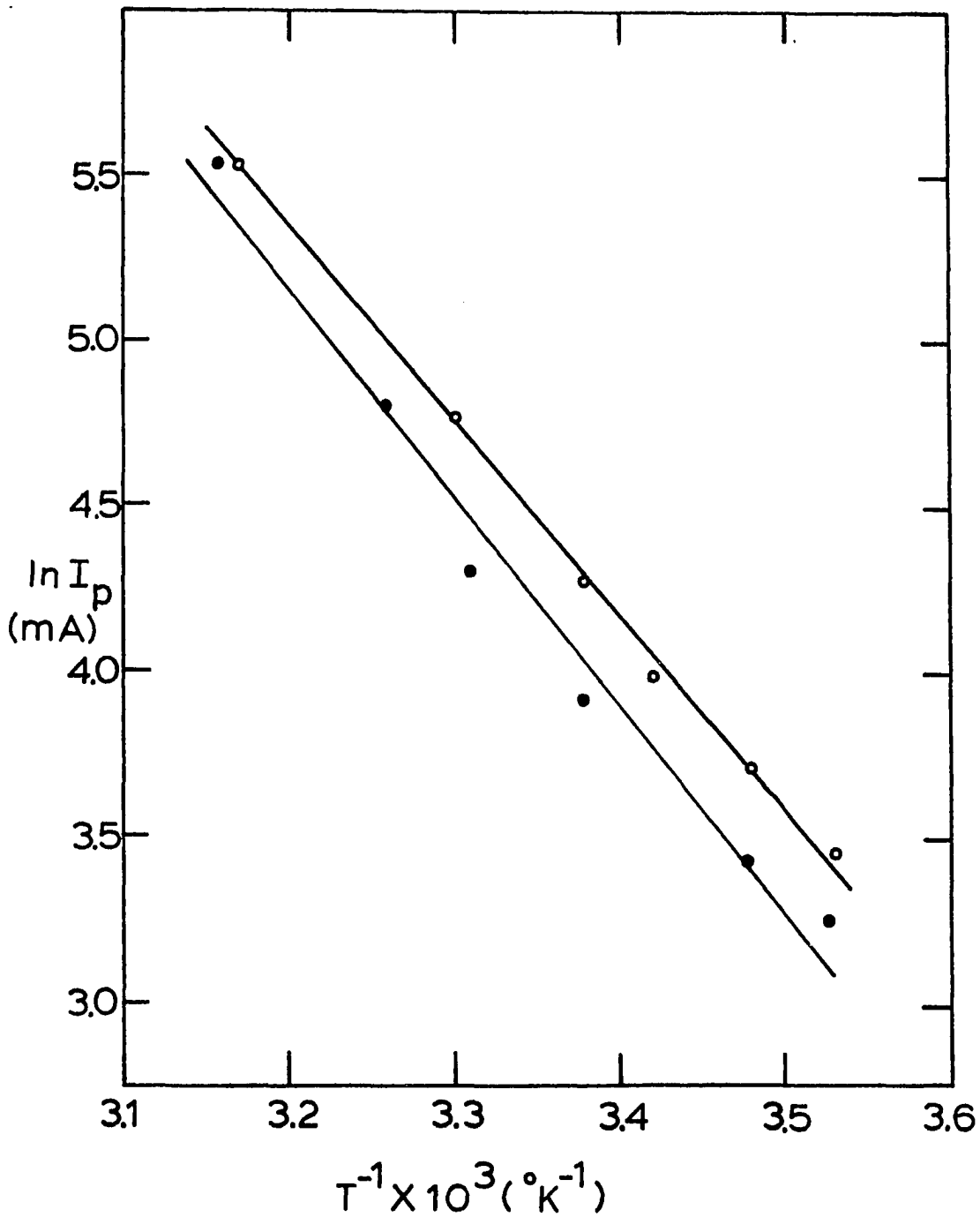
5.5
5.0
4.5
ln I_p
(mA)
4.0
3.5
3.0
3.1
3.2
3.3
3.4
3.5
3.6
$T^{-1} \times 10^3 (°K^{-1})$

together with the value of ΔG_3^* obtained from

$$\Delta G_3^* = -S \cdot R \qquad (V\text{-}16)$$

are shown in Table V-3.

Table V-3. The values of S, ln Z and ΔG_3^* obtained from the plots of ln I_p *vs.* 1/T for the oxidation of HCOOH on the Pt-RDE in 0.50 M H_2SO_4

Peak	Bi ad-atoms	S (°K)	ln Z	ΔG_3^* (kJ mole^{-1})
A	absent	-2500	11	21
A	present	-5100	20	42
D	absent	-5800	24	48
D	present	-6300	25	52

The values of ln Z and ΔG_3^* calculated for Peak D (negative scan) are not significantly affected by the presence of the Bi ad-atoms. This is understandable because, during the negative potential sweep, the electrode surface is not significantly covered by the Bi ad-atoms in the acidic medium in the potential range of Peak D. However, the values of ln Z and ΔG_3^* calculated from Peak A (positive scan) are significantly increased by the presence of the Bi ad-atoms. This indicates that whereas the activation barrier for desorption of P from the electrode surface is greater in the presence of the Bi ad-atoms,

the desorption is greatly enhanced in the presence of the Bi ad-atoms, as reflected by the larger value of the pre-exponential term Z in the Arrhenius Equation (see Equation V-14).

D. Conclusion

Bi ad-atoms significantly increase the activation barrier for the desorption of poisons formed during the oxidation of HCOOH on the Pt electrode. However, the desorption process is greatly enhanced by the Bi ad-atoms with the result that the observed anodic current is greatly enhanced.

VI. SUMMARY AND CONCLUSIONS

The electrochemical oxidation of formic acid was studied on a Pt electrode in acidic solutions, and that of dextrose was studied on Pt and Au electrodes in alkaline solutions. Loss of electrode activity, i.e., poisoning, was observed during the oxidation of both formic acid and dextrose on the Pt electrode. However, this phenomenon was not observed for dextrose on the Au electrode. The poisoning phenomenon is concluded to result from the strong adsorption of by-products of the electrochemical reactions on the Pt surface, rather than from adsorption of impurities in the electrolyte. While the exact structures of the poisons are not known, it is likely that they are free-radicals whose partially filled orbitals can overlap with the partially filled d-orbitals of the Pt atoms on the electrode surface.

The effects of metal ad-atoms on the electrochemical oxidation of formic acid and dextrose on the Pt and Au electrodes were characterized using linear sweep cyclic voltammetry. Several heavy-metal species, especially Pb, Bi and Tl, were found to enhance greatly the anodic currents for both formic acid and dextrose on the Pt electrode. The transition metals, including Cu and Zn, were found to inhibit the oxidations of the organic compounds on the Pt electrode. Correlation of the enhancement effects of the metal ad-atoms with their electron configuration reveals that, in general, enhancement increases as the number of partially filled orbitals in the 6-p level increases. The

maximum enhancement comes from the optimum coverage (θ_M) of the electrode with respect to the metal ad-atoms. The optimum value of θ_M differs for the different metals studied, ranging from approximately 0.3 (Bi) to 0.8 (Tl) for the oxidation of formic acid, and 0.5 (Pb) to > 0.9 (Bi) for the oxidation of dextrose on the Pt electrode. Saturation of the electrode surface with respect to the metal ad-atoms, i.e., $\theta_M \longrightarrow 1$. results in a decrease of the enhancement effects.

All metal ad-atoms tested showed an inhibitory effect on the oxidation of organic compounds on the Au electrode for all values of θ_M. This is concluded to result from the fact that, since the Au electrode is immune to the poisoning phenomenon, the metal ad-atoms serve only to block the active sites on the Au surface, thereby decreasing the effective surface area of the electrode.

Amperometric data obtained at constant potential demonstrated that a Pt electrode is completely deactivated within 10 sec during the electrochemical oxidation of dextrose without the benefit of ad-atoms. The Au electrode, on the other hand, retains much of its activity even after 10 minutes. However, the activity of the Pt electrode can be maintained much longer than 10 sec in the presence of the metal ad-atoms. The time taken for the anodic current to decay to 10% of the maximum value obtained during the amperometric studies on the Pt-RDE, the Bi-coated Pt-RDE and the Au-RDE are approximately 5 sec, 5 min and 60 min, respectively. From this observation, the conclusion is made that the amount of poison that can remain adsorbed on the Pt electrode is drastically decreased in the presence of the metal

ad-atoms. The same conclusion is made based on the observation of the equivalency of the anodic currents obtained per unit concentration of dextrose per active site ($I_p/C^b \cdot N_{act}$) on the Bi-coated Pt-RDE with that for the Au-RDE.

In the absence of the metal ad-atoms, the anodic currents associated with the electrochemical oxidation of dextrose and formic acid on the Pt-RDE were independent of the rotation speed (W) of the electrode, but increased as the rate of potential scan (ϕ) was increased. Hence, the oxidation reactions are totally surface-controlled. However, the reverse was observed for the oxidation of dextrose and formic acid on the Bi-coated Pt electrode. It is concluded that the oxidation reactions are closer to being mass transport-limited in the presence of the ad-atoms.

Studies which involved the variation of temperature during a study of the electrochemical oxidation of formic acid on the Bi coated Pt-RDE revealed that the peak potentials and the peak widths of the anodic peaks were not affected by changes in temperature. Hence, the steps in the reaction up to and including the rate determining step are concluded to not involve electron transfer. Furthermore, it is concluded that the metal ad-atoms do not increase the rate of electron transfer, i.e., the reversibility of the anodic reactions. In other words, the metal ad-atoms do not truly catalyze the anodic reactions of the organic compounds.

The peak potentials (E_p) obtained for the oxidation of formic acid and dextrose were observed to be shifted slightly negative along the

potential axis in the presence of the metal ad-atoms. The value of E_p for the positive sweep in the presence of the metal ad-atoms was the result of the transformation of the oxidation state of the metal. However, the negative shifts observed were very small, e.g., < 50 mV, and are concluded to be too small to indicate an increase in the rate of the electron transfer step in the presence of the ad-atoms.

The enhancement of the anodic currents for formic acid and dextrose at a Pt electrode by deposition of metal ad-atoms is concluded to result not from an increase in the rate of electron transfer of the anodic reactions but rather from an increase in the rate of desorption of the adsorbed poisons. The activation energy (ΔG_3^*) of the desorption step in the oxidation of formic acid was calculated based on the Arrehenius theory using data obtained in the temperature studies. The value of ΔG_3^* was found to be increased by the Bi ad-atoms, indicating that the Bi ad-atoms actually increase the energy barrier of the desorption step. However, the pre-exponential factor in the Arrehenius Equation was drastically increased by the presence of Bi ad-atoms. The pre-exponential factor in the Arrehenius Equation is frequently interpreted as a frequency term for unimolecular reactions (111). In an analogous manner, it is concluded that the Bi ad-atoms increase the 'frequency' of vibrational desorption of the poisons at the electrode surface resulting in an increase in the rate of regeneration of active Pt sites. Physically, the metal ad-atoms may help to break the chemical bonds between the Pt atoms and the poisons by a process visualized as surface-site exchange. The motions of the

ad-atoms from site-to-site on the electrode surface quite literally result in "scraping" of the adsorbed poisons from the electrode surface.

It was observed that the enhancement effects of the metal ad-atoms were lost as soon as either the noble metal substrate or the metal ad-atoms were oxidized. It is concluded that the bi-functional theory (see Section II.C.2.c) proposed by some workers to explain the enhancement effects of the metal ad-atoms is not applicable to the heavy-metal ad-atoms studied in this research. In fact, in the oxidized form, the ad-atoms offer no enhancement of the oxidation reactions studied.

VII. SUGGESTIONS FOR FUTURE RESEARCH

The Au electrode needs to be studied in greater detail for the electrochemical oxidation of simple sugars as well as other simple organic compounds because it was shown to be highly active for the electrochemical oxidation of dextrose. Such investigations would reveal whether the Au electrode is in general immune to poisoning by the organics and, if so, further studies need to be conducted to reveal the surface properties of the Au that contribute to the immunity.

Alloy electrodes, such as Bi/Pt or Pb/Pt electrodes, should be investigated for their activities in the electrochemical oxidation of organic compounds in an alkaline medium. Although selective leaching of the less noble component of an alloy electrode is a problem in acidic media, this should not be a severe problem in neutral or alkaline media. The catalyst metal in an alloy electrode would also better resist desorption by organic molecules, which is a problem with precoated electrodes. The alloy electrodes may offer exciting possibilities for the in-vivo determination of serum glucose and other biologically important molecules.

Application of the enhancement effects of metal ad-atoms to the electrochemical oxidation of a wide variety of organic compounds offers the possibility of designing a highly efficient 'electrochemical incinerator'. Such an incinerator can be used for the destruction of harmful organic compounds, including the organic carcinogens.

VIII. BIBLIOGRAPHY

1. Adams, R. N. "Electrochemistry at Solid Electrodes", 1st ed.; Marcel Dekker, Inc.: New York, 1969; Chapter 2.

2. Taylor, L. R.; Parkinson, B. A.; Johnson, D. C. Electrochim. Acta 1975, 20, 1005.

3. McIntyre, J. D. E.; Peck, W. F., Jr. In "Electrochemical Catalysis by Foreign Metal Ad-atoms", Bruckenstein, S., Ed.; "Proceedings of the Third Symposium on Electrode Processes", The Electrochemical Society: Princeton, 1980.

4. Sherwood, G. A. Ph.D. Dissertation, Iowa State University, Ames, IA, 1978.

5. Adzic, R. R.; Yeager, E.; Cahan, B. D. J. Electrochem. Soc. 1974, 12, 474.

6. Haber, F. Z. Physik. Chem. 1900, 32, 193.

7. Russ, R. Z. Physik. Chem. 1903, 44, 641.

8. Weinberg, N. L. In "Electrochemical Oxidation of Organic Compounds", Weinberg, N. L., Ed.; "Technique of Electroorganic Synthesis"; John Wiley and Sons: New York, 1974; Vol. 5, pt. 1, Chapter 4.

9. Rifi, M. R. In "Electrochemical Reduction of Organic Compounds", Weinberg, N. L., Ed.; "Technique of Electroorganic Synthesis"; John Wiley and Sons: New York, 1974; Vol. 5, pt. 1, Chapter 8.

10. Sandstede, G. In "From Electrocatalysis to Fuel Cells", Sandstede, G., Ed.; University of Washington Press: Seattle, 1972.

11. Müller, E. Z. Electrochem. 1923, 29, 264.

12. Müller, E.; Tanaka, S. Z. Electrochem. 1928, 34, 256.

13. Brummer, S. B.; Makrides, A. D. J. Phys. Chem. 1963, 68, 1448.

14. Capon, A.; Parsons, R. J. Electroanal. Chem. 1973, 44, 239.

15. Breiter, M. W. Electrochim. Acta 1965, 10, 503.

16. Gottlieb, M. H. J. Electrochem. Soc. 1964, 111, 465.

17. Munson, R. A. J. Electrochem. Soc. 1964, 111, 372.

18. Johnson, P. R.; Kuhn, A. T. J. Electrochem. Soc. 1965, 112, 599.

19. Rhodes, D. R.; Steigelmann, E. F. J. Electrochem. Soc. 1965, 112, 16.

20. Piersma, B. J.; Warner, T. B.; Schuldiner, S. J. Electrochem. Soc. 1966, 113, 841.

21. Bagotzky, V. S.; Vassiliev, Y. B. Electrochim. Acta 1966, 11, 1439.

22. Brummer, S. B. J. Phys. Chem. 1965, 69, 562.

23. Bockris, O'M. J.; Swinkels, D. A. J. J. Electrochem. Soc. 1964, 111, 736.

24. Bockris, O'M. J.; Green, M.; Swinkels, D. A. J. J. Electrochem. Soc. 1964, 111, 743.

25. Capon, A.; Parsons, R. J. Electroanal. Chem. 1973, 45, 205.

26. Breiter, M. W. Electrochim. Acta 1963, 8, 447.

27. Fleischmann, C. W.; Johnson, G. K.; Kuhn, A. T. J. Electrochem. Soc. 1964, 111, 602.

28. Breiter, M. W. Electrochim. Acta 1963, 8, 457.

29. Jayaram, R.; Lal, H. J. Electroanal. Chem. 1977, 79, 121.

30. Belanger, G.; Vijh, A. K. "Oxide and Oxide Films"; Marcel Dekker, Inc.: New York, 1977; Vol. 5, Chapter 1.

31. Podlovchenko, B. I.; Petry, O. A.; Frumkin, A. N.; Lal, H. J. Electroanal. Chem. 1966, 11, 12.

32. Breiter, M. W. J. Electroanal. Chem. 1967, 15, 221.

33. Sidheswaran, P.; Lal, H. J. Electroanal. Chem. 1972, 40, 143.

34. Fleury, M. B.; Letellier, S. J. Electroanal. Chem. 1978, 88, 123.

35, Raicheva, S. N.; Kalcheva, S. V.; Christov, M. V.; Sokolova, E. J. J. Electroanal. Chem. 1974, 55, 213.

36. Kalcheva, S. V.; Christov, M. V.; Sokolova, E. I.; Raicheva, S. N. J. Electroanal. Chem. 1974, 55, 223.

37. Kalcheva, S. V.; Christov, M. V.; Sokolova, E. I.; Raicheva, S. N. J. Electroanal. Chem. 1974, 55, 231.

38. Loučka, T.; Weber, J. J. Electroanal. Chem. 1969, 21, 329.

39. Breiter, M. W. Electrochim. Acta 1963, 8, 973.

40. Breiter, M. W. J. Electroanal. Chem. 1968, 19, 131.

41. Sidheswaran, P. J. Electroanal. Chem. 1972, 38, 101.

42. Sundholm, G. J. Electroanal. Chem. 1971, 31, 265.

43. Sobkowski, J.; Cinak, J. J. Electroanal. Chem. 1971, 30, 499.

44. Kamath, V. N.; Lal, H. J. Electroanal. Chem. 1968, 19, 137.

45. Trasatti, S.; Formaro, L. J. Electroanal. Chem. 1968, 17, 343.

46. Bagotzky, V. S.; Vasilyev, Y. B. Electrochim. Acta 1964, 9, 869.

47. Bockris, O'M. J.; Piersma, B. J.; Gileadi, E. Electrochim. Acta 1964, 9, 1329.

48. Yao, S. J.; Appleby, A. J.; Geisel, A.; Cash, H. R.; Wolfson, S. K., Jr. Nature 1969, 224, 921.

49. Wolfson, S. K., Jr.; Gofberg, S. L.; Prusiner, P.; Nanis, L. Trans. Am. Soc. Artif. Intern. Organs 1968, 14, 195.

50. Wan, B. Y. C.; Tseung, A. C. C. Med. and Biol. Engng. 1974, 12, 14.

51. Gebhardt, V.; Rao, J. R.; Richter, G. J. J. Appl. Electrochem. 1976, 6, 127.

52. Massie, H.; Racie, P.; Parker, R.; Hank, A. W. Med. and Biol. Engng. 1968, 6, 503.

53. Tseung, A. C. C.; King, W. J.; Wan, B. Y. C. Med. and Biol. Engng. 1971, 9, 175.

54. Chang, K. W.; Aisenberg, S.; Soeldner, J. S.; Hiebert, J. M. Trans. Am. Soc. Artif. Intern. Organs 1973, 19, 352.

55. Gough, D. A.; Anderson, F. L.; Giner, J.; Colton, C. K.; Soeldner, J. S. Anal. Chem. 1978, 50, 941.

56. Skon, E. Electrochim. Acta 1977, 22, 313.

57. Rao, M. L. B.; Drake, R. F. J. Electrochem. Soc. 1969, 116, 334.

58. Ernst, S.; Heitbaum, J. J. Electroanal. Chem. 1979, 100, 173.

59. Marinčic, L.; Soeldner, J. S.; Colton, C. K.; Giner, J. Morris, S. J. Electrochem. Soc. 1979, 127, 43.

60. Lerner, H.; Giner, J.; Soeldner, J. S.; Colton, C. K. J. Electrochem. Soc. 1979, 126, 237.

61. Hough, L.; Richardson, A. C. In "The Monosaccharides, Pentoses, Hexoses, Heptoses and Higher Sugars", Coffey, S., Ed.; "Rodd's Chemistry of Carbon Compounds"; Elsevier: New York, 1967; Vol. 1F, Chapter 23.

62. Lehninger, A. L. "Biochemistry: The Molecular Basis of Cell Structure and Function", 2nd ed.; Worth: New York, 1970; Chapter 10.

63. Speck, J. C. Adv. Carbohydr. Chem. 1958, 13, 63.

64. Angerstein-Koglowska, H.; MacDougall, B.; Conway, B. E. J. Electrochem. Soc. 1973, 120, 756.

65. Breiter, M. W. Electrochim. Acta 1965, 10, 503.

66. Spasojevic, M. D.; Adzic, R. R.; Despic, A. R. J. Electroanal. Chem. 1980, 109, 261.

67. Adzic, R. R.; Spasojevic, M. D.; Despic, A. R. J. Electroanal. Chem. 1978, 92, 31.

68. Tindall, C. W.; Bruckenstein, S. Anal. Chem. 1968, 40, 1051.

69. Bowles, B. J. Electrochim. Acta 1965, 10, 717.

70. Bowles, B. J. Electrochim. Acta 1965, 10, 731.

71. Bowles, B. J. Electrochim. Acta 1965, 15, 737.

72. Cadle, S. H.; Bruckenstein, S. Anal. Chem. 1972, 44, 1993.

73. Lorenz, W. J.; Hermann, H. D.; Wüthrich, N.; Hilbert, F. J. Electrochem. Soc. 1974, 121, 1167.

74. Szabo, S. J. Electroanal. Chem. 1977, 77, 193.

75. Lindstrom, T. R. Ph.D. Dissertation, Iowa State University, Ames, IA, 1980.

76. Takamura, T.; Sato, Y.; Takamura, K. J. Electroanal. Chem. 1973, 41, 31.

77. Adzic, R. R.; Yeager, E.; Cahan, B. D. J. Electrochem. Soc. 1974, 121, 474.

78. Kolb, D. M.; Prazasnyski, M.; Gerischer, H. J. Electroanal. Chem. 1974, 54, 25.

79. Trasatti, S. Zeitschrift für Physikalische Chemie Neue Folge Bd. 1975, 98, 75.

80. Furuya, N.; Motoo, S. J. Electroanal. Chem. 1979, 98, 189.

81. Furuya, N.; Motoo, S. J. Electroanal. Chem. 1980, 107, 159.

82. Furuya, N.; Motoo, S. J. Electroanal. Chem. 1976, 72, 165.

83. Furuya, N.; Motoo, S. J. Electroanal. Chem. 1977, 78, 243.

84. Furuya, N.; Motoo, S. J. Electroanal. Chem. 1979, 98, 195.

85. Adzic, R. R.; Simic, D. N.; Despic, A. R.; Drazic, D. M. J. Electroanal. Chem. 1975, 65, 587.

86. Adzic, R. R.; Despic, A. R.; Simic, D. N.; Drazic, D. M. National Bureau of Standards Special Publication 456, 1976, p. 191.

87. Adzic, R. R.; Simic, D. N.; Drazic, D. M.; Despic, A. R. J. Electroanal. Chem. 1975, 61, 117.

88. Adzic, R. R.; Simic, D. N.; Despic, A. R.; Drazic, D. M. J. Electroanal. Chem. 1977, 80, 81.

89. Motoo, S.; Watanabe, M. J. Electroanal. Chem. 1979, 98, 20.

90. Taylor, A. H.; Kirkland, S.; Brummer, S. B. Trans. Faraday Soc. 1971, 67, 809.

91. Despic, A. R.; Adzic, R. R.; Tripkovic, A. V. Soviet Electrochem. 1977, 13, 568.

92. Janssen, M. M. P.; Moolhuysen, J. Electrochim. Acta 1976, 21, 869.

93. Janssen, M. M. P.; Moolhuysen, J. Electrochim. Acta 1976, 21, 861.

94. Mcnicol, B. D.; Chapman, A. G.; Short, R. T. J. Appl. Electrochem. 1976, 6, 221.

95. Andrew, M. R.; Drury, J. S.; Mcnicol, B. D.; Pinnington, C.; Short, R. T. J. Appl. Electrochem. 1976, 6, 99.

96. Janssen, M. M. P.; Moolhuysen, J. J. Catalysis 1977, 46, 289.

97. Watanabe, M.; Motoo, S. J. Electroanal. Chem. 1975, 60, 259.

98. Watanabe, M.; Motoo, S. J. Electroanal. Chem. 1975, 60, 267.

99. Cathro, K. J. J. Electrochem. Soc. 1969, 116, 1608.

100. Motoo, S.; Watanabe, M. J. Electroanal. Chem. 1976, 69, 429.

101. Koch, D. F. A.; Rand, D. A. J.; Woods, R. J. Electroanal. Chem. 1976, 70, 73.

102. Motoo, S.; Shibata, M.; Watanabe, M. J. Electroanal. Chem. 1980 110, 103.

103. Motoo, S.; Watanabe, M. J. Electroanal. Chem. 1980, 111, 261.

104. Watanabe, M.; Motoo, S. J. Electroanal. Chem. 1975, 60, 275.

105. Takamura, K.; Sakamoto, M. J. Electroanal. Chem. 1980, 113, 273.

106. Jayaran, R.; Lal, H. J. Electroanal. Chem. 1977, 79, 121.

107. Taylor, A. H.; Pearce, R. D.; Brummer, S. B. Trans. Faraday Soc. 1971, 67, 801.

108. Lown, J. A. Ph.D. Dissertation, Iowa State University, Ames, IA, 1979.

109. "The Handbook of Chemistry and Physics", 47th ed.; Weast, R. C., Ed.; The Chemical Rubber Co.: Cleveland, 1966.

110. Johnson, D. C. "Introduction to Electrochemical Methods of Analysis"; University Bookstore: Ames, IA., 1977; Chapter 3.

111. Espenson, J. H. "Chemical Kinetics and Reaction Mechanisms", 1st ed.; McGraw-Hill: New York, 1981; Chapter 6.

IX. ACKNOWLEDGEMENTS

I would like to thank Dr. Dennis C. Johnson for his support and guidance throughout my career as a graduate student. I would also like to express my gratitude to members of his research group for their valuable contribution to my graduate experience.

Financial support from the Department of Chemistry, Ames Laboratory and Phillips Petroleum Corporation is gratefully acknowledged.

Finally, I thank my parents for their support and encouragement throughout my education.